AFRL-RQ-WP-TR-2020-0017

JET FUEL PROPERTIES

James T. Edwards

Fuels & Energy Branch
Turbine Engine Division

JANUARY 2020
Interim Report

AIR FORCE RESEARCH LABORATORY
AEROSPACE SYSTEMS DIRECTORATE
WRIGHT-PATTERSON AIR FORCE BASE, OH 45433-7542
AIR FORCE MATERIEL COMMAND
UNITED STATES AIR FORCE

NOTICE AND SIGNATURE PAGE

This report was cleared for public release by the USAF 88th Air Base Wing (88 ABW) Public Affairs Office (PAO) and is available to the general public, including foreign nationals.

Copies may be obtained from the Defense Technical Information Center (DTIC) (https://discover.dtic.mil/).

AFRL-RQ-WP-TR-2020-0017 HAS BEEN REVIEWED AND IS APPROVED FOR PUBLICATION IN ACCORDANCE WITH ASSIGNED DISTRIBUTION STATEMENT.

REPORT DOCUMENTATION PAGE

Form Approved
OMB No. 0704-0188

1. REPORT DATE *(DD-MM-YY)*	2. REPORT TYPE	3. DATES COVERED *(From - To)*
January 2020	Interim	1 July 2019 – 1 January 2020

4. TITLE AND SUBTITLE
JET FUEL PROPERTIES

5a. CONTRACT NUMBER
In-house

5b. GRANT NUMBER

5c. PROGRAM ELEMENT NUMBER
62203F

6. AUTHOR(S)
James T. Edwards

5d. PROJECT NUMBER
5330

5e. TASK NUMBER

5f. WORK UNIT NUMBER
Q1AP

7. PERFORMING ORGANIZATION NAME(S) AND ADDRESS(ES)
Fuels & Energy Branch (AFRL/RQTF)
Turbine Engine Division
Air Force Research Laboratory Aerospace Systems Directorate
Wright-Patterson Air Force Base, OH 45433-7542
Air Force Materiel Command, United States Air Force

8. PERFORMING ORGANIZATION REPORT NUMBER
AFRL-RQ-WP-TR-2020-0017

9. SPONSORING/MONITORING AGENCY NAME(S) AND ADDRESS(ES)
Air Force Research Laboratory
Aerospace Systems Directorate
Wright-Patterson Air Force Base, OH 45433-7542
Air Force Materiel Command
United States Air Force

10. SPONSORING/MONITORING AGENCY ACRONYM(S)
AFRL/RQTF

11. SPONSORING/MONITORING AGENCY REPORT NUMBER(S)
AFRL-RQ-WP-TR-2020-0017

12. DISTRIBUTION/AVAILABILITY STATEMENT
DISTRIBUTION STATEMENT A. Approved for public release. Distribution is unlimited.

13. SUPPLEMENTARY NOTES
PA Clearance Number: 88ABW-2020-0271; Clearance Date: 28 January 2020.

14. ABSTRACT
This report contains a summary of jet fuel physical properties for conventional and alternative (non-petroleum) fuels. Amongst the properties included in the report are density, viscosity, distillation, composition, derived cetane number, enthalpy, surface tension, freeze point, flash point, and net heat of combustion. Several properties are demonstrated to need further study.

15. SUBJECT TERMS
jet fuel, density, viscosity, distillation, composition, derived cetane number, enthalpy, surface tension, freeze point, flash point, net heat of combustion

16. SECURITY CLASSIFICATION OF:			17. LIMITATION OF ABSTRACT:	18. NUMBER OF PAGES	19a. NAME OF RESPONSIBLE PERSON (Monitor)
a. REPORT	b. ABSTRACT	c. THIS PAGE			James T. Edwards
Unclassified	Unclassified	Unclassified	SAR	136	19b. TELEPHONE NUMBER (Include Area Code) N/A

TABLE OF CONTENTS

LIST OF FIGURES

LIST OF TABLES

1. INTRODUCTION

A significant amount of jet fuel physical property data has become available as the result of alternative fuel programs (ramping up in 2006) and other programs such as the CRC World Fuel Survey. This data has appeared in Research Reports and data compilations, but an attempt to gather it in one place and assess its consistency has not been done. This report is designed to be an update/complement to jet fuel physical property data compilations[1,2,3,15]. This report does not include much description on jet fuels themselves - good introductory documents are available[1,17,18]. Jet fuels are about 10% of the liquid transportation fuel market in the U.S., smaller than gasoline and diesel. All are predominantly produced from crude oil at the present time. The three transportation fuels are quite different in properties (Table 1) – this report focusses on jet fuels.

The World Fuel Survey consisted of 54 conventional jet fuels, as well as Stoddard solvent and two Sasol synthetic jet fuels[2]. In the data following (Table 1), the focus will be on the 54 conventional fuels in the Survey. The fuels were primarily Jet A-1 and Jet A fuels from Europe and North America, but included JP-8 and a few JP-5 fuels. Often the CRC Handbook includes typical properties for the various jet fuels (presented as best-fit lines, such as density versus temperature)[1], and those lines are often included in the discussion that follows.

Table 1 – Typical transportation fuel properties

	Jet	Diesel[19]	Motor gasoline[19]
Density	0.805	0.85	0.74
Avg MW	160	210	95
Carbon number range	C8 - C16	C9 to C23	C4 – C10
Flash point, C	50	60	
Freeze point, C	-52	-18	
VABP (volume molecular weight boiling point), C	210	275	105

NOTE: Gasoline and diesel data from Chevron diesel and gasoline technical reviews available on-line.

Within the class of jet fuels, there are a number of separately specified fuels, as illustrated in Table 2. The basic jet fuel specification has been remarkable constant since the early 1940s, as shown in Table 3 (although that statement totally ignores the decades of JP-4 use by the military; fuel specification history is found in References 17 and 15). All of these current jet fuels fall into the class of kerosene (or kerosine) fuels, defined by their boiling range. This report also includes data on some of the more notable alternative jet fuels evaluated since 2006. A decoder for these alternative fuels is presented in Table 4. Although many labs have participated in the evaluation of the alternative fuels, most of the data comes from Southwest Research Institute (SwRI), Air Force Research Laboratory/University of Dayton Research Institute (AFRL/UDRI), the U.S. Navy, and the Nat'l Institute of Standards and Technology (NIST). The National Jet Fuel Combustion Program (NJFCP) has acquired three fuels that span the range of jet fuel properties typically encountered in operational use. Data on these three Category A fuels is presented in most of the following sections to benchmark the data[14]. The A-2 fuel was obtained as a jet fuel with average properties, and data and correlations on this fuel in the following sections can be used as a typical jet fuel. Comparisons are also provided to industry analytical correlations[4,5,6]. Many of these analytical correlations use distillation data and density/specific gravity to correlate other properties, so distillation (Section 3) and density (Section 4) are discussed first, after a brief discussion of the reference fuels. JP-10 missile fuel (exo-tetrahydro dicyclopentadiene) is not included in this report. The use of detailed composition data to calculate properties has been recently

reviewed[25], and is mentioned only in passing in this report. Forthcoming DoD reports will expand on this topic.

Most of this data was measured at temperatures between -40 and 200 °C. Older higher-temperature data, (typically) calculations, is also included although its validity has yet to be confirmed[8,9,10,11,12,13]. In the sections that follow, typically properties of conventional fuels are presented, followed by alternative fuels (data from References 20 to 24), and then a discussion of estimation techniques for those properties. Fuels are often identified by the AFRL internal ID number, POSF XXXXX. This report includes alternative data from fuels used/tested by AFRL. Additional alternative aviation fuel data is available[118,119,120].

Table 2 – Common fuel specifications

Jet Fuel	Specification
Jet A	ASTM D1655, DEFSTAN 91-91
Jet A w/ additives	NATO F-24
Jet A-1	ASTM D1655, DEFSTAN 91-91, NATO F-35
JP-8, Jet A-1 w/ additives	MIL-DTL-83133, NATO F-34
JP-5	MIL-DTL-5624, NATO F-44
JPTS	MIL-DTL-25524
JP-4	MIL-DTL-5624, NATO F-40
JP-7	MIL-DTL-38219 (inactive)
JP-10	MIL-DTL-87107

NOTE: NATO in Reference 8

Table 3 – Jet fuel specifications

Property	AN-F-32, 1944 "JP-1"	ASTM D1655, 1959 "Jet A"	ASTM D1655, 2018 "Jet A"	JP-8, 2018	World Survey Avg[2]
Density	0.85 max	0.775-0.83	0.775-0.84	0.775-0.84	0.804
Flash point, C	43 min	44-66	38 min	38 min	49.5
Viscosity (cSt)	10 at -40 °C, max	15 at -34 °C, max	8 at -20 °C, max	8 at -20 °C, max	4.3
Freeze point, C	-60 °C max	-40 max (Jet A), -50 (Jet A-1)	-40 max (Jet A), -47 (Jet A-1)	-47 °C max	-52.1
Aromatics, vol%	20, max	20, max	25, max	25, max	17.5
Heat of Combustion, MJ/kg	--	42.8, min	42.8, min	42.8, min	43.05
Heat of Combustion, BTU/gal	--	121,500-126,500	--	--	
Sulfur content, mass%	0.2 max	0.3	0.3	0.3	0.049
Mercaptan sulfur, mass %	--	0.003	0.003	0.002	0.0002
Acid number	--	0.1	0.1	0.015	0.006
Distillation, C					
IBP					160
10%	210 max	205	205	205	176
20%					183
50%		233			201
90%	254 max				238
FBP	300 max	288	300	300	254
Smoke point, mm	--	20 min	18 min	18 min	--

Table 4 – Alternative fuels evaluated to be added to ASTM D7566

Fuel	Production Process	Fuel Overview	Companies	D7566 Approval
Synthetic Paraffinic Kerosene (SPK)	Synthesis gas production from coal, natural gas, or biomass, then Fisher-Tropsch synthesis to hydrocarbons	Predominantly jet-fuel-range iso-paraffins	Sasol "Isoparaffinic Kerosene, IPK", Shell, Syntroleum "S-8"	2009 (up to 50% blend)
Hydroprocessed Esters and Fatty Acids (HEFA, aka HRJ)	Hydroprocessing of triglycerides (animal fats, plants oil)	Predominantly jet-fuel-range iso-paraffins	UOP, Dynamic Fuels	2011 (up to 50% blend)
SIP	Direct fermentation of sugars to hydrocarbons	Single component, farnesane (2,6,10 trimethyl dodecane)	Amyris/Total	2014 (up to 10% blend)
IPKA	Addition of aromatics to production process for IPK	Kerosene containing aromatics	Sasol	2015 (up to 50% blend)
Alcohol-to-Jet (ATJ) SPK	Dehydration of iso-butanol and/or ethanol to alkenes, then oligomerization to jet fuel range hydrocarbons	Jet fuel range iso-paraffins	Gevo, LanzaTech	2016/2018 (up to 50% blend)
CHJ	"Catalytic Hydrothermolysis" of plant oils	Kerosene containing aromatics	ARA	2020 (up to 50% blend)
ATJ SKA	Similar to ATJ SKA, but contains aromatics	Kerosene containing aromatics	Swedish Biofuels, Byogy	pending
Hydroprocessed Depolymerized Cellulosic Jet (HDCJ)	Pyrolysis of lingo-cellulosic biomass to liquids, with subsequent upgrading to hydrocarbons	Heavily aromatic/ cycloparaffinic kerosene	KiOR, UOP	pending
Hydro-deoxygenated Synthesized Kerosene (HDO SK)	Catalytic upgrading of cellulosic "sugars" to hydrocarbons	Cycloparaffinic kerosene	Virent/Shell	pending
Hydro-deoxygenated Synthesized Aromatic Kerosene HDO SAK	Catalytic upgrading of cellulosic "sugars" to hydrocarbons	Aromatic kerosene	Virent/Shell	pending

Table 4 (cont) - Alternative fuels evaluated to be added to ASTM D7566

Fuel	Production Process	Fuel Overview	Companies	D7566 Approval
Bb-SPK	Hydroprocessing of algae oil (predominantly hydrocarbon) using HEFA process	Predominantly jet-fuel-range hydrocarbons, including cycloparaffins (no aromatics)	IHI	pending
Cycloparaffinic Kerosene (CPK-0)	Integrated hydropyrolysis and hydroconversion of lignocellulosic biomass	Predominantly jet-fuel-range cycloparaffins	Shell	pending

2. REFERENCE FUELS, PHASE DIAGRAM

This report focusses on jet fuels in the liquid phase. Some calculated physical properties are available for fuels in the vapor phase (e.g., Reference 13), but few measurements have been made in the vapor phase. The CRC Handbook of Aviation Fuel Properties[1] typically includes liquid fuel data from roughly -40 °C to 120 °C, but this report will include higher temperature data (both experiments and calculations) when available. This higher temperature data may be needed for fuel system and combustor design. The emphasis is on jet fuels in current use – Jet A, Jet A-1, JP-8, and JP-5.

Conventional jet fuel is a hydrocarbon distillate in the kerosene boiling range. In fact, the specification for kerosine for home heating applications (ASTM D3699) closely resembles the jet fuel specification, and the actual kerosine product commercially available in Ohio typically meets the jet fuel specification – and is a lot easier to obtain.

Since the jet fuel specification is a rather loose specification, there can be significant variations in physical properties amongst on-specification fuels. For example, the density results for jet fuels in the PQIS database[3] are widely distributed across the permissible 0.775 to 0.84 range, as shown in Figure 1. The NJFCP Category A fuels mentioned in Section 1 are also labeled, and well represent the range of fuel densities found in practice. Density is often a correlating parameter for physical properties[4], along with average boiling point. For this reason, much of the data that follows is anchored by the three Category A fuels: A-1 (POSF 10264, a JP-8), A-2 (POSF 10325, a Jet A), and A-3 (POSF 10289, a JP-5).

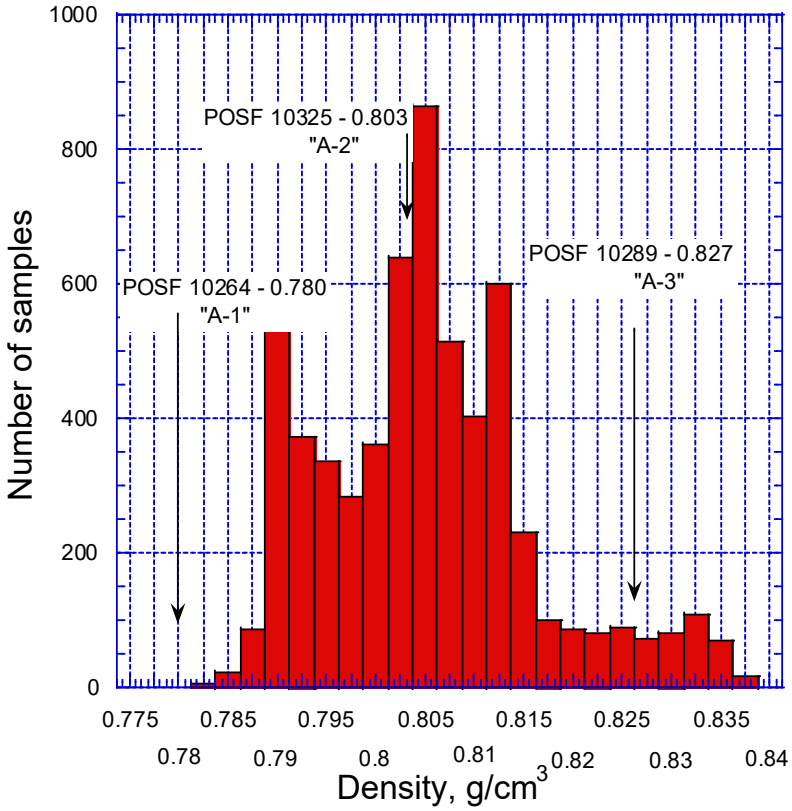

Figure 1 – Density histogram from 2013 PQIS, with Category A fuels labeled.

Another view of statistics can be obtained with a box (or box and whisker) plot, where the data is divided up into quartiles. The two quartiles surrounding the median form the box, while the range of the other two quartiles forms the whiskers. The thickness of the box (the center 50% of the distribution)

is defined at the inter-quartile distance (IQD). In the program used to plot Figure 2, data that falls outside the upper limit + 1.5*IQD or below the lower limit – 1.5*IQD is defined as an outlier (the circles in Figure 2). The long higher density tail in the distribution of Figure 1 results in a few density values being defined as outliers. In any case, one can see that the three Category A reference fuels do well-represent the range of densities present in jet fuels. Box plots are used again in the composition section below. Further discussion of density follows in Section 4. Figures 1 and 2 include data for approximately 6000 fuel samples.

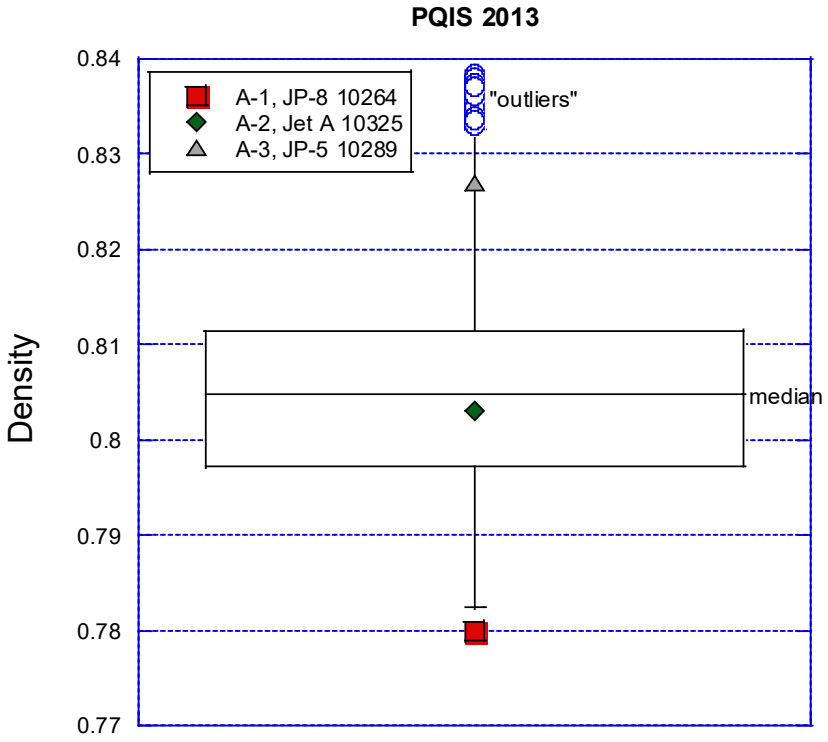

Figure 2 – Density data from Figure 1 as a box plot.

Measured phase diagram data for jet fuel is rare, but one set of measured data from UTRC was found[26]. The phase diagrams are reproduced in Figure 3. ERBS (Environmental Reference Broadened Specification Fuel[27]) is a prototype jet fuel with some of the specification limited relaxed, such as aromatic content and freeze point. ERBS was designed to increase the availability of jet fuel in a time of perceived shortage, and resembled diesel fuel (as shown in Figure 3). Ultimately, these broadened specification limits were not adopted. In any case, one can see that the critical temperature of jet fuel is roughly 680 K (400 °C, 750 °F) from Figure 3, consistent with literature data[28]. Further discussion of critical properties follows in Section 3. The critical temperature and pressure are not controlled by specification. What is controlled are some distillation limits and the flash and freeze points, as discussed in the next few sections.

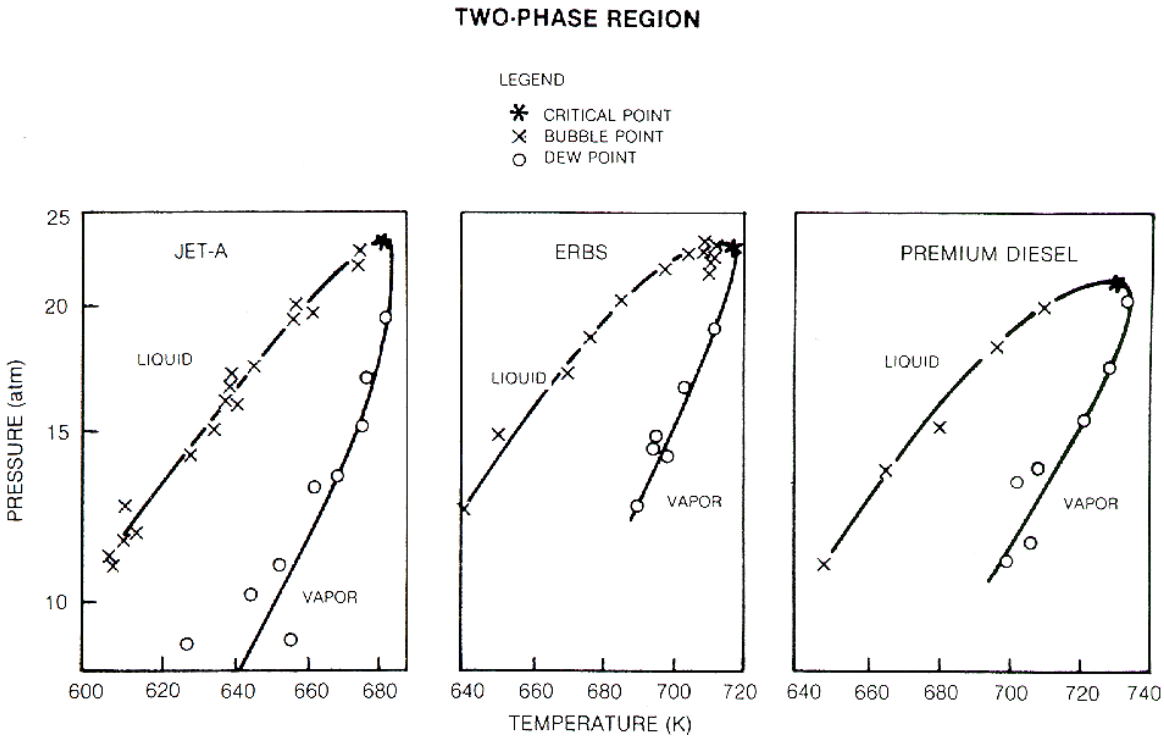

Figure 3 – Phase diagrams[26]

In terms of phase behavior, one can also note that jet fuel has a relatively large liquid range at ambient pressures, enabling its ease of handling and use in aircraft. For example, a typical jet fuel (NJFCP A-2), is completely liquid from -51 °C (freeze point) to 159 °C (initial boiling point) at atmospheric pressure, as compared to the 100 °C liquid range for water.

3. DISTILLATION, FLASH POINT, VAPOR PRESSURE, CRITICAL PROPERTIES

3.1 Distillation

As mentioned in connection with Table 1, distillation properties are often used to characterize jet fuels, typically by the venerable ASTM D86 (Standard Test Method for Distillation of Petroleum Products and Liquid Fuels at Atmospheric Pressure) distillation. This is a simple pot-boiling type of characterization, which does not produce results consistent with the true boiling point, although conversion approaches are available. However, ASTM D86 is the referee method for most jet fuel specifications, so this type of data is commonly available for most jet fuels. There is also a mini version of ASTM D86 denoted as ASTM D7345 (Standard Test Method for Distillation of Petroleum Products and Liquid Fuels at Atmospheric Pressure: Micro Distillation Method), as well as a gas chromatographic technique that more closely resembles the true boiling point (ASTM D2887: Standard Test Method for Boiling Range Distribution of Petroleum Fractions by Gas Chromatography). Additionally, NIST has developed an "advanced distillation column" (ADC)[29,30,31,32,33,38]. As shown in Figure 4 for the A-2 (average) fuel, D2887 gives results that resemble the true boiling point (as estimated from D86 data using a method in reference[4]), while D86 and D7345 give higher initial boiling points and lower final boiling points than the true result. For the NIST ADC device, the head temperature (T_h) is similar to the D86 temperatures, while the kettle temperature (T_k) is higher. Note that one advantage of the NIST ADC device is that it allows the composition of distillation fractions to be obtained, although NIST used the D2789 (Standard Test Method for Hydrocarbon Types in Low Olefinic Gasoline by Mass Spectrometry [39]) method to analyze the fractions. The scope of D2789 only cites gasoline. ASTM D2789 has been found to be inaccurate for kerosene aromatics[34].

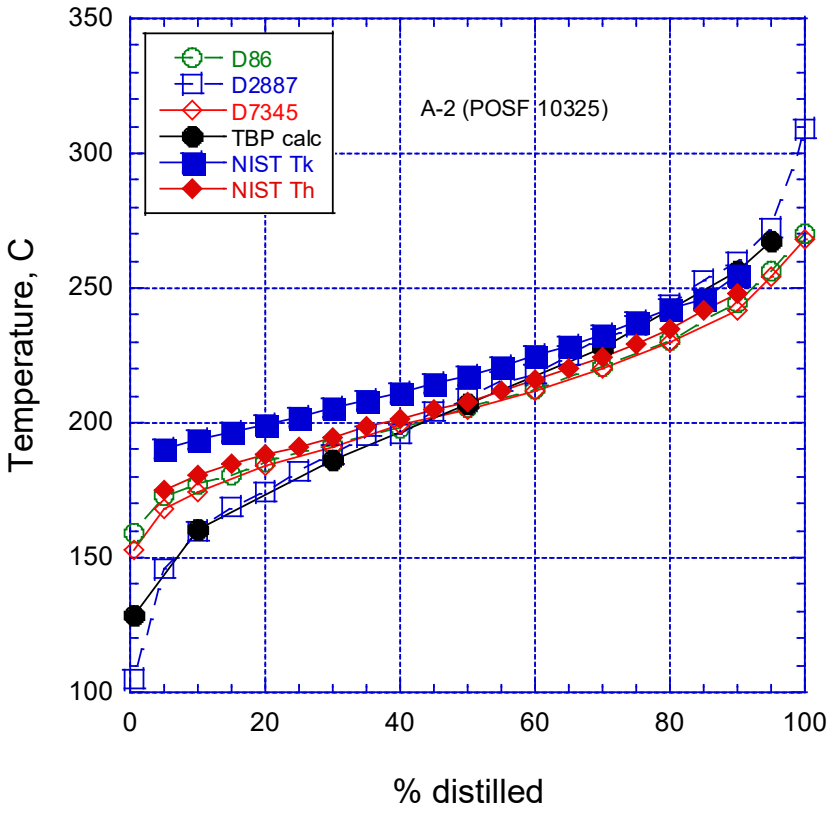

Figure 4 – Distillation of POSF 10325 Jet A (A-2) by various methods.

D86 data have been used to characterize jet fuels since the 1940s (e.g., Table 1). D86 data is also used with density/specific gravity data to estimate physical properties of petroleum fractions such as jet fuel[4,5,6,15]. Figure 5 shows the distillation data for the three Category A fuels, with World Fuel Survey[2] averages and standard deviations. The Category A distillation data is in Tables 5 and 6[14,38]. The jet fuel specification limits are T10 < 205 °C and FBP (final boiling point) < 300 °C, as shown in Table 1.

The standard deviation lines on Figure 5 come from an analysis of the statistics. For example, the raw data for T10 for Jet A/Jet A-1/JP-8 is shown in Figure 7.

Table 5 – ASTM D86 distillation and D4052 density (SwRI)

D86 distillation, °C	A-1	A-2	A-3	World Fuel Survey avg
0%	150.0	159.2	177.9	160
5%	162.2	173.1	190.2	
10%	164.3	176.8	194.2	176
15%	167.4	180.8	197.7	
20%	171.1	185.4	201.3	182
30%	176.9	191.5	207.9	
40%	183.0	198.2	213.8	
50%	189.7	205.4	219.6	201
60%	197.0	212.6	225.3	
70%	206.5	220.8	231.0	
80%	218.5	230.9	237.5	
90%	233.9	244.6	245.8	238
95%	245.0	256.0	252.5	
100%	256.7	270.5	259.5	253
Density (60 °F/15.5 °C)	0.780	0.804	0.827	0.8032

Table 6 – NIST ADC data for Category A fuels, reproduced from Reference 38

	Jet A-10325		JP-8-10264		JP-5-10289	
	83.1 kPa		83.2kPa		83.6 kPa	
DVF(%)	T_k(°C)	T_h(°C)	T_k(°C)	T_h(°C)	T_k(°C)	T_h(°C)
5	190.4	175.0	176.5	168.2	206.7	198.0
10	193.7	180.3	179.4	171.8	209.6	202.0
15	196.7	184.5	181.9	174.8	212.3	205.4
20	199.6	188.2	184.4	177.4	215.2	208.7
25	202.4	191.1	187.0	180.2	217.6	211.3
30	205.5	194.5	189.5	183.2	220.2	214.3
35	208.2	198.4	192.3	186.2	222.4	217.0
40	211.0	201.3	195.1	188.9	224.8	219.4
45	214.4	204.7	198.4	192.7	227.0	222.2
50	217.4	207.9	201.9	196.2	229.3	224.8
55	220.7	211.8	205.2	199.4	231.3	227.5
60	224.7	216.1	208.5	204.0	233.7	230.3
65	228.6	220.2	214.2	208.7	236.3	232.9
70	233.0	224.5	219.2	214.1	238.9	236.3
75	237.6	229.3	224.8	219.8	241.6	239.7
80	242.7	234.5	231.7	226.8	245.3	243.3
85	246.1	241.4	238.5	234.1	248.5	247.2
90	255.2	248.1	244.3	243.2	253.0	252.6

NOTE: These temperatures in the kettle and in the head (T_k and T_h, respectively) have been adjusted to 1 atm with the modified Sydney Young equation; the average experimental atmospheric pressures are provided to allow recovery of the actual measured temperatures.

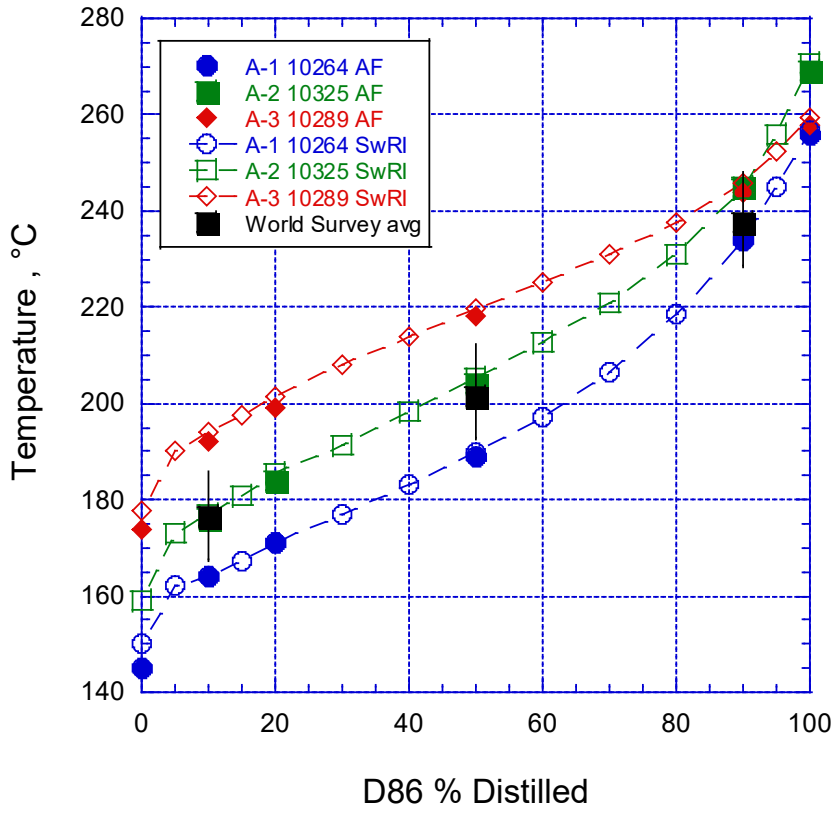

Figure 5 – ASTM D86 distillation for Category A fuels[14]

D86 distillation data is typically incorporated into property correlations by converting to an average boiling point[29]. D86 data naturally produces a volume-average boiling point. Maxwell[6] shows in chart form how one converts from volume average to weight average, mean average, and/or molal average (reproduced in Figure 6 – note that temperature unit is F!). The slope of the distillation curve can be calculated in various ways (e.g., [T70-T10]/60 in Figure 6). Note that for the A-2 fuel, (T70-T10)/60 ~ 1.3 F/%, so the correction between the various average boiling points is relatively small from Figure 6.

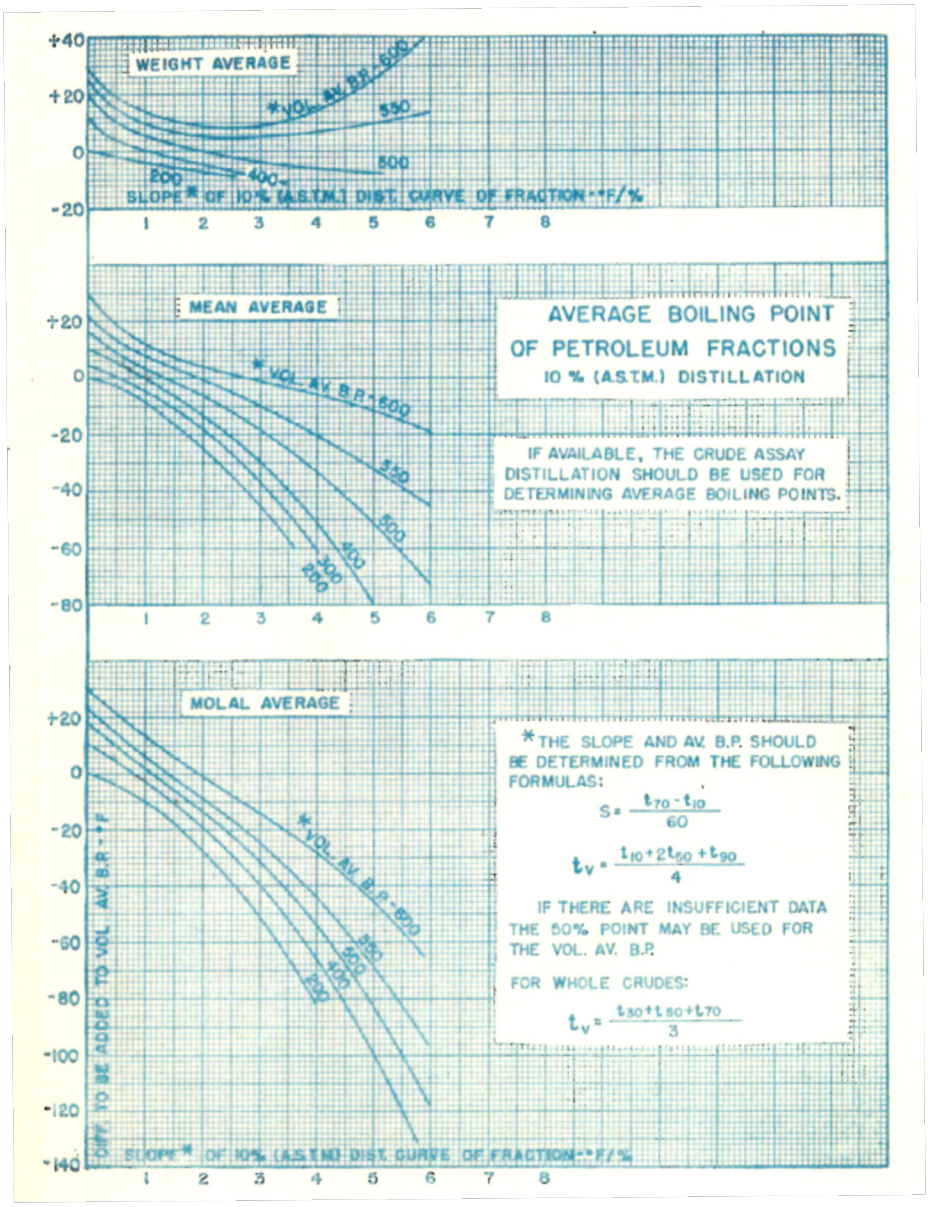

Figure 6 – Conversions between various average boiling point[6]

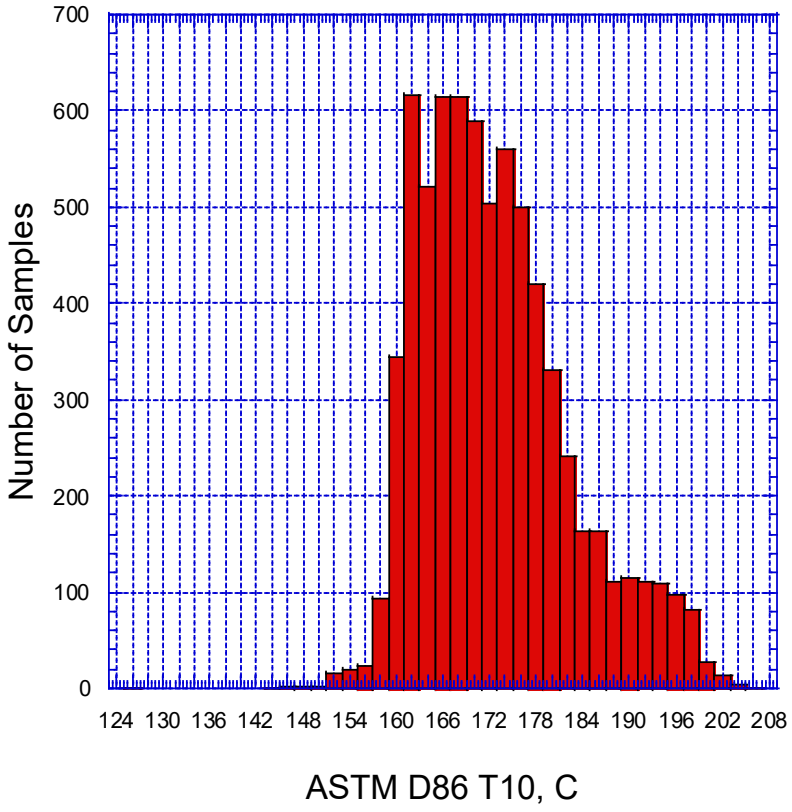

Figure 7 – ASTM D86 T10 from PQIS 2013 for Jet A/Jet A-1/JP-8.

3.2 Flash Point

Several fuel properties are primarily controlled by the distillation curve. The flash point is controlled by the front end (low temperature end) of the distillation curve. This can be seen in two ways. First, it can be seen in Figure 8, where the first 10% of the POSF 10289/A-3 JP-5 fuel is distilled off, raising the flash point from 60 to 70 °C (and also changing freeze point and viscosity). One can also see this relationship in Figure 9, which plots PQIS T10 data versus flash point[3]. The correlation isn't perfect, but illustrates the effect of distillation on flash point. Riazi[4] correlates flash point as (T in K):

$$T_F = 15.48 + 0.70704T_{10}$$

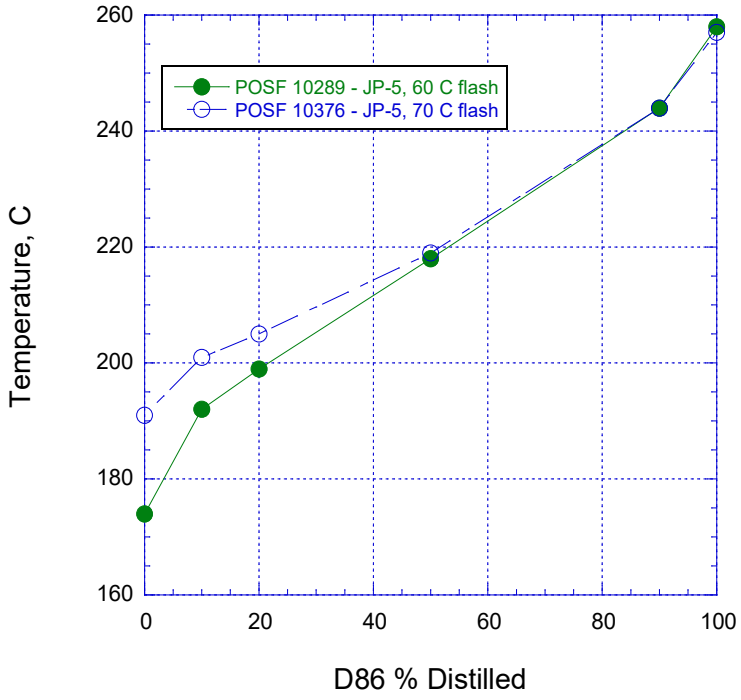

Figure 8 – Change in D86 results obtained by distilling off low boiling point material to raise flash point of A-3 (JP-5) fuel from 60 to 70 ℃.

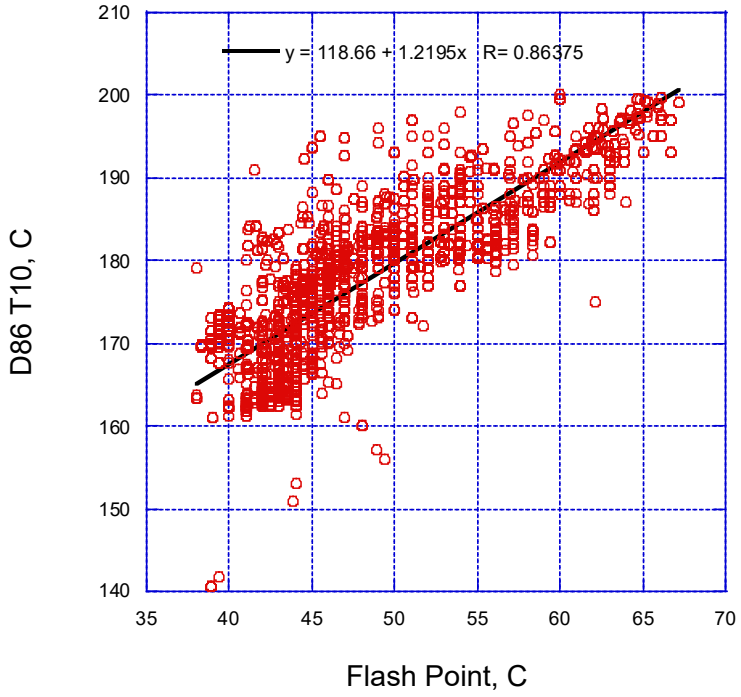

Figure 9 – Correlation of flash point with D86 10% distillation temperature[3].

It would be more logical to expect flash point to correlate to the initial boiling point (IBP), but Riazi states that the IBPs are relatively inaccurate compared to the 10% point. The range (distribution) of flash points in PQIS 2016 is shown in Figure 10. Navy JP-5 high flash point kerosene dates back to the early 1950s[17], and has a minimum 60 °C flash point, as is evident in Figure C-6. Lefebvre[68] shows plot (from Maxwell Smith's book) of straight-line relationship between the 10% D86 temperature and flash

point, for fuels ranging from avgas to gas oils. A comparison of the distribution of flash points from kerosene fuels (not including JP-5) is shown in Figure 11.

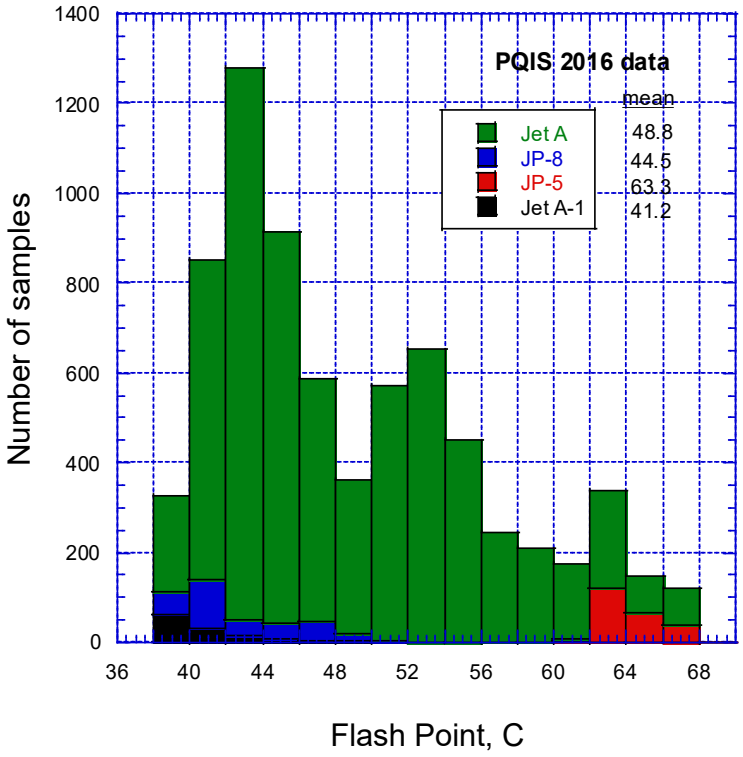

Figure 10 – Statistical distribution of flash points[3]

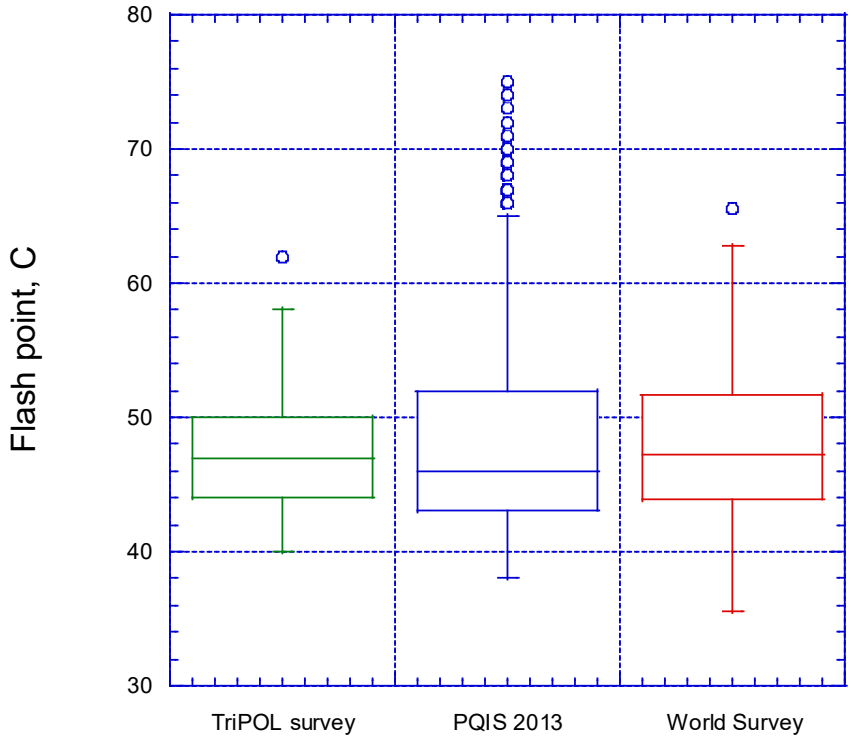

Figure 11 – Flash point distribution for jet fuels (JP-8/Jet A/Jet A-1, no JP-5)

3.3 Vapor Pressure vs. T

Vapor pressure is not a specification property. Vapor pressure is not independent of the other properties discussed – it is likely that one could calculate the vapor pressure from the D86 distillation curve and/or flash point. For example, the CRC Handbook[1] shows separate vapor pressure curves for JP-8/Jet A/Jet A-1 (flash >38 °C) and JP-5 (flash > 60 °C). The vapor pressures of the three Category A fuels was measured at SwRI by ASTM D6378 (Standard Test Method for Determination of Vapor Pressure (VPX) of Petroleum Products, Hydrocarbons, and Hydrocarbon-Oxygenate Mixtures) yielding the results shown in Figure 12[14]. And, yes, the data comes as vapor pressure in psia versus temperature in C, so those mixed units are plotted directly. The vapor pressures track with D86 and flash point, as expected. Barnett & Hibbard[15] correlate vapor pressure as a function of temperature with the slope of the distillation curve at T10 (i.e., (T15-T5)/10). This appears to be a method of getting around the inaccuracy of IBP measurements. Lefebvre[68] has plot of vapor pressure versus temperature, citing Barnett and Hibbard. That plot is reproduced in Figure 13. Considering that the fuels included in Barnett and Hibbard were those in use in the mid-1950s (JP-1, JP-3, JP-4, JP-5, Grade 115/145 avgas and various grade of fuel oils) – it is not clear what Lefebvre's "Jet A/Jet A-1" line is based on.

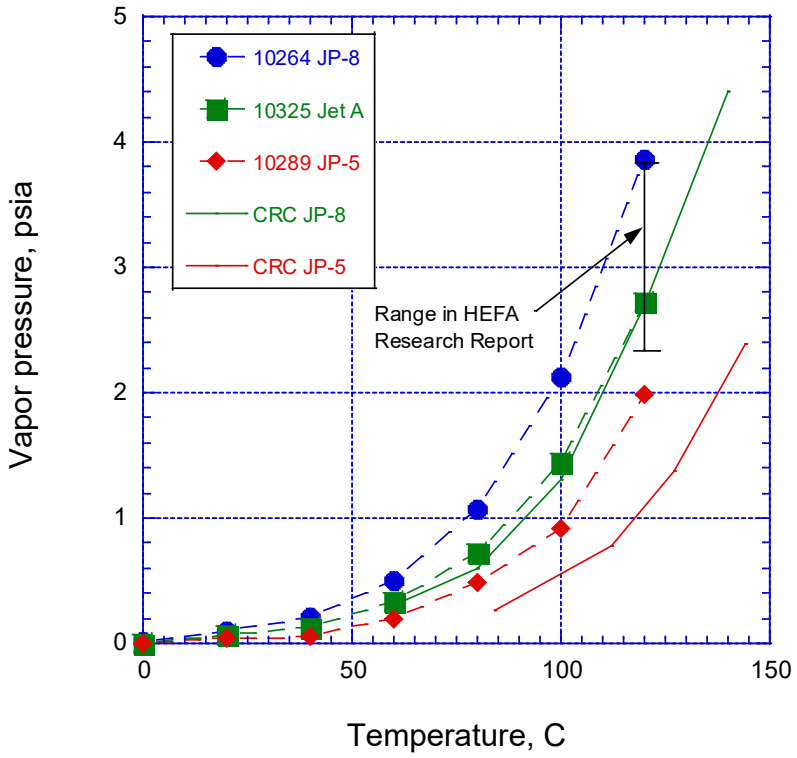

Figure 12 – Vapor pressure vs. T data for Category A fuels

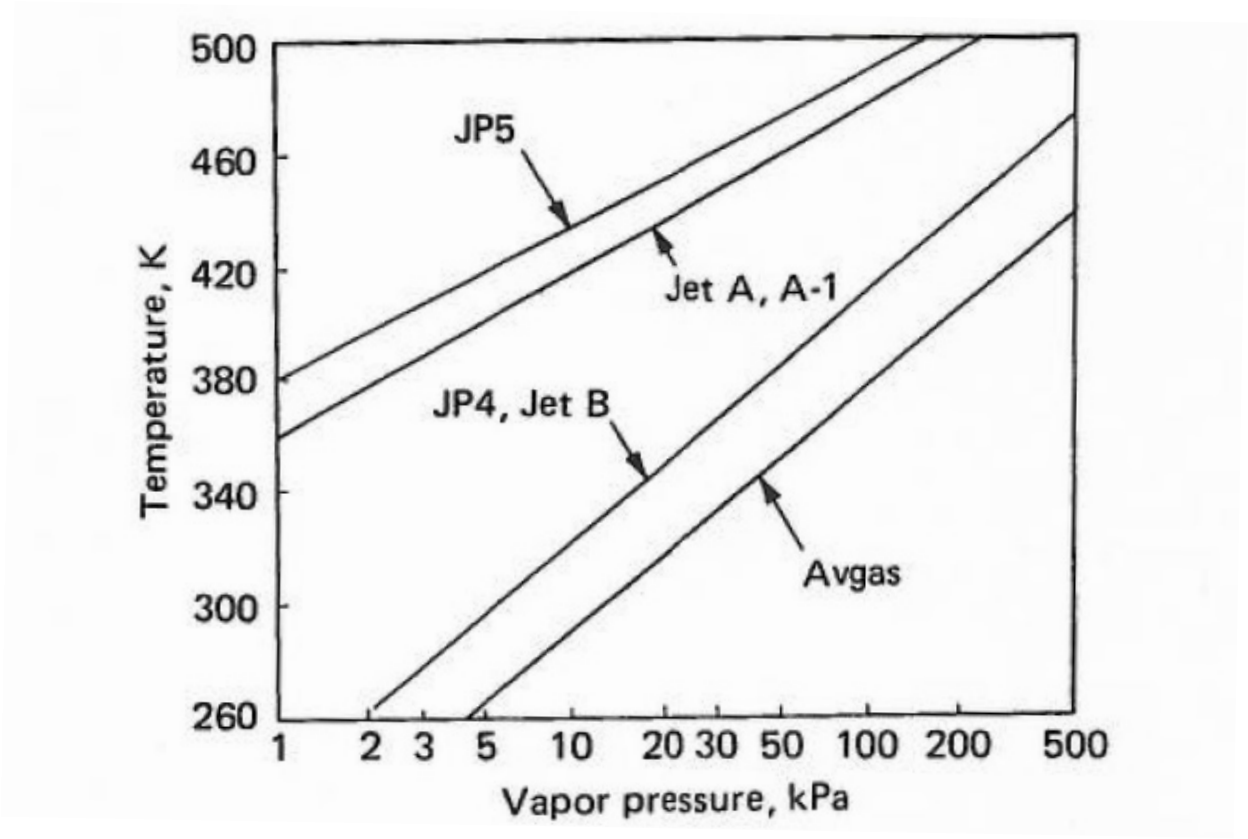

Figure 13 – Vapor pressure as a function of temperature[68]

3.4 Alternative fuels

Flash point and D86 data for various (neat) alternative fuels is presented in Tables 5 and 6, respectively. A number of these fuels were made in JP-5/high flash point versions, with two examples shown in Tables 7 and 8 (SPK and CHJ). Note that the distillation behavior of the two is similar to that seen in Figure 14, with a higher initial boiling point for the higher-flash-point fuel. Vapor pressure versus temperature data for alternative fuels is indistinguishable from comparable conventional fuels of similar flash point, as would be expected. Distillation and flash point data for a variety of alternative fuels blends has been published[55,56].

Table 7 – flash points for selected (neat) alternative fuels

Fuel	Manufacturer	POSF	Flash point, °C
Synthetic Paraffinic Kerosene (SPK)	Sasol IPK	7629	42
	Shell SPK	5729	46
	Syntroleum S-8	5018	48
	Syntroleum S-5	4705	67
Hydroprocessed Esters and Fatty Acids (HEFA, aka HRJ)	UOP camelina	10301	46
	UOP tallow	10298	44
	Dynamic Fuels (mixed fats)	7635	44
ATJ SPK	Gevo (isobutanol)	11498	50
CHJ-8	ARA	8455	48
CHJ-5	ARA	13676	64
ATJ SKA	Swedish Biofuels	12924	44
Hydro-deoxygenated Synthetic Kerosene (HDO SK)	Virent/Shell	8535	50

Table 8 – ASTM D86 distillation data for selected (neat) alternative fuels

Fuel	Companies	POSF	IBP, C	T10	T20	T50	T90	FBP
Synthetic Paraffinic Kerosene (SPK)	Sasol IPK	7629	156	164	166	177	201	224
	Shell SPK	5729	156	162	164	169	185	200
	Syntroleum S-8	5018	147	170	180	209	247	259
	Syntroleum S-5	4705	189	201	202	216	253	268
Hydroprocessed Esters and Fatty Acids (HEFA, aka HRJ)	UOP (camelina)	10301	147	164	174	220	273	283
	UOP (tallow)	10298	144	162	173	216	263	272
	Dynamic Fuels (mixed fats)	7635	147	179	192	222	258	270
ATJ SPK	Gevo (isobutanol)	11498	173	178	179	182	228	263
CHJ-8	ARA	8455	164	180	185	200	229	240
CHJ-5	ARA	13676	181	189	192	204	232	248
ATJ SKA	Swedish Biofuels	12924		164		185	232	256
Hydro-deoxygenated Synthetic Kerosene (HDO SK)	Virent/Shell	8535	159	178	186	213	260	282

3.5 Property estimation techniques

Most estimation techniques use density/specific gravity and some variation of average boiling point to estimate/correlate properties. There are different types of average boiling points – volume average, weight average, mean average, molal average, as discussed in relation to Figure 6. Averaging D86 data results in volume average boiling point (VABP), typically

$$VABP = \left(\frac{T_{10} + T_{30} + T_{50} + T_{70} + T_{90}}{5}\right) \text{ or } = \left(\frac{T_{10}+T_{50}+T_{90}}{3}\right)$$

Riazi has equations converting VABP to the other average boiling points[4], while Maxwell and others have tables and graphs[5,6]. The ASTM slope or Engler slope ((T90 – T10)/80) is used to characterize the width of the boiling range, where narrow boiling petroleum fractions have the various average boiling points being fairly similar. Riazi defines narrow boiling as having (T90-T10)/80 < 0.8 °C/%. Jet fuels typically have slopes near this 0.8 value, so they mostly qualify as narrow boiling (whereas diesel fuel typically does not). The point being that most property correlations use the mean average boiling point, rather than VABP – but for jet fuels the mean and volume average boiling points are very similar, so VABP can be used directly (Riazi[4] also states mean average boiling point ~ T50 for narrow boiling petroleum fractions). Note that the correlations often use specific gravity (SG) rather than density, where SG = density of fuel at 15.5 C (60 °F) /density of water at 15.5 °C. The density of water at 15.5 °C/60 °F is 0.999 g/cm^3, so the specific gravity and specification density in g/cm^3 or g/mL are essentially equivalent for engineering purposes. Some correlations use API gravity, where

$$API = \left(\frac{141.5}{SG(at\ 60\ F}\right) - 131.5.$$

The Watson K_w or characterization factor is also sometimes used as a measure of the paraffin content of the fuel, where

$$K_w = \frac{T_b^{0.33}(in\ R)}{SG}$$

(K_w=11.85 for POSF 10325/A-2 fuel, using VABP as T_b).

One could use composition data to estimate boiling range, but most correlations assume that density and D86 distillation are measured, and the other properties are predicted from them. This may change as advanced compositional techniques become more widely used. Riazi[4] describes analytical techniques for estimating vapor pressure of petroleum fractions.

3.6 Critical Properties

Critical property measurements for jet fuel are rare. These are not easy measurements, since jet fuel breaks down (thermally cracks) at near-critical temperatures over the course of the measurements. Penn State measured the critical temperature and estimated the critical pressure of a number of jet fuels[28], with the results shown in Table 9. One can see the variations between conventional jet fuels and the coal-derived (naphthenic) fuels (JP-8C/JP-8CA/JP-8CB), but in general one can state that the critical temperature and pressure of jet fuels are 730 to 770 °F (388 to 410 °C) and 21-33 atm, respectively. Thus, the typical temperature range for the physical properties in the CRC Handbook is well below the critical temperature, so near-critical effects should be absent. The importance of the critical temperature and pressure arises in the non-linear physical property variations near the critical point. This will become evident in some of the higher-temperature data sets presented later in this report.

Table 9 – Penn State measured critical properties, where JP-8C, JP-8CA, and JP-8CB are coal-derived, with the rest petroleum-derived[28]

Fuel	Tc, F	Pc, atm (calc)
JP-8P	740	24.1
JP-8P2	757	22.4
Jet A	752	23.5
Jet A-1	732	23.1
JP-7	761	20.7
JPTS	719	23.1
JP-8C	761	32.3
JP-8CA	753	33.3
JP-8CB	773	31.3

Critical property correlations for estimating T_c and P_c for fuels are given in References 4 and 28. Equations that worked for conventional fuels did not work as well for naphthenic (coal-derived) fuels[28]. Riazi[4] has equations for T_c, P_c that result in T_c ~ 737 °F (392 °C), P_c ~ 21.2 bar for the A-2 fuel.

$$T_c = 19.0623 T_b^{1.58848} \cdot SG^{0.3596}$$

$$P_c = 5.53027E^7 \cdot T_b^{-2.3145} \cdot SG^{2.301}$$

where T is in °K. Maxwell[6] (p. 72) has a chart that correlates critical temperature as a function of density and average boiling point, yielding pseudocritical T_c ~ 725 °F and true T_c ~ 735 °F for the A-2 fuel. This data is roughly consistent with Table 9. An estimate for critical density and acentric factor for JP-5 can be found at the end of the Appendix.

4. DENSITY

For specification purposes, density is typically measured by ASTM D4052 (Standard Test Method for Density, Relative Density, and API Gravity of Liquids by Digital Density Meter) at 60 °F/15.5 °C. The distribution of densities was shown in Figures 1 and 2. As shown in the CRC Handbook[1] and the World Survey[2], density is a linear function of temperature from -40 °C to about 100 °C. That linearity extends to pure hydrocarbons and alternative fuels, as shown in Moses[16] (see also[7]). Figure 14 illustrates this linearity with data from the three reference fuels[14] as well as World Survey fuels and "Jet A" from the CRC Handbook. The line from the 1983 Handbook was used, since some questions have arisen over the slope of the density line in the later editions. This will be discussed further below.

Older (calculated) data[8,9,10,11,12,13] shows that linearity begins to fail (as it should) as the critical temperature is neared (Figure 15). And, being older data, it comes in English units. Figure 16 shows that above the critical temperature in the vapor region, the calculated densities are strongly dependent on pressure (as they should be). Liquid density as a function of pressure is presented in the bulk modulus Section 10. Figures 15 and 16 are specific examples of more generalized density diagrams such as Figure 17[69].

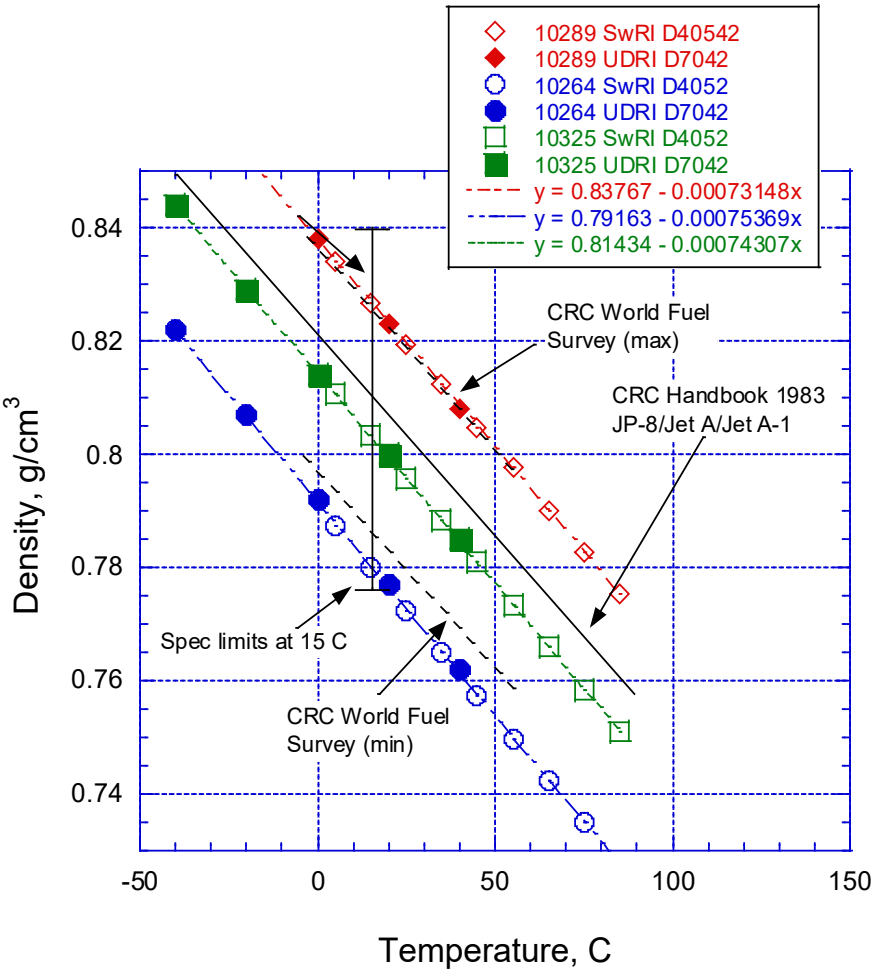

Figure 14 – Density data for Category A fuels[14], Jet A[1], World Survey[2].

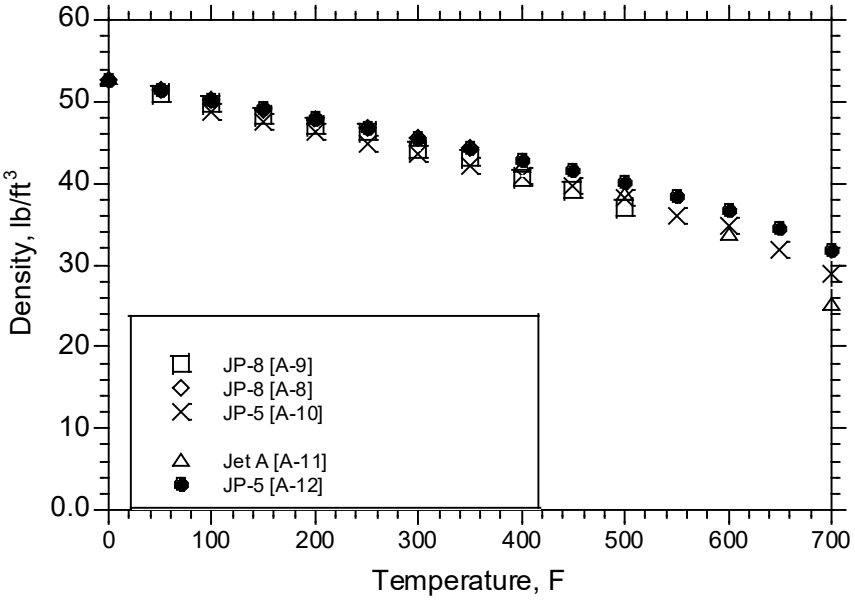

Figure 15 – Older density data up to 700 °F (62.43 lb/ft³ = 1 g/cm³)[8,9,10,11,12,13]

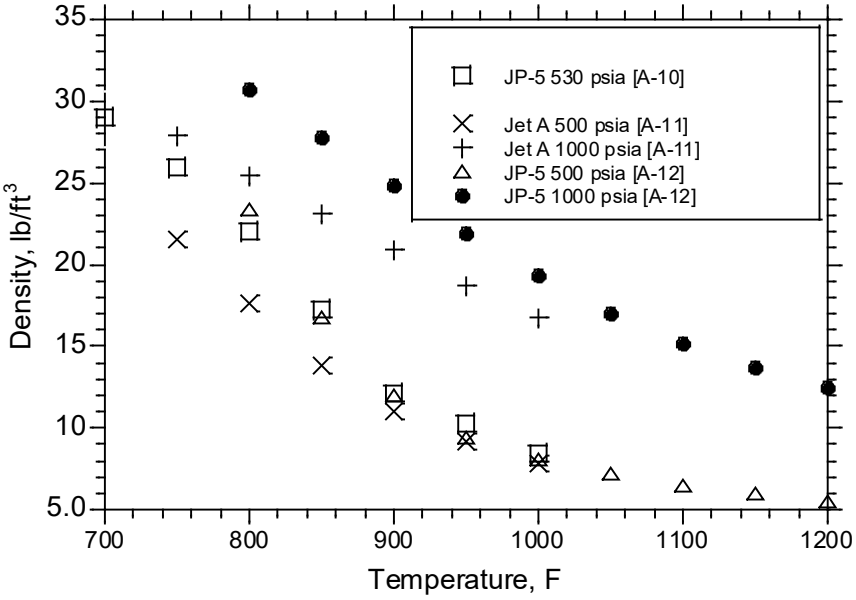

Figure 16 – Older density data 700 to 1200 °F (calculated)[8,9,10,11,12,13]

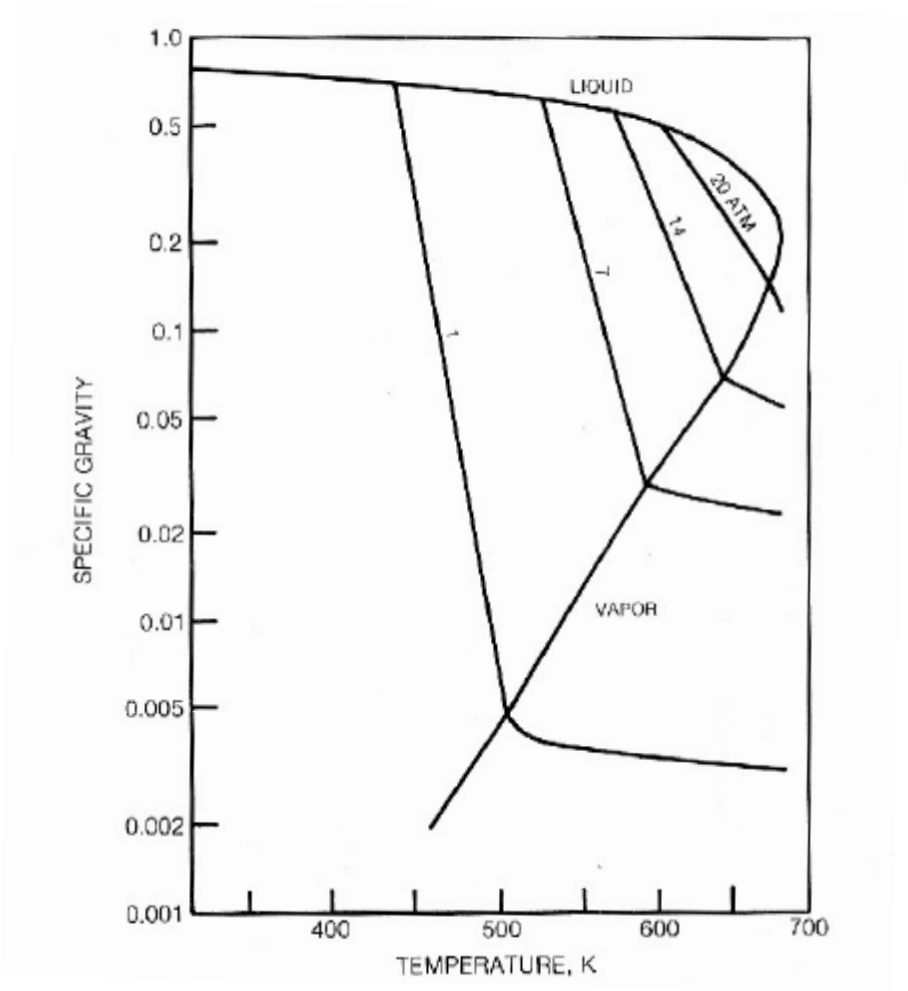

Figure 17 – General density phase diagram[69]

For reference, refractive index is directly proportional to density, as shown in Figure 18 with data taken from the World Fuel Survey[2] and elsewhere[37].

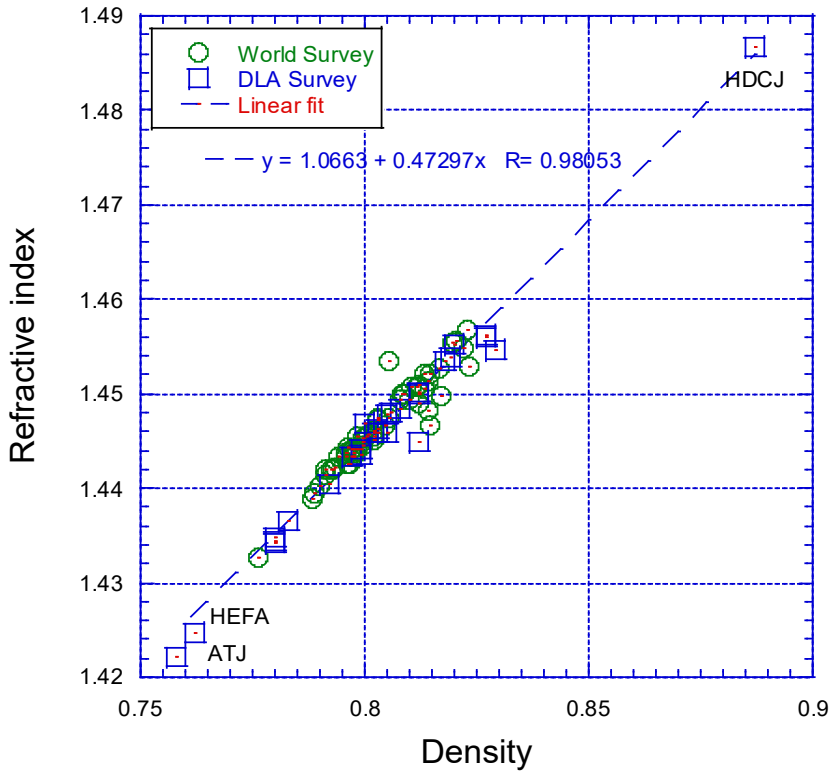

Figure 18 – Relationship between refractive index (20 ℃) and density (15 ℃)[2,37]

4.1 TriPOL Density Re-Evaluation

At the request of the Navy, ASTM D7042 measurements of density as a function of temperature were performed by AFRL/UDRI on the DoD Survey fuels in 2019. There was concern that the slope of the density-versus-temperature line had shifted over time in the various CRC Handbooks and other data sources. This data (along with dielectric constant-versus-density data) is used in most fuel gauging systems. The 2019 DoD data was compared to CRC Handbook data from 1983, 2004, and 2016, as well as the 2006 CRC World Fuel Survey and the ARINC Report 611 data (fuel gauging reference world-wide data set). It was found that the slope of the density vs temperature line in the DoD World Survey was very consistent with the CRC Word Fuel Survey and the ARINC 611 survey (roughly 1% difference). However, all of the survey data were NOT consistent with CRC Handbook data. For example, the slope of the density-temperature line in the 2016 CRC Handbook is ~10% greater than the various surveys. It is recommended that the CRC Handbook density-temperature data NOT be used in DoD aircraft designs or assessments.

4.2 DoD World Survey Measurements

As of this writing, DoD Survey data is available on 68 fuels from -40 °C to +40 °C (data taken at -40 °C, -20 °C, 0 °C, +20 °C, +40 °C). The fuels are equally divided between F-24 (CONUS) and JP-8 (OCONUS). As reference data, the current CRC Handbook (CRC Report 663, 2014) presents the following equations for density (1 kg/m^3 = 0.001 g/cm^3):

- JP-5: Density (kg/m3) = -0.8195*T [C] + 825.4
- Jet A, JP-8: Density = -0.8122*T [C] + 819.3
- Jet A-1: Density = -0.8111* T [C] + 814.1

It must be noted that the completion of DoD's conversion to commercial fuel in 2014 has rendered this fuel classification somewhat obsolete. JP-8 now is purchased as Jet A-1 OCONUS, so densities for JP-8 in the ongoing DoD Survey should match Jet A-1 densities, not Jet A. In the new data presented, the fuels would naturally be separated into F-24/Jet A and JP-8/Jet A-1.

The best way of presenting the data in a useful form is not immediately obvious. The CRC Handbook shows no data points, so the scatter in the data is not clear. In this section, the results will be presented in several ways to illustrate the results. Note that PQIS data exists also at 16 °C, so the range of densities at a given temperature can be compared to other data sets. World Survey data also exists, as well as data from earlier CRC Handbooks, such as CRC Report 635 (2004) and CRC Report 530 (1983).

First, all the CRC Handbooks and other data sources all show density to be linear with temperature over the range of -40 °C to +40 °C. This is also found to be the case in the DoD Survey fuels. Rather than show all 68 fuels on one graph (as the CRC World Survey often does), 10 F-24 fuels are shown in Figure 19. Note the high R values. Another way of assessing linearity would be to least-square fit each fuel and compare the R value. The range of R values is shown in Figure 20. Evidently, the current D7042 data confirms the linearity of the density data over this range. As it turns out, both the densest and least dense fuel in the DoD Survey are shown in Figure 19.

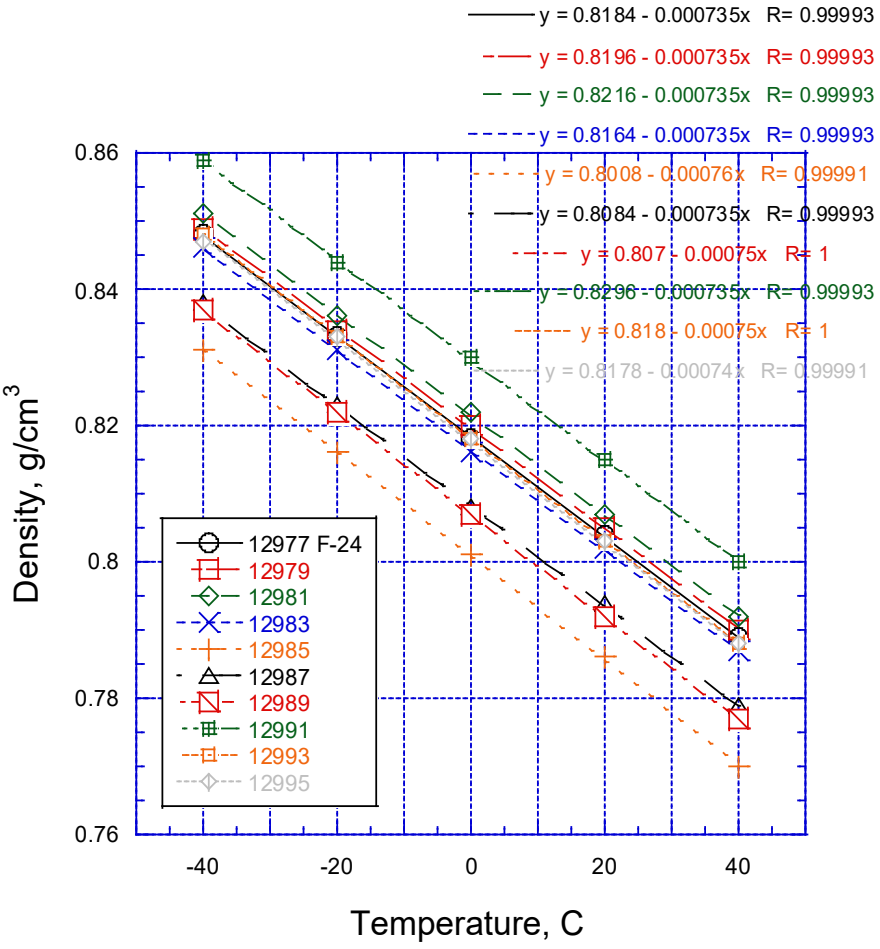

Figure 19 – Sample of DoD survey data demonstrating linearity of density-temperature relationship

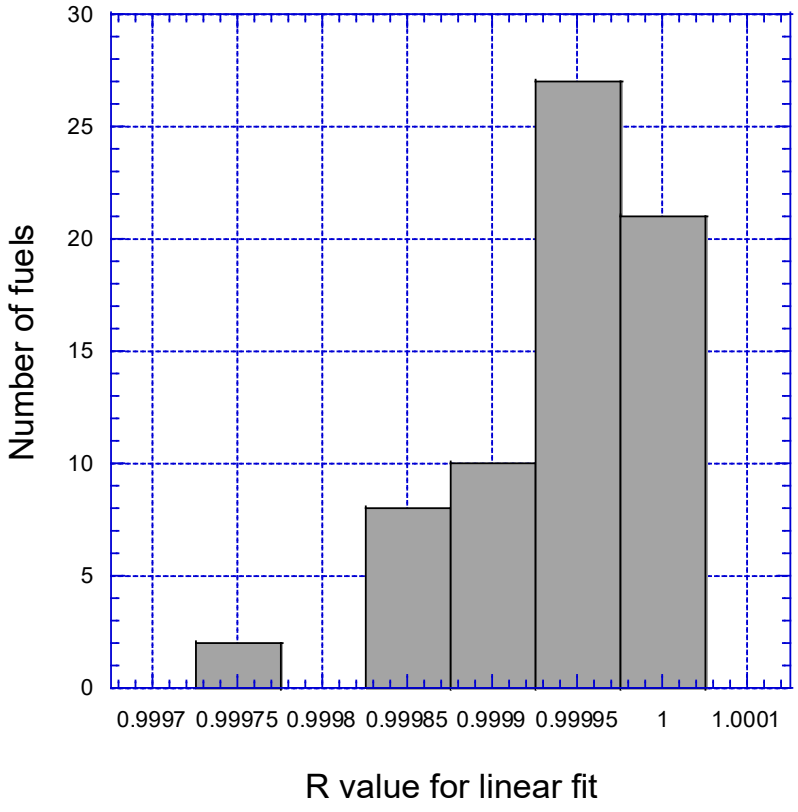

Figure 20 – Distribution of R values indicating linearity of density-temperature data from DoD survey.

Are the absolute values and the distribution of densities for this DoD survey similar to other data sets (such as PQIS)? The distribution of densities at a given temperature for this survey can be compared to that from PQIS. For example, the range of densities for F-24 from PQIS in 2016 (16 °C) is shown in Figure 21, while the F-24 data in the current survey is shown in Figure 22. The range of densities encountered is similar, as is the mean/median. Similar plots for JP-8 are shown in Figures 23 and 24. The absolute values of the JP-8 densities in 2016 PQIS are similar to those for JAA/F-24 in PQIS, which contrast with this DoD survey, where the JP-8 fuels are slightly less dense than the Jet A/F-24 fuels.

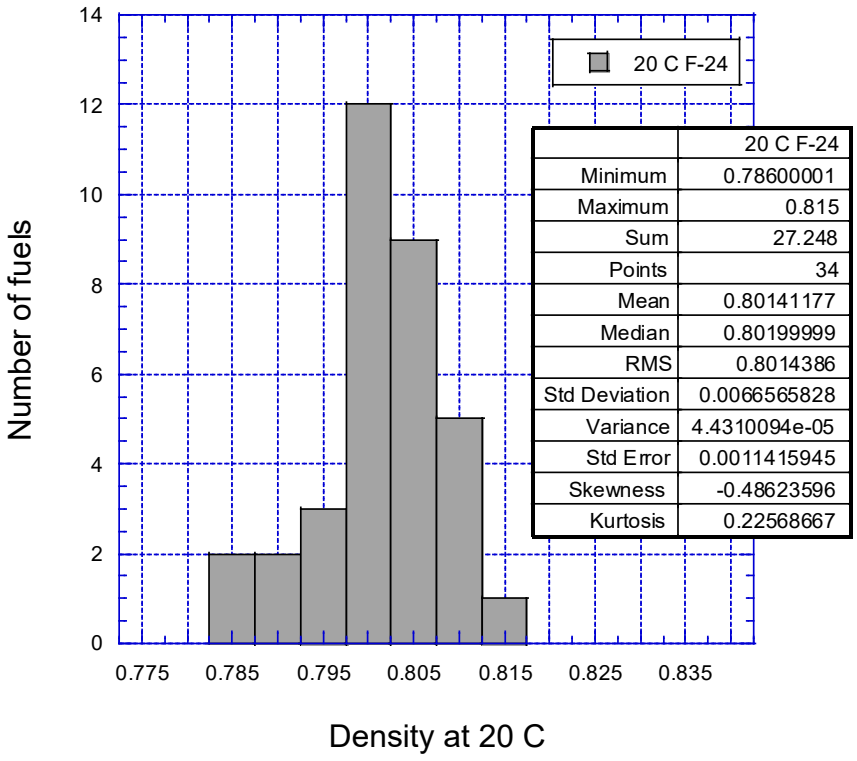

	20 C F-24
Minimum	0.78600001
Maximum	0.815
Sum	27.248
Points	34
Mean	0.80141177
Median	0.80199999
RMS	0.8014386
Std Deviation	0.0066565828
Variance	4.4310094e-05
Std Error	0.0011415945
Skewness	-0.48623596
Kurtosis	0.22568667

Figure 21 – Distribution of F-24 densities in DoD World Survey

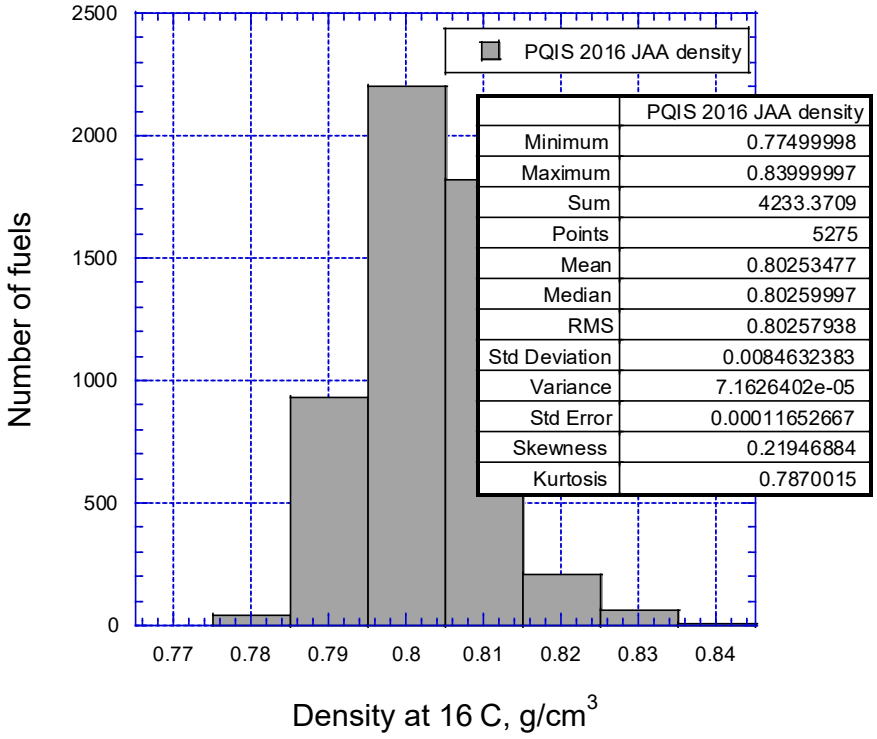

	PQIS 2016 JAA density
Minimum	0.77499998
Maximum	0.83999997
Sum	4233.3709
Points	5275
Mean	0.80253477
Median	0.80259997
RMS	0.80257938
Std Deviation	0.0084632383
Variance	7.1626402e-05
Std Error	0.00011652667
Skewness	0.21946884
Kurtosis	0.7870015

Figure 22 – Distribution of F-24 densities in 2016 PQIS (15 ℃).

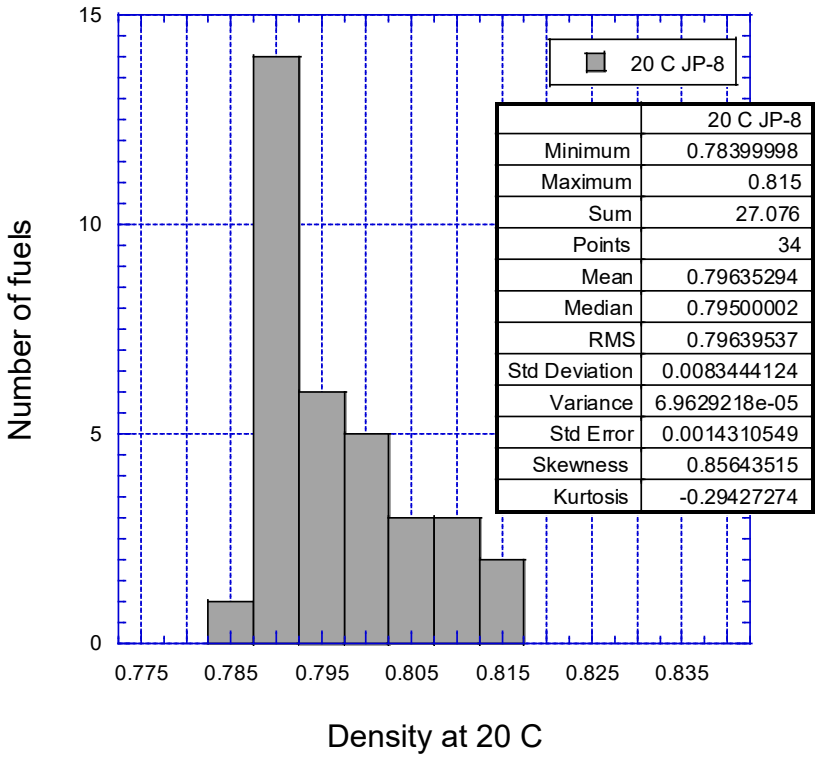

Figure 23 – Distribution of JP-8 densities in DoD World Survey

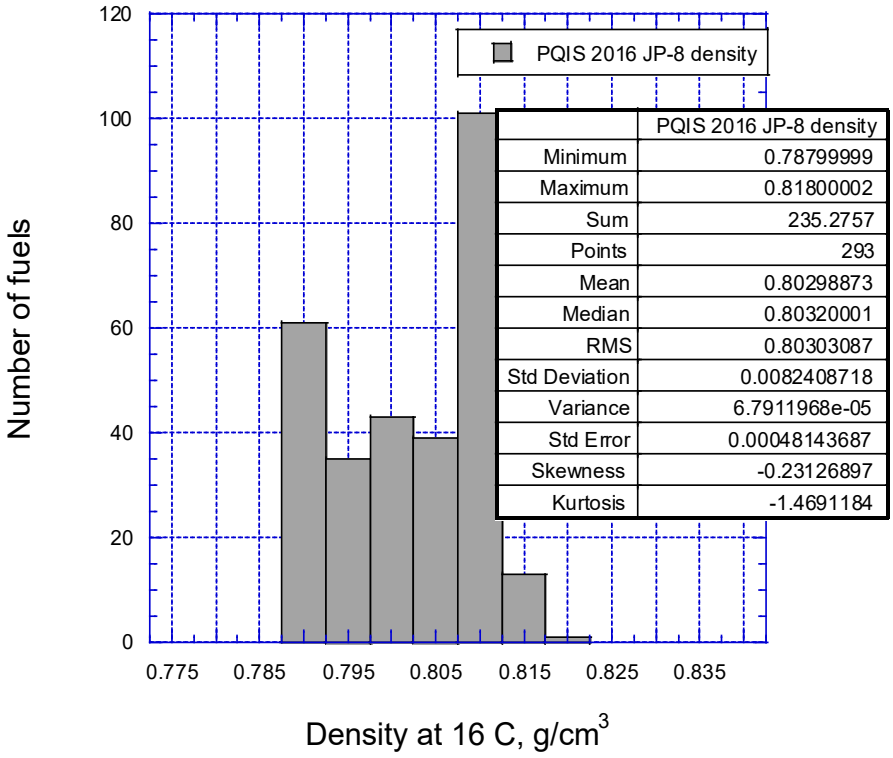

Figure 24 – Distribution of JP-8 densities in 2016 PQIS

Consistency of the data with earlier surveys is important, but the major objective of this study is the slope of the density-versus-temperature line – does the current data agree with the slope in the CRC handbook (as shown in the equations above)? At this point, fuel gauges would not be separately calibrated for F-24 or JP-8, so the slope data will be for complete data set of 68 fuels. In Figure 25, it can be seen the slopes of the 68 DoD survey density-vs-T lines are narrowly distributed around an average value of 0.744 g/cm^3 per °C. For this linear data, a similar result can be obtained by just plotting all of the density data and doing a least square fit (Figure 26). There are two other data sets that can be treated similarly – the CRC World Fuel Survey and the ARINC 611 fuel gauging data set – both are roughly 20 years old, but give very similar results to the current DoD world survey, as shown in Figures 27 and 28. This similarity of behavior is shown in Figure 29 where all three data sets are shown with best fit lines. The slopes are within roughly 1% of each other.

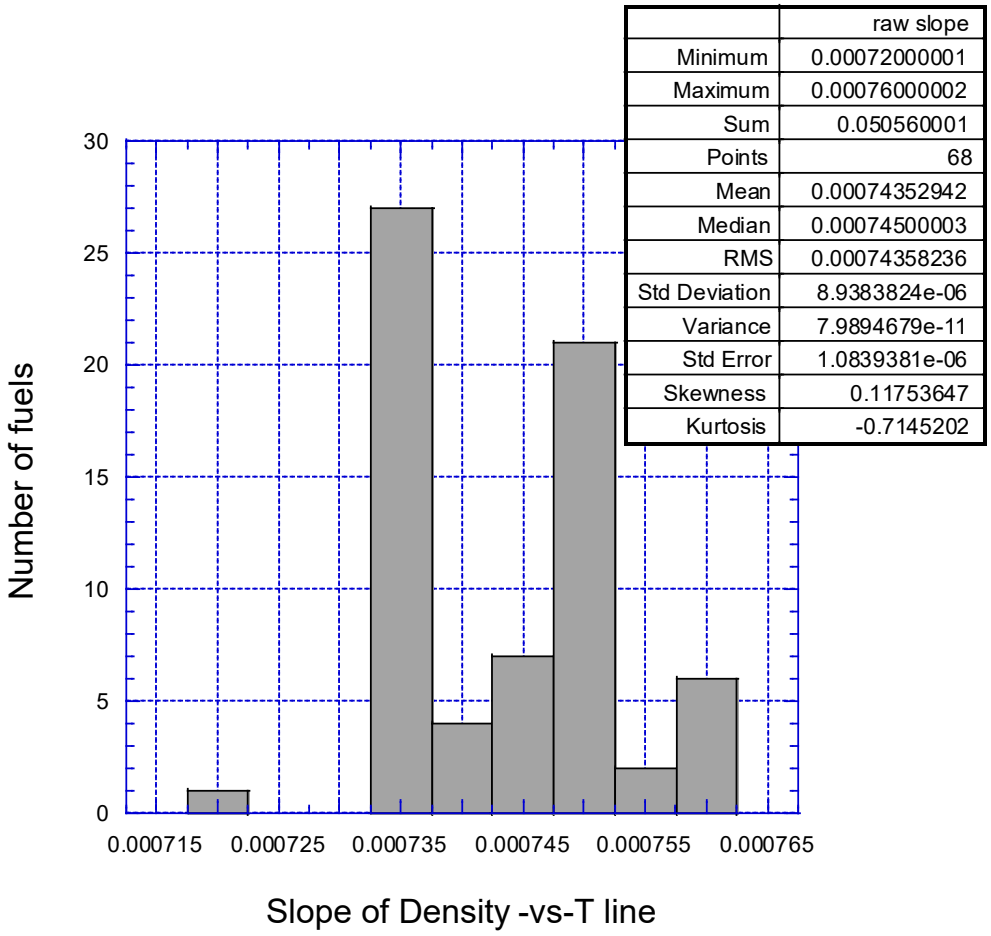

Figure 25 – Distribution of density-temperature slopes in DoD world survey

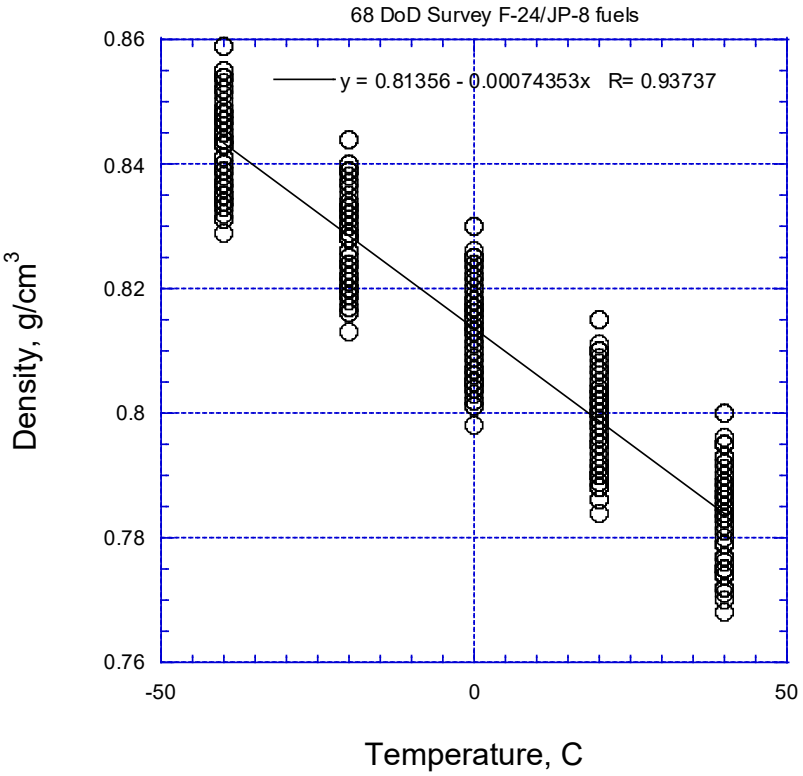

Figure 26 – Fit of all 68 fuels in DoD world survey

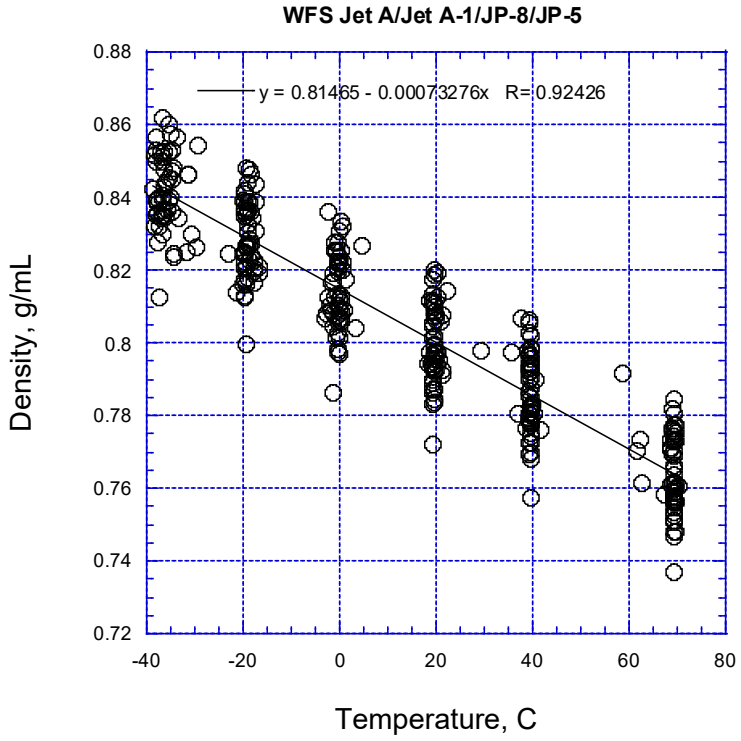

Figure 27 – CRC World Fuel Survey density-temperature data set

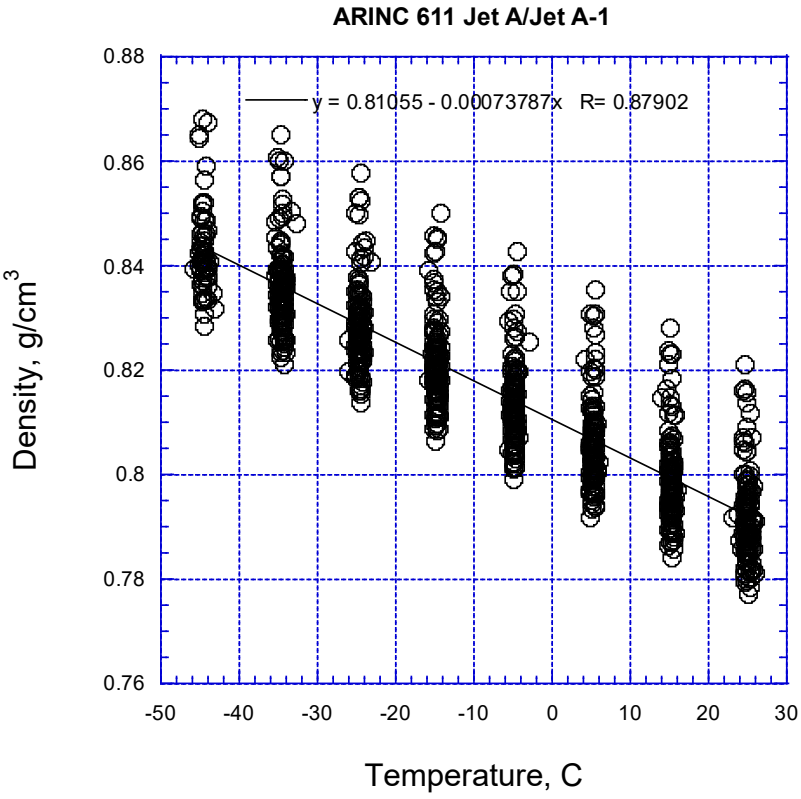

Figure 28 – ARINC 611 density-temperature data set

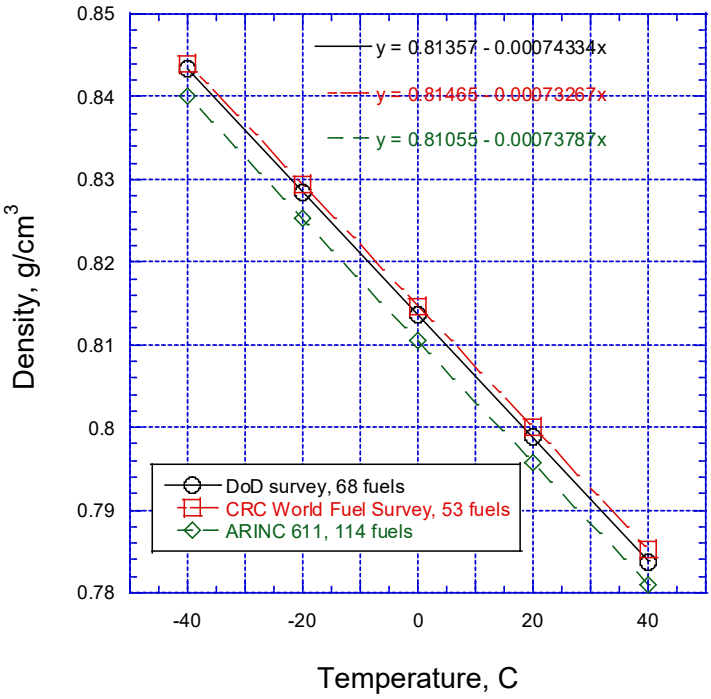

Figure 29 – Comparison of various world surveys

However, when compared to various CRC Handbook lines, a noticeable discrepancy is seen. As shown in Figure 30, the most recent CRC handbook density-temperature relationship has a slope that is roughly 10% greater than the current DoD and older CRC World Survey data. The older CRC Handbook data also differs from the various world surveys, but with a lower slope than the surveys. A drawback of the CRC Handbook is that the source of the data is not well-described – so the source of this apparently incorrect data is not known. It is recommended that the current CRC Handbook density-temperature data NOT be used in DoD aircraft designs or assessments. It is the author's understanding that Airbus and Boeing and their suppliers use the CRC and ARINC 611 survey data in design and assessment of commercial aircraft fuel gauging systems – not the CRC Handbook relationships.

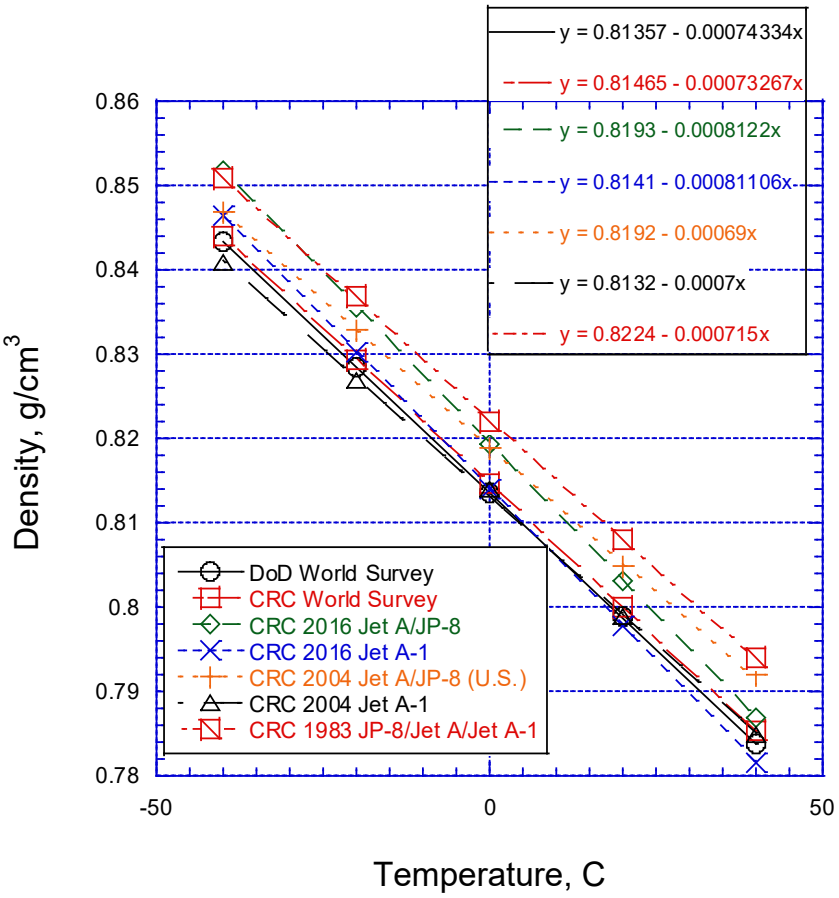

Figure 30 – Comparison of various density-temperature lines

4.3 Alternative fuels

The density of various alternative fuels is shown in Table 10. In Research Reports, the density as a function of temperature is usually included for alternative fuel blends[16]. However, it closely resembles Figure 14, so this data is not particularly interesting and is not included in this report. NIST has published density data on a number of alternative fuels and published parameters for density equations[72,73,74,75,79].

Table 10 – Density of selected alternative fuels

Fuel	Companies	POSF*	Density, 16 C (g/cm^3)
Synthetic Paraffinic Kerosene (SPK)	Sasol IPK	7629	0.760
	Shell SPK	5729	0.737
	Syntroleum S-8	5018	0.756
Hydroprocessed Esters and Fatty Acids (HEFA, aka HRJ)	UOP (camelina)	10301	0.762
	UOP (tallow)	10298	0.760
	Dynamic Fuels (mixed fats)	7635	0.762
SIP	Amyris/Total	n/a	0.773
IPKA	Sasol	n/a	0.782
ATJ SPK	Gevo (isobutanol)	11498	0.761
	LanzaTech (ethanol)	12756	0.762
CHJ	ARA	8455	0.803
ATJ SKA	Swedish Biofuels	12924	0.782
	Byogy	7614	0.782
Hydroprocessed Depolymerized Cellulosic Jet (HDCJ)	KiOR	9818	0.888
Hydro-deoxygenated Synthetic Kerosene (HDO SK)	Virent/Shell	8535	0.812
SAK	Virent/Shell	n/a	0.814

*n/a = data from Research Report, other data is USAF data

4.4 Density estimation

Density can be predicted from GCxGC compositional data (discussed in next section), e.g., References 35 and 25. Since density is typically measured for most fuels sold commercially and is a relatively simple measurement, this calculation capability is of questionable value. What IS interesting is observing the density of the various classes of hydrocarbons, as shown in Figure 31, using data from reference 35 (plot is not in Reference 35). The explanation for the low density of the paraffinic alternative fuels is apparent. For estimating density as a function of temperature, one could also just curve fit existing data. For example fitting the data for A-2 yields density (kg/m^3) = 1018.26 – 0.714617*T (K)[36]. Parameters for the Rackett and Tait equations are given by NIST in various papers (e.g., Reference 79).

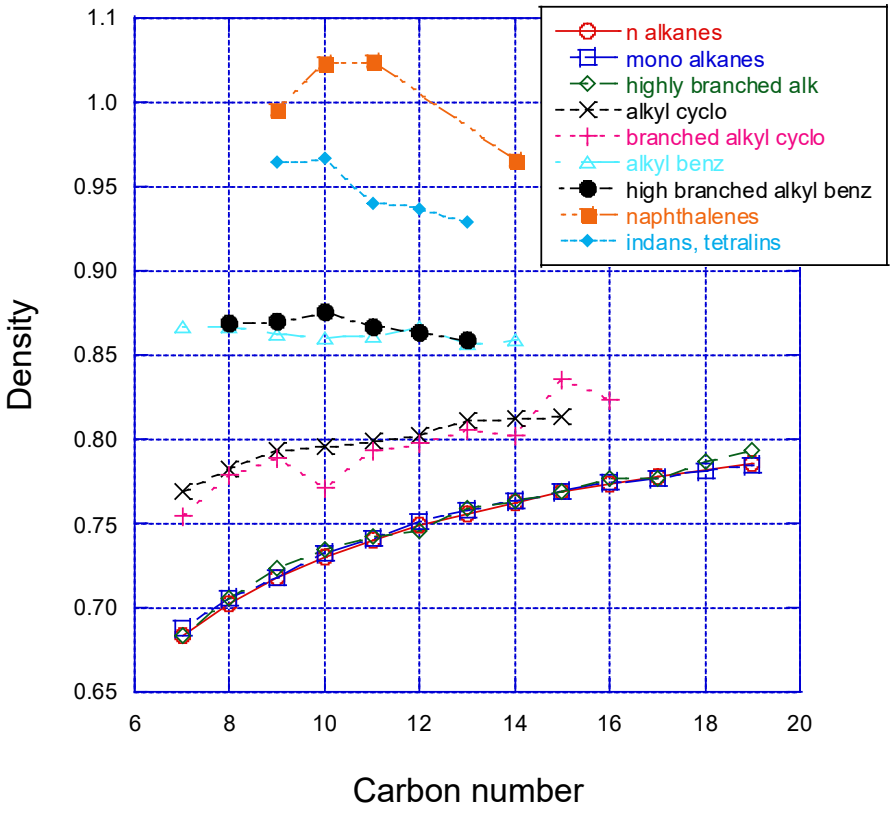

Figure 31 – Density data for various hydrocarbons from Reference 35

5. BULK HYDROCARBON COMPOSITION, MOLECULAR WEIGHT

5.1 Hydrocarbon Composition

Various chromatographic techniques have been used to assess the hydrocarbon composition of jet fuels in various programs over the past several decades. On the simplest level, on can compare the GC-MS trace of fuels to roughly compare molecular weight distributions of various fuels. Figure 32 is an example from the ATJ SPK Research Report. Other than a rough comparison of molecular distribution (and identification of the n-paraffins), this technique has shortcomings in identifying chemical class breakdown since many of the fuel peaks are not well-resolved and/or identified. But organizations are still using this approach to characterize fuels[38]. The limitations of GC-MS analysis led to the use of ASTM D2789 (reported in Reference 34) and ASTM D2425 (Standard Test Method for Hydrocarbon Types in Middle Distillates by Mass Spectrometry)[40] to characterize fuels during the early part of the alternative fuel program to assess the hydrocarbon class breakdown of fuels into paraffins (n- plus iso-), cycloparaffins, and aromatics. D2789 was not reliable for jet fuels, at least for total aromatic content. It was also discovered that D2425 had shortcomings in differentiating highly-branched iso-paraffins from cycloparaffins, so multi-dimensional GCxGC was developed for the jet fuel application[41,42]. This GCxGC data has the additional advantage over D2425 of showing the distribution over carbon number of the various hydrocarbon classes. As an example of the type of data available from GCxGC, Figure 33 shows the mean of the World Survey distribution of the various hydrocarbon classes. Data for the reference fuels is shown in Table 11. Hydrogen content can also be estimated from this data (see also[47]).

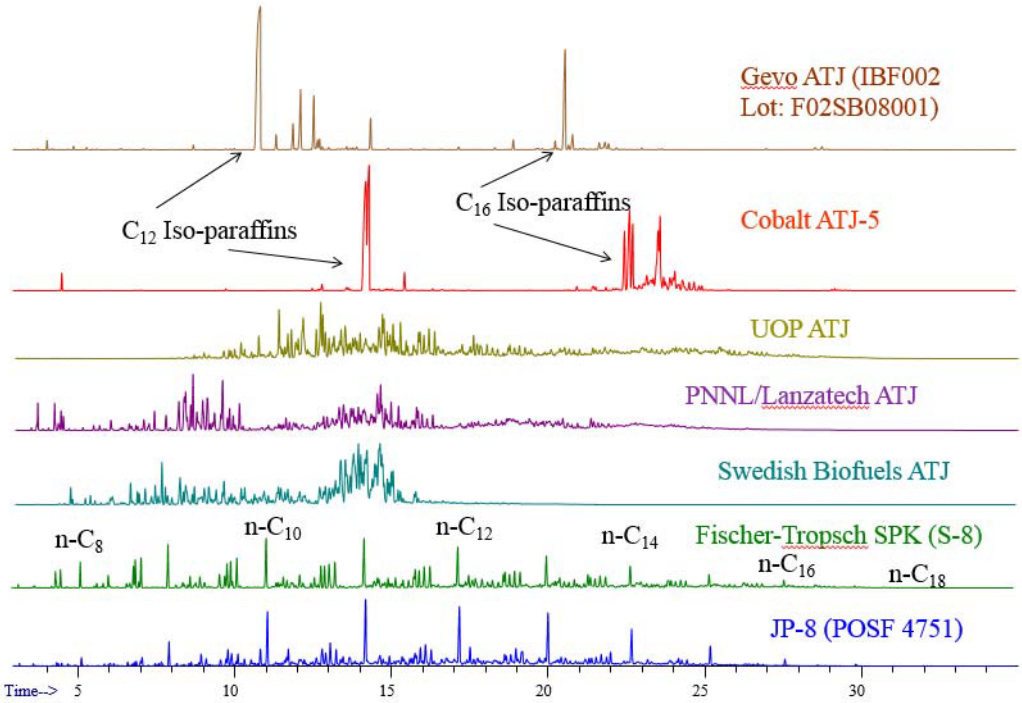

Figure 32 – Gas chromatograms of various alternative fuels

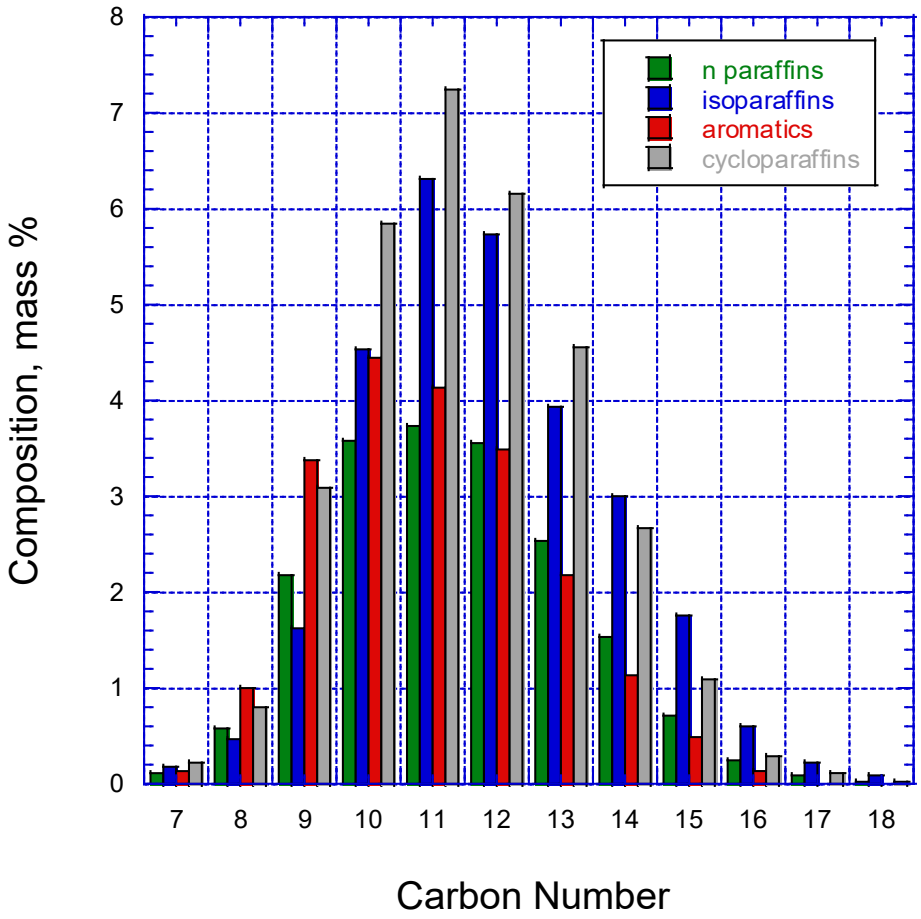

Figure 33 – GCxGC data averaged across World Fuel Survey

Table 11 – GCxGC composition data for reference fuels.

Hydrogen content (weight %)	14.4		14.0		13.7		
Average Molecular Wt (g/mole)	152		159		166		World Fuel Survey average
	A-1 POSF-10264 JP-8		A-2 POSF-10325 Jet A		A-3 POSF-10289 JP-5		
	Weight %	Volume %	Weight %	Volume %	Weight %	Volume %	Weight %
Aromatics							
Alkylbenzenes							
benzene (C06)	0.01	0.01	0.01	0.01	<0.01	<0.01	0.14
toluene (C07)	0.23	0.21	0.16	0.14	0.03	0.02	1.00
C2-benzene (C08)	1.98	1.77	1.10	1.00	0.41	0.38	3.27
C3-benzene (C09)	4.17	3.73	2.97	2.73	1.32	1.24	3.56
C4-benzene (C10)	2.33	2.09	3.32	3.05	2.09	1.97	2.36
C5-benzene (C11)	1.19	1.07	2.22	2.03	1.98	1.86	1.55
C6-benzene (C12)	0.66	0.59	1.45	1.33	1.80	1.70	0.84
C7-benzene (C13)	0.25	0.22	0.73	0.67	1.24	1.16	0.54
C8-benzene (C14)	0.12	0.11	0.52	0.48	1.05	0.99	0.27
C9-benzene (C15)	0.06	0.05	0.28	0.25	0.39	0.37	0.12
C10+-benzene (C16+)	<0.01	<0.01	0.15	0.14	0.03	0.03	<0.01
Total Alkylbenzenes	**11.00**	9.85	**12.90**	11.84	**10.33**	9.72	**13.65**
Diaromatics (Naphthalenes, Biphenyls, etc.)							
diaromatic-C10	0.10	0.08	0.22	0.17	0.09	0.07	0.20
diaromatic-C11	0.33	0.25	0.66	0.51	0.33	0.26	0.55
diaromatic-C12	0.41	0.32	0.86	0.68	0.60	0.48	0.66
diaromatic-C13	0.18	0.14	0.43	0.34	0.29	0.24	0.31
diaromatic-C14+	0.04	0.03	0.17	0.14	0.04	0.03	0.15
Total Alkylnaphthalenes	**1.06**	0.82	**2.34**	1.84	**1.34**	1.09	**1.88**
Cycloaromatics (Indans, Tetralins,etc.)							
cycloaromatic-C09	0.02	0.02	0.02	0.02	0.03	0.03	0.12
cycloaromatic-C10	0.19	0.15	0.26	0.21	0.57	0.48	0.68
cycloaromatic-C11	0.37	0.30	0.66	0.56	1.91	1.66	1.22
cycloaromatic-C12	0.38	0.32	0.89	0.76	2.67	2.34	1.28
cycloaromatic-C13	0.34	0.29	0.85	0.73	2.27	2.01	1.04
cycloaromatic-C14	0.16	0.14	0.44	0.38	1.08	0.96	0.44
cycloaromatics-C15+	0.03	0.02	0.17	0.15	0.14	0.12	0.21
Total Cycloaromatics	**1.49**	1.24	**3.29**	2.81	**8.69**	7.60	**4.98**
Total Aromatics	**13.56**	**11.91**	**18.53**	**16.49**	**20.36**	**18.41**	**20.51**
Paraffins							
iso-Paraffins							
C07 & lower -isoparaffins	0.21	0.24	0.15	0.18	0.02	0.02	0.17
C08-isoparaffins	0.88	0.97	0.44	0.50	0.13	0.15	0.46
C09-isoparaffins	2.59	2.80	1.05	1.17	0.48	0.54	1.63
C10-isoparaffins	8.15	8.67	4.20	4.57	1.66	1.85	4.55
C11-isoparaffins	8.38	8.73	5.70	6.08	2.73	2.98	6.32
C12-isoparaffins	5.41	5.64	5.63	6.02	3.36	3.67	5.73
C13-isoparaffins	4.63	4.73	4.22	4.41	3.57	3.82	3.92
C14-isoparaffins	3.96	4.00	4.20	4.35	3.54	3.76	3.01
C15-isoparaffins	2.28	2.30	2.51	2.59	2.70	2.85	1.76
C16-isoparaffins	0.75	0.75	1.00	1.03	0.65	0.68	0.59
C17-isoparaffins	0.20	0.20	0.39	0.40	0.08	0.09	0.22
C18-isoparaffins	0.03	0.03	0.11	0.11	<0.01	<0.01	0.09
C19-isoparaffins	<0.01	<0.01	0.03	0.03	<0.01	<0.01	<0.01
C20-isoparaffins	<0.01	<0.01	0.03	0.03	<0.01	<0.01	<0.01
C21-isoparaffins	<0.01	<0.01	<0.01	<0.01	<0.01	<0.01	<0.01
C22-isoparaffins	<0.01	<0.01	<0.01	<0.01	<0.01	<0.01	<0.01
C23-isoparaffins	<0.01	<0.01	<0.01	<0.01	<0.01	<0.01	<0.01
C24-isoparaffins	<0.01	<0.01	<0.01	<0.01	<0.01	<0.01	<0.01
Total iso-Paraffins	**37.48**	39.07	**29.69**	31.46	**18.91**	20.42	**28.45**

	A-1 POSF 10264		A-2 POSF 10325		A-3 POSF 10289		WFS avg
n-Paraffins							
n-C07 & lower	0.24	0.27	0.17	0.20	0.02	0.02	0.11
n-C08	1.11	1.22	0.54	0.61	0.19	0.22	0.58
n-C09	2.97	3.20	1.42	1.57	0.64	0.72	2.17
n-C10	6.46	6.84	3.26	3.53	1.41	1.57	3.57
n-C11	5.22	5.44	4.29	4.58	2.60	2.85	3.73
n-C12	3.99	4.11	3.74	3.94	3.09	3.33	3.55
n-C13	2.97	3.03	2.80	2.93	2.50	2.68	2.53
n-C14	1.97	1.99	2.02	2.09	1.92	2.04	1.53
n-C15	0.83	0.83	1.03	1.06	0.86	0.90	0.71
n-C16	0.23	0.23	0.43	0.44	0.11	0.12	0.24
n-C17	0.06	0.06	0.21	0.22	0.01	0.01	0.09
n-C18	<0.01	<0.01	0.05	0.05	<0.01	<0.01	0.02
n-C19	<0.01	<0.01	0.01	0.01	<0.01	<0.01	<0.01
n-C20	<0.01	<0.01	<0.01	<0.01	<0.01	<0.01	<0.01
n-C21	<0.01	<0.01	<0.01	<0.01	<0.01	<0.01	<0.01
n-C22	<0.01	<0.01	<0.01	<0.01	<0.01	<0.01	<0.01
n-C23	<0.01	<0.01	<0.01	<0.01	<0.01	<0.01	<0.01
Total n-Paraffins	**26.05**	27.23	**19.98**	21.23	**13.35**	14.47	**18.84**
Cycloparaffins							
Monocycloparaffins							
C07 & lower monocycloparaffins	0.51	0.51	0.36	0.37	0.08	0.08	0.23
C08-monocyclocycloparaffins	1.01	0.99	0.78	0.78	0.35	0.36	0.77
C09-monocyclocycloparaffins	3.06	2.98	2.30	2.29	1.53	1.57	2.46
C10-monocyclocycloparaffins	4.47	4.22	4.11	3.97	3.25	3.22	4.69
C11-monocyclocycloparaffins	3.55	3.44	5.43	5.38	5.77	5.86	5.30
C12-monocyclocycloparaffins	2.45	2.36	3.73	3.68	6.25	6.32	4.39
C13-monocyclocycloparaffins	2.25	2.15	4.19	4.09	6.11	6.11	3.12
C14-monocyclocycloparaffins	1.19	1.14	2.19	2.14	4.22	4.24	1.82
C15-monocyclocycloparaffins	0.77	0.74	1.33	1.29	2.27	2.27	0.90
C16-monocyclocycloparaffins	0.11	0.10	0.42	0.41	0.41	0.41	0.27
C17-monocyclocycloparaffins	0.02	0.02	0.18	0.18	0.01	0.01	0.10
C18-monocyclocycloparaffins	<0.01	<0.01	0.04	0.04	<0.01	<0.01	0.02
C19+-monocyclocycloparaffins	<0.01	<0.01	0.02	0.02	<0.01	<0.01	<0.01
Total Monocycloparaffins	**19.41**	18.66	**25.08**	24.64	**30.25**	30.44	**24.09**
Dicycloparaffins							
C08-dicycloparaffins	0.03	0.03	0.03	0.03	0.03	0.02	0.03
C09-dicycloparaffins	0.35	0.31	0.43	0.39	0.46	0.42	0.62
C10-dicycloparaffins	0.47	0.40	0.72	0.63	1.04	0.94	1.14
C11-dicycloparaffins	0.71	0.65	1.52	1.41	2.84	2.69	1.86
C12-dicycloparaffins	0.77	0.70	1.57	1.47	4.33	4.14	1.75
C13-dicycloparaffins	0.52	0.47	1.21	1.12	4.53	4.32	1.43
C14-dicycloparaffins	0.45	0.41	0.81	0.76	3.14	3.00	0.85
C15-dicycloparaffins	0.08	0.07	0.20	0.19	0.63	0.61	0.20
C16-dicycloparaffins	<0.01	<0.01	0.04	0.04	0.03	0.03	0.02
C17+-dicycloparaffins	<0.01	<0.01	0.02	0.02	<0.01	<0.01	0.01
Total Dicycloparaffins	**3.39**	3.05	**6.56**	6.06	**17.02**	16.17	**7.92**
Tricycloparaffins							
C10-tricycloparaffins	<0.01	<0.01	<0.01	<0.01	<0.01	<0.01	0.01
C11-tricycloparaffins	0.11	0.09	0.16	0.13	0.10	0.09	0.09
C12-tricycloparaffins	<0.01	<0.01	<0.01	<0.01	<0.01	<0.01	0.01
Total Tricycloparaffins	**0.11**	0.09	**0.16**	0.13	**0.10**	0.09	**0.11**
Total Cycloparaffins	**22.91**	21.79	**31.79**	30.83	**47.37**	46.70	**32.12**
Average Molecular Formula - C	10.8		11.4		11.9		
Average Molecular Formula - H	21.7		22.1		22.6		

There are several data sets of GCxGC data that can be used to show the variations in overall hydrocarbon classes. In Figure 34, the 54 conventional fuels in the World Survey are shown as a box plot similar to the box show in Figure 2. It can be seen that conventional fuels in the Survey (from the early 2000s) have relatively consistent amounts of n-paraffins, iso-paraffins, cycloparaffins, and aromatics. One can see that typical alternative fuels like SPK, HEFA, and ATJ SPK that are essentially entirely iso-paraffins fall well outside of experience. An ongoing DOD world-wide survey of fuels is producing GCxGC data very similar to Figure 34.

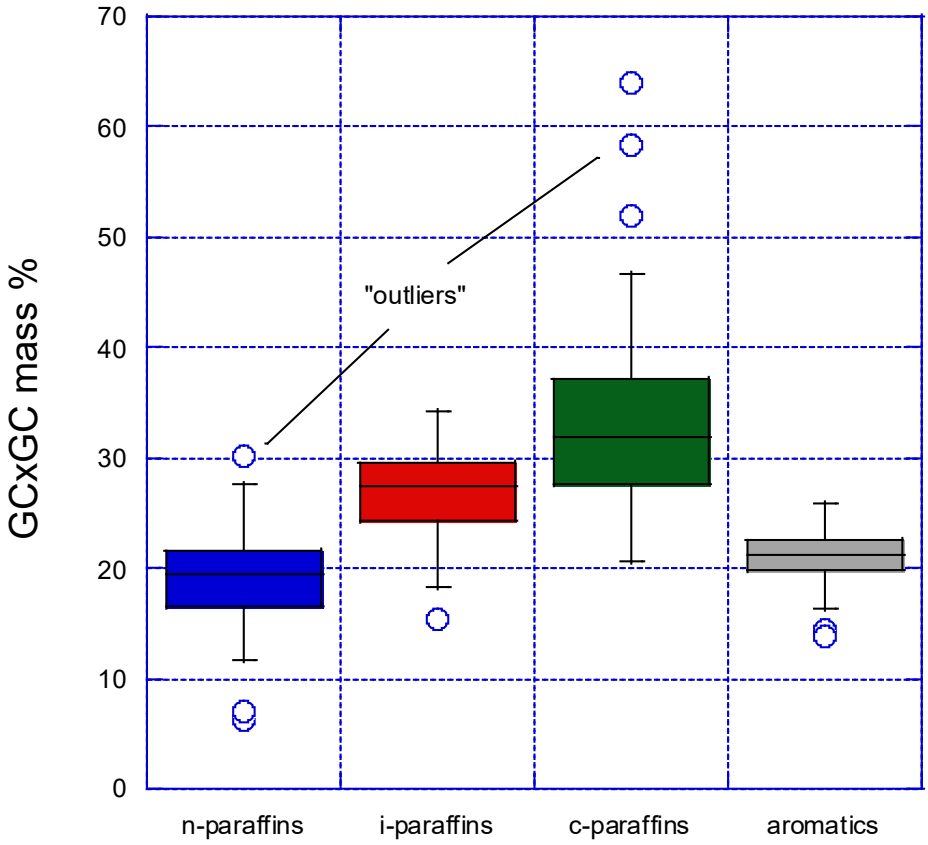

Figure 34 – World Fuel Survey distribution of hydrocarbon types via GCxGC

As shown in Table 12, GCxGC data is sufficiently detailed that it can be broken out as either mass % or volume %. This is very useful when comparing results from other test methods that might be reported out as either mass % or volume %. For example, aromatics in ASTM D1319 (Standard Test Method for Hydrocarbon Types in Liquid Petroleum Products by Fluorescent Indicator Adsorption) are reported as volume %, while D6379 (Standard Test Method for Determination of Aromatic Hydrocarbon Types in Aviation Fuels and Petroleum Distillates—High Performance Liquid Chromatography Method with Refractive Index Detection) and D5186 (Standard Test Method for Determination of the Aromatic Content and Polynuclear Aromatic Content of Diesel Fuels By Supercritical Fluid Chromatography) report out in mass % aromatics. Using total aromatics from GCxGC data from several data sets (including those with ~25 vol% aromatics), one can plot mass % versus volume % for total aromatics in jet fuel to get an accurate conversion, as shown in Figure 35. One can also further examine a given class of hydrocarbons, such as aromatics, to determine the statistics of the distribution, as shown in Figure 36. The Sasol Fully

Synthetic Jet Fuel from the World Survey is included in Figure 36 to demonstrate that the aromatics are outside of experience.

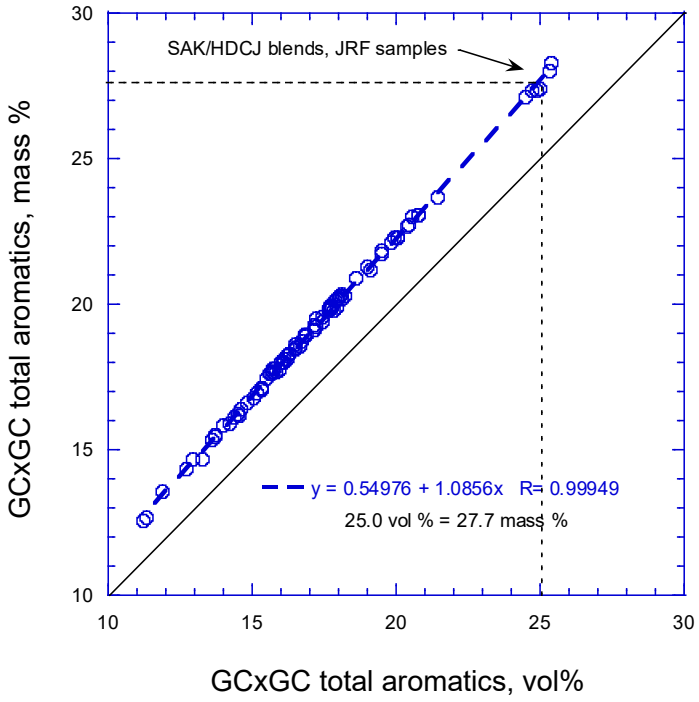

Figure 35 – GCxGC relation between mass % and vol % aromatics

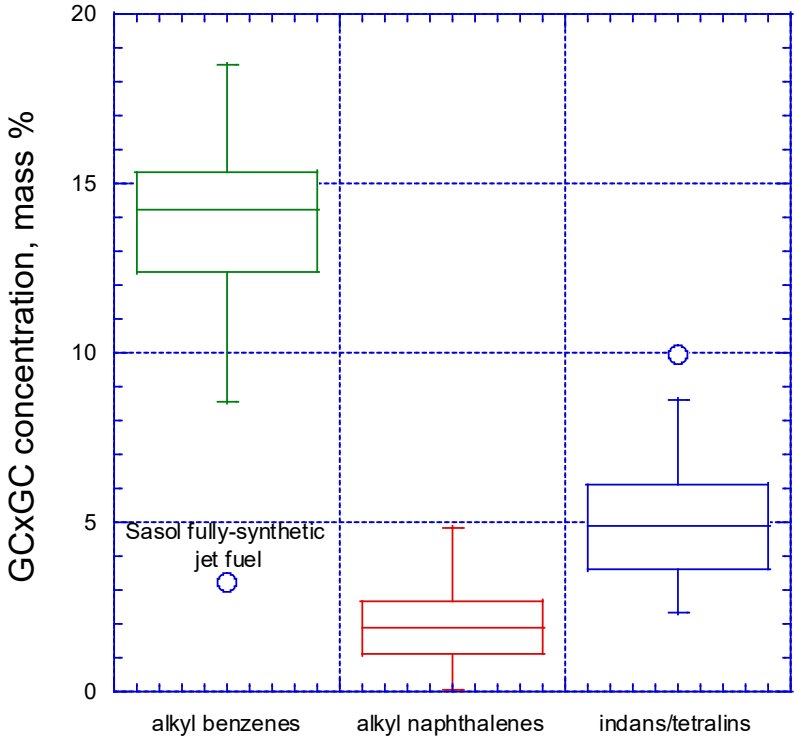

Figure 36 – GCxGC distribution of aromatic types in World Survey

5.2 Molecular weight

The equivalent molecular weight of a complex mixture can be estimated from correlations[4,5,6], GCxGC data, or direct measurements[43]. Table 12 shows GCxGC MW estimates for a variety of jet fuels, including alternative fuels.

For the average Jet A/POSF 10325, Fig 5-5 in Nelson[5] yields MW~ 160 (Maxwell's chart shown in Figure 39 yields ~160[6]); GCxGC ~ 159 (Table 12). Princeton's direct measurement yielded ~148[43]. Riazi[4] has:

$$MW = 1.6604E^{-4} \cdot T_b^{2.1962} \cdot SG^{-1.0164} \; (T_b \; in \; K)$$

which yields a MW of ~ 159. Lefebvre[68] has molecular mass = 11,280/(API)$^{1.1}$, which yields a molecular weight of ~ 172 (API gravity = 44.7 for POSF 10325).

The distribution of molecular weights from GCxGC analysis of the World Survey fuels (unpublished) is shown in Figure 37, resulting in a mean of ~156. GCxGC data can also be used to estimate an average carbon number, with the distribution shown in Figure 38. Given a mean carbon number and mean molecular weight, one can estimate an average fuel molecule from the World Survey, resulting in $C_{11.2}H_{21.5}$.

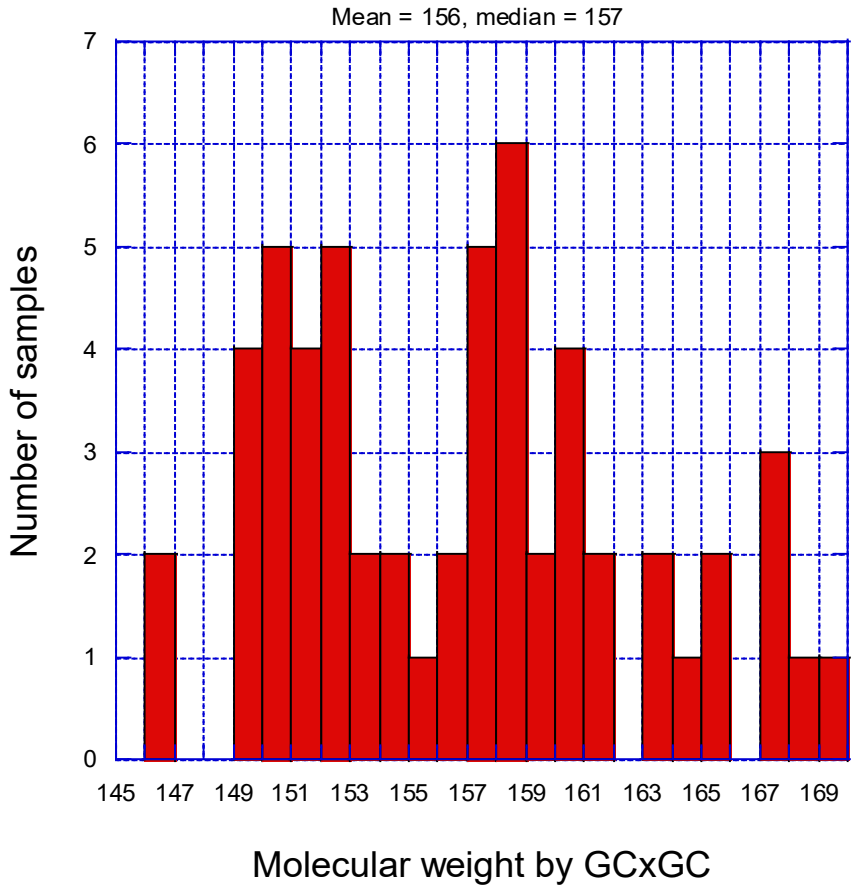

Figure 37 – GCxGC molecular weight distribution for World Survey fuels

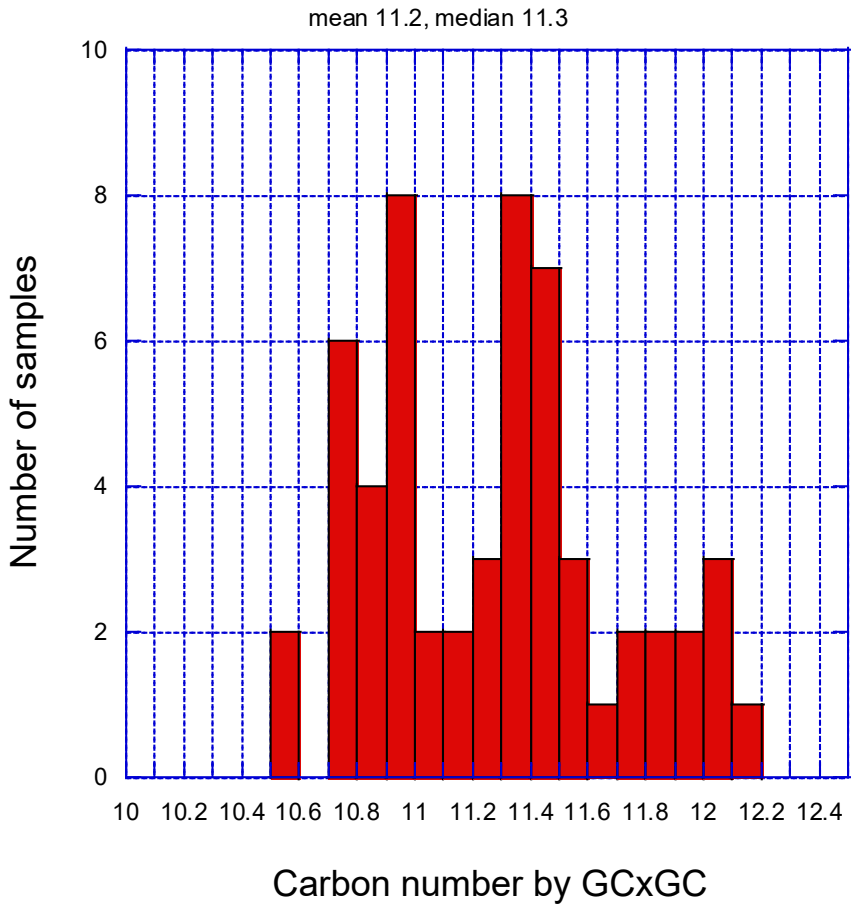

Figure 38 – GCxGC average carbon number distribution for World Survey fuels

Table 12 – Molecular weights of jet fuels using GCxGC analysis

Fuel	MW by GCxGC (g/mol)
Jet A POSF 4658	163
JP-8 POSF 6169	159
JP-8 POSF 5699	157
S-8 FT SPK, POSF 4734	166
Sasol IPK, POSF 7629	153
Shell SPK, POSF 5729	144
Tallow HEFA, POSF 6308	171
Camelina HEFA, POSF 7720	177
JP-8/SPK blend, POSF 7717	152
JP-8/IPK Blend, POSF 7718	156
JP-8/tallow HEFA blend, POSF 7719	165
JP-8/camelina HEFA blend, POSF 7721	167
Gevo ATJ, POSF 10151	177
JP-8/Gevo ATJ blend, POSF 10153	168
Jet A, POSF 10325 “A-2”	159
JP-8, POSF 10264 “A-1”	152
JP-5, POSF 10289 “A-3”	166
NJFCP C10 blend component, POSF 8296	142
NJFCP C14 blend component, POSF 9405	191
Norpar 12	162
Aromatic 100	122
Aromatic 150	136

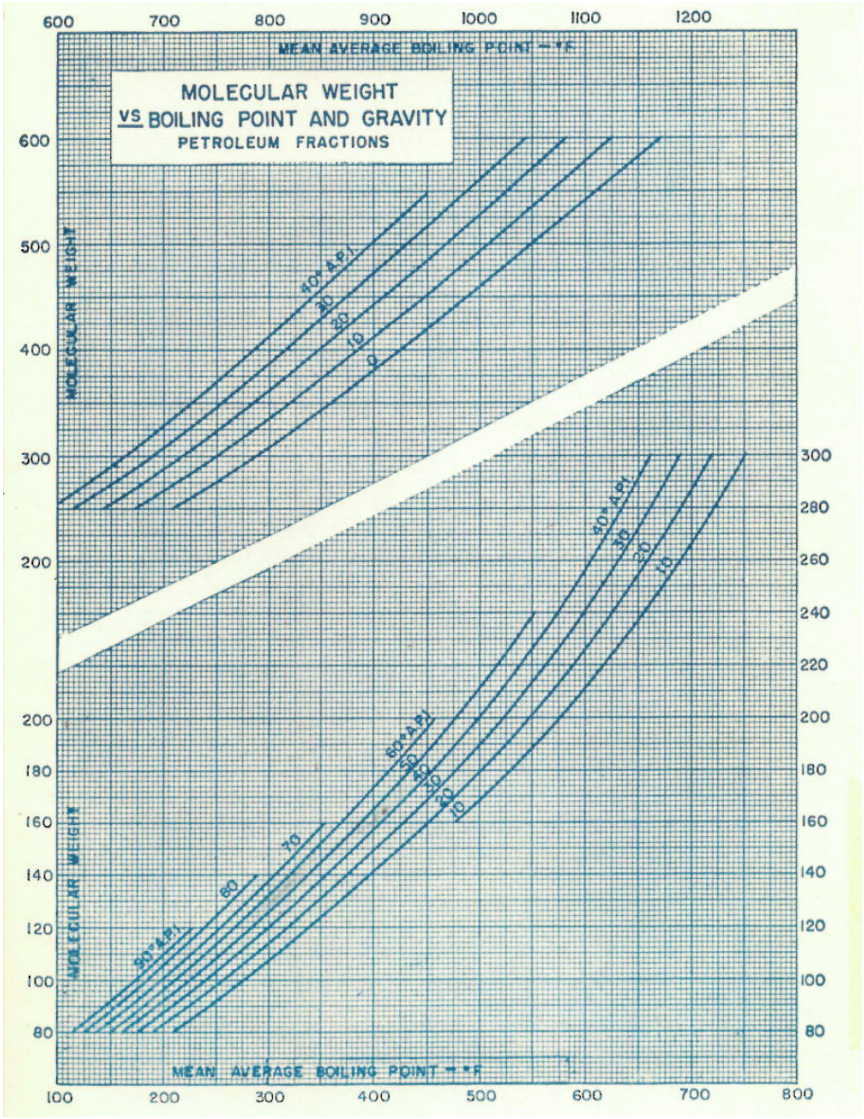

Figure 39 – Molecular weight as a function of average boiling point and density[6]

5.3 Alternative fuels

Detailed GCxGC compositional information can be found in the various Research Reports. It is interesting to compare the iso-paraffin distribution in the various approved fuels, as shown in Table 12. The SPK, HEFA, and ATJ fuels are predominantly iso-paraffinic, as can be seen by the total at the bottom of the table. The Shell SPK fuel is relatively narrow and has a high n-paraffin content (remainder of the fuel). The HEFA fuels consistently have a wider carbon number distribution. Note that several of the HEFA fuels show a peak at C16/C17, reflecting decarboxylation of the original fatty acid. The Gevo ATJ fuel is predominantly C12 and C16, due to its being built up from iso-butanol. These iso-paraffin distributions can be compared to those of conventional fuels shown in Table 11.

Table 13 – GCxGC distribution of iso-paraffins (mass %) in selected alternative jet fuels

Alternative Fuel ->	Shell SPK	Syntroleum S-8 SPK	Sasol IPK	UOP camelina HEFA	Dynamic Fuels HEFA	UOP tallow HEFA	Gevo ATJ
POSF number ->	5172	5018	7629	10301	7635	6308	8092
Carbon number							
C07 & lower	0.04	0.01	0.04	0.02	0.01		0.09
C08	0.21	1.48	0.49	1.39	1.77	2.10	0.36
C09	5.71	6.28	10.69	10.87	3.65	9.40	0.08
C10	20.9	8.29	22.07	11.67	6.69	9.69	0.18
C11	18.5	9.89	34.28	10.24	10.33	9.69	0.32
C12	9.24	10.93	21.56	8.54	12.37	9.25	79.74
C13	0.30	11.50	7.16	8.48	11.54	9.53	1.20
C14	0.05	11.16	1.72	6.41	13.98	7.84	15.99
C15	0.04	9.92	0.29	5.75	4.29	11.75	1.20
C16	0.01	5.84	0.07	10.95	20.73	12.83	
C17		0.56	0.02	11.56	0.29	5.92	
C18		0.02	0.01	0.81	3.44	0.34	
Total	55.1	75.88	98.41	86.7	89.1	88.3	99.1

5.4 Structural characterization by IR, NMR

GCxGC has some shortcomings for use in understanding/predicting jet fuel properties – primarily in that the amount of branching in iso-paraffins and side chains of aromatics/cycloparaffins is not resolved. This branching is directly related to combustion properties such as ignition delay and/or DCN. One can use spectroscopic techniques such as IR[44,45] or NMR[46] to characterize this branching, at least approximately. For example, both IR (Figure 37) and NMR (Figure 38) can enable characterization of the number of CH3 and CH2 groups in an average molecule. Highly branched iso-paraffins (low DCN) would have a higher ratio of CH3 to CH2 groups than n-paraffins (high DCN).

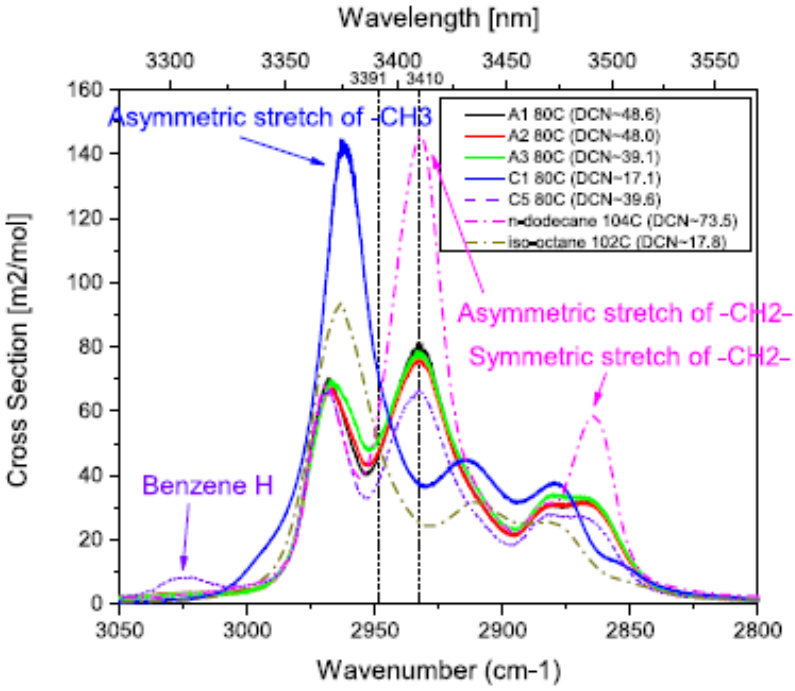

Figure 40 – Jet fuel FTIR spectra at 80 ℃[44]

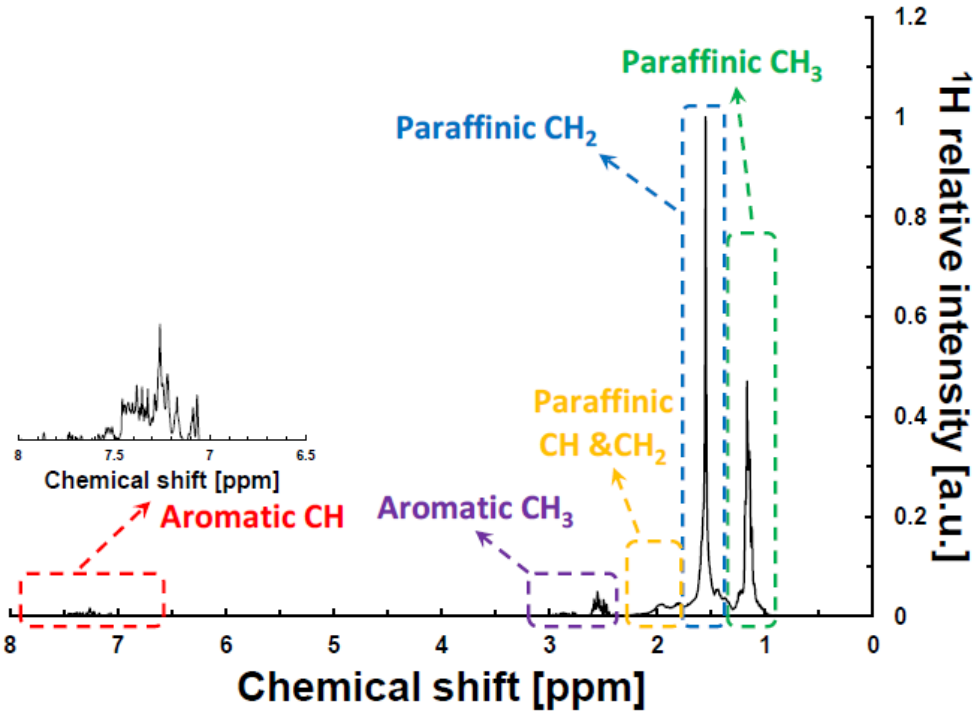

Figure 41 – Hydrocarbon ^{1}H NMR spectrum[46]

6. H CONTENT, HEAT OF COMBUSTION, HEAT OF FORMATION

6.1 H content

Jet fuels are predominantly hydrocarbons. The H/C ratio of jet fuels can be calculated from the measured hydrogen content, which is an optional specification test for most jet fuels performed using ASTM D3701 (Standard Test Method for Hydrogen Content of Aviation Turbine Fuels by Low Resolution Nuclear Magnetic Resonance Spectrometry) or ASTM D7171(Standard Test Method for Hydrogen Content of Middle Distillate Petroleum Products by Low-Resolution Pulsed Nuclear Magnetic Resonance Spectroscopy). The JP-8 specification (MIL-DTL-83133) included a 13.8 mass% minimum H content, while ASTM D1655 does not. Additionally, H content can be inferred from GCxGC composition data as presented in Section 4. ASTM D3701 H content data is included in the World Fuel Survey[2]. The distribution of H contents in the World Survey is shown in Figure 42. DLA Energy funded a survey[7] that included H content measurements (by D3701, D7171, and GCxGC) for about 25 fuels. As shown in Figures 43 and 44, there is general agreement, although the D3701 data appears to have some outliers. This data includes several alternative fuels, hence the much wider range of H contents than the World Survey. Interestingly, the agreement between D3701 and GCxGC H content does not seem to hold for the World Survey. As shown in Figure 45, the D3701 data in the World Survey seems to be biased a bit higher than the GCxGC data and is apparently unreliable. Given the correlation with heat of combustion (discussed below), it appears the World Survey D3701 data is indeed biased high (as opposed to the World Survey fuels being unusual).

The H content in mass % can be converted to molar H/C ratio:

$$H/C = \frac{12.0107(wt\%\ H)}{100.794\left(1-\left(\frac{wt\ \%\ H}{100}\right)\right)}$$

With the molecular weight (as described earlier) for C_aH_b, one can calculate the stoichiometric coefficients:

$$MW(C_aH_b) = 12.0107a + 1.008b$$

b/a is the molar H/C ratio as calculated above.

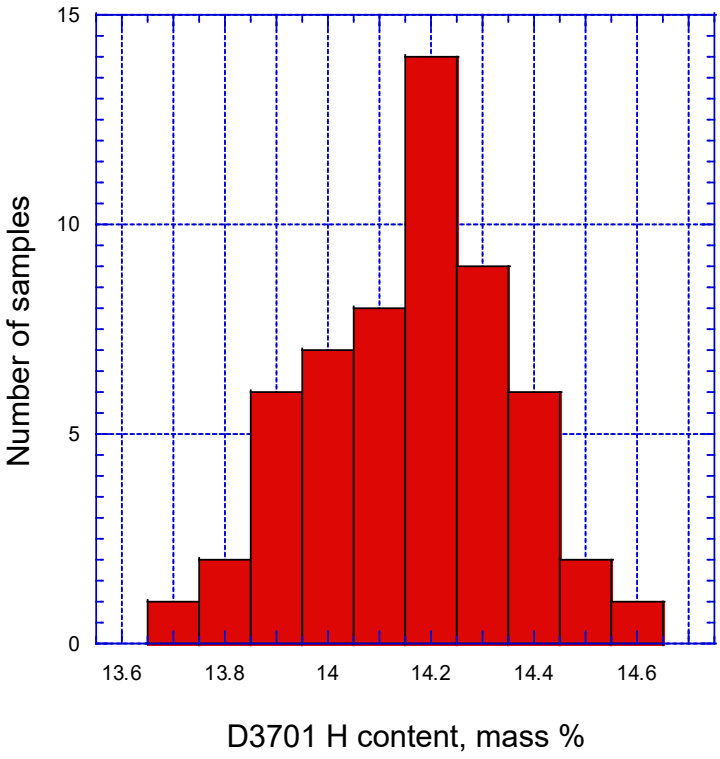

Figure 42 – World Survey H content distribution

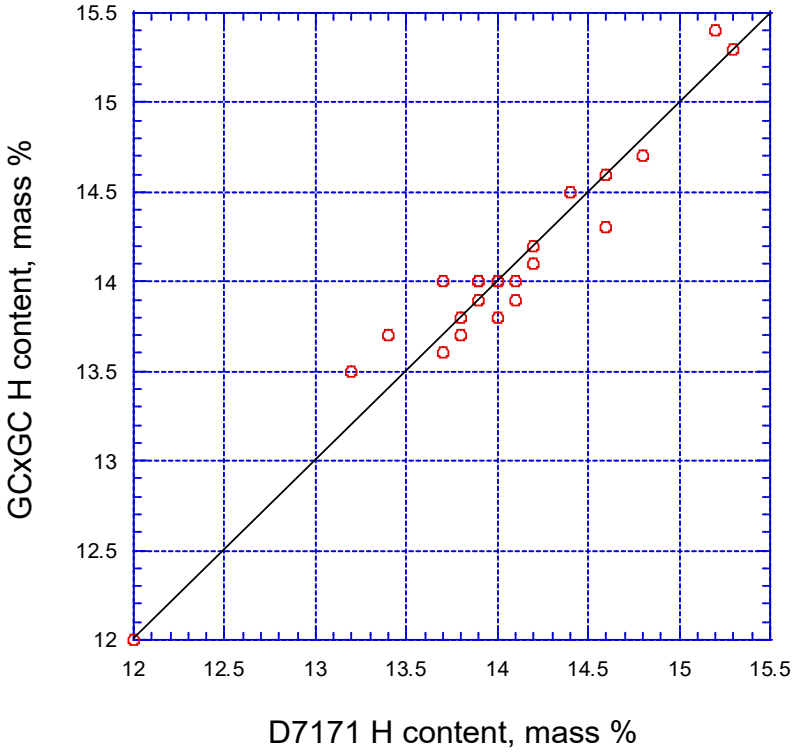

Figure 43 – Correlation of GCxGC H content and D7171 H content results from DLA Survey[7]

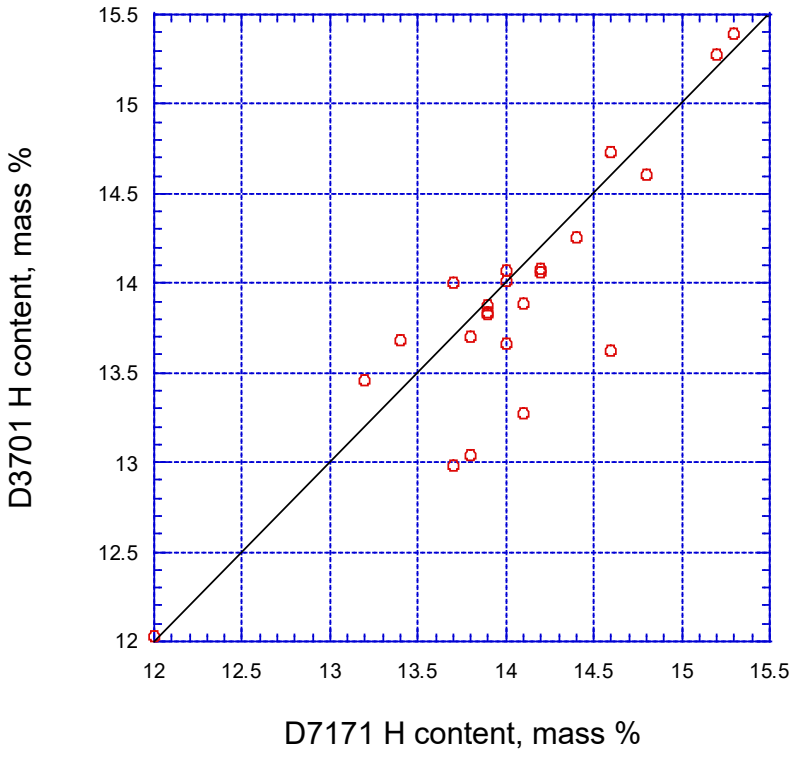

Figure 44 – Correlation of D3701 and D7171 H content results from DLA Survey[7]

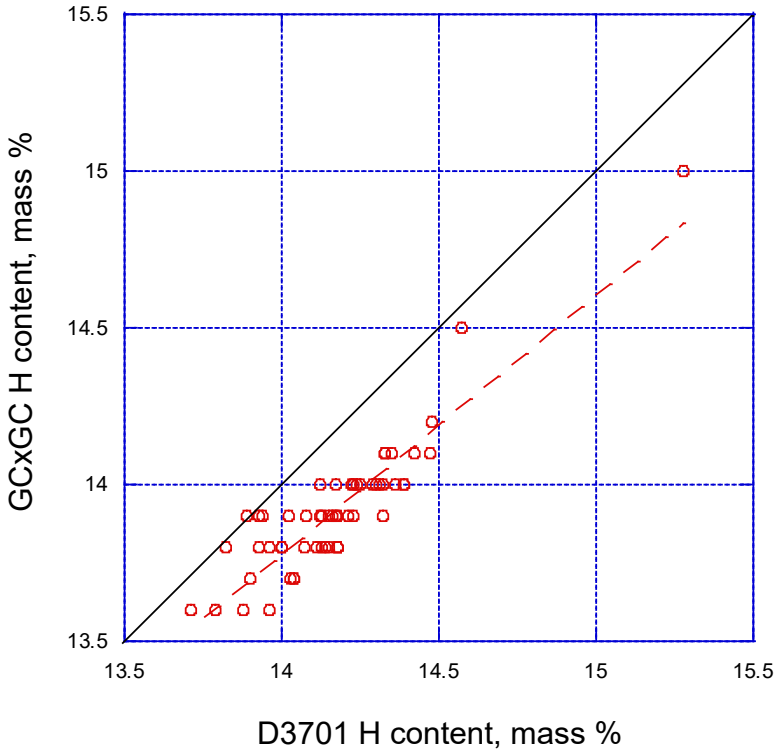

Figure 45 – Correlation of GCxGC H content and D3701 for CRC World Survey

6.2 Heat of Combustion

The net heat of combustion is a specification property and can be measured via ASTM D4809 (Standard Test Method for Heat of Combustion of Liquid Hydrocarbon Fuels by Bomb Calorimeter) or calculated via ASTM D3338 (Standard Test Method for Estimation of Net Heat of Combustion of Aviation Fuels) using the equation below (using aromatic content (***A***, volume %), volatility (***T***, boiling point or average of Test Method D86/D2887 10%, 50% and 90% points in C), and density (***D***, kg/m^3)).

$$Q_p\ (in\ MJ/kg) = \frac{5528.73 - 9264.88A + 10.1601T + 0.314169AT}{D + 0.0791707A - 0.00944893T - 0.000292178AT + 35.9936}$$

Similar to H content, there are two sets of measured heat of combustion data[2,7]. The distribution of net heat of combustion for the World Survey is shown in Figure 46. The values are fairly narrowly distributed. There are three apparent outliers. The high heat of combustion outlier is the Sasol Fully Synthetic Jet Fuel, and the high NHOC is consistent with its composition. The two fuels that are below the specification requirement (42.8 MJ/kg) are West Coast Jet A fuels that are highly cycloparaffinic and have relatively high densities. Again, the measured value is consistent the composition of these fuels. However, the net heat of combustion values for the two fuels are below the specification limit (42.8 MJ/kg).

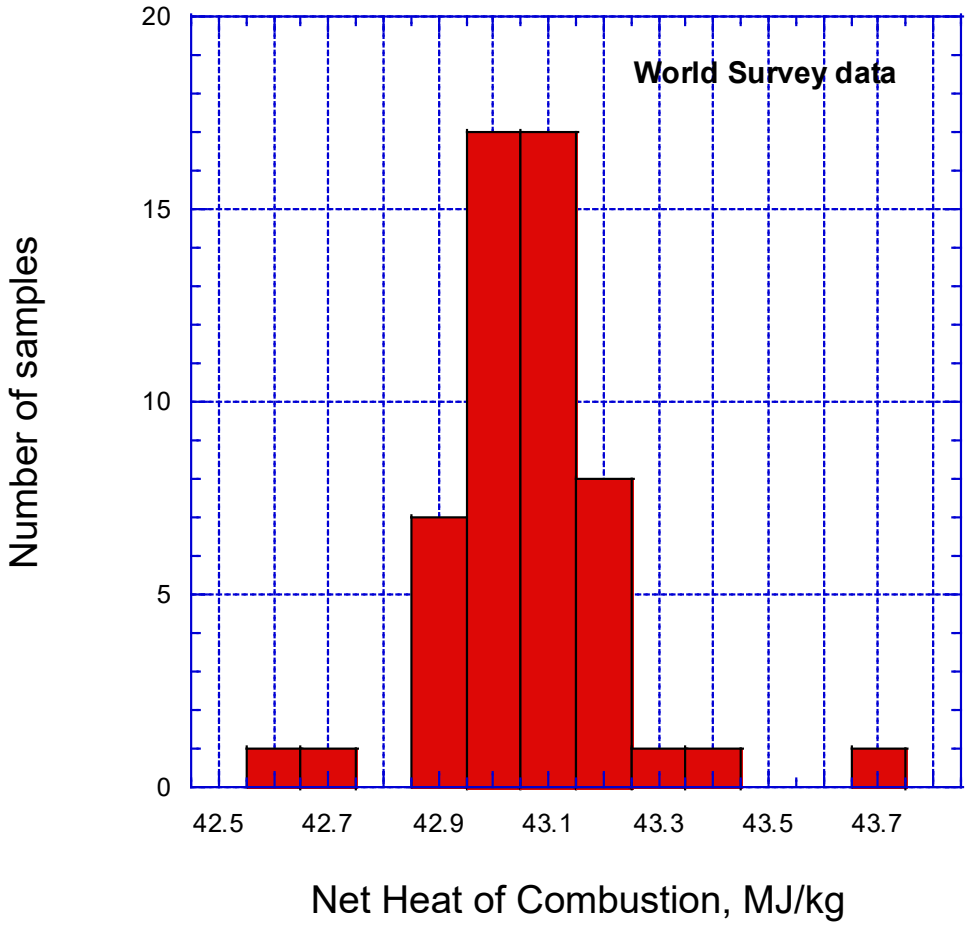

Figure 46 – Net heat of combustion (measured) from World Survey[2]

Typically, net heat of combustion correlates with fuel hydrogen content. Net heat of combustion as a function of H content is shown in Figure 47 for the World Survey data fuels[2]. Also plotted is the data from the DLA survey fuels[7], using D7171 and D3701 as the measure of H content. Interestingly, there seems to be a bias between the two benchmark data sets examined. This is apparently due to the issue of the World Survey D3701 H content being biased high, as mentioned previously. Plotting the two data sets versus GCxGC H content produces a better correlation as shown in Figure 48. This seems to confirm that the World Survey D3701 H content data is biased high.

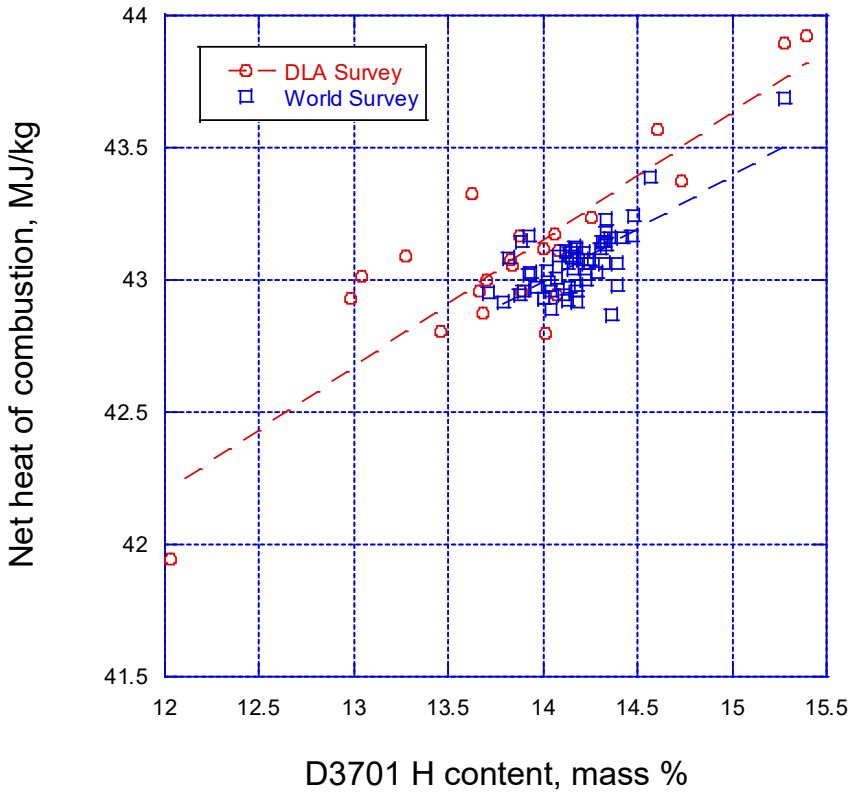

Figure 47 – Correlation of net heat of combustion with H content

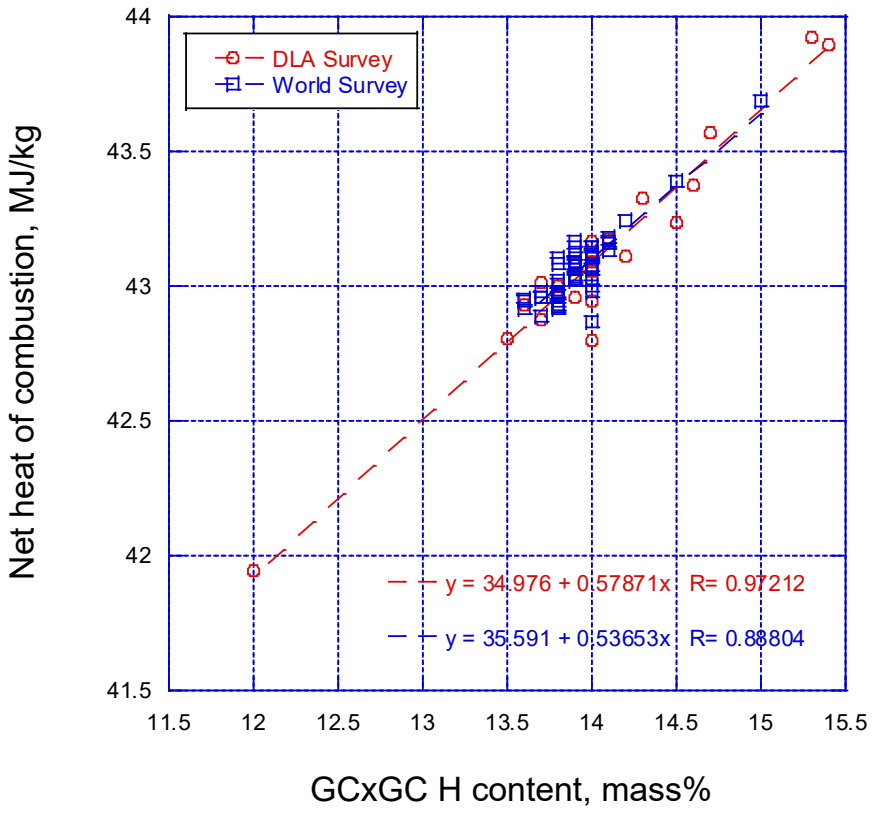

Figure 48 – Correlation of net heat of combustion with H content by GCxGC

6.3 Alternative fuels

The H content and net heat of combustion for various alternative fuels is shown in Table 14. This data is consistent with trends discussed above, as shown in Figure 49.

Table 14 – H content and net heat of combustion for alternative fuels

Fuel	Companies	POSF	H content, mass% (D7171)	NHOC, MJ/kg (D4809)
Synthetic Paraffinic Kerosene (SPK)	Sasol IPK	7629	15.7	43.9
	Shell SPK	5729	15.5	44.3
	Syntroleum S-8	5018	15.2	43.9
Hydroprocessed Esters and Fatty Acids (HEFA, aka HRJ)	UOP (camelina)	10301	15.3	43.9
	UOP (tallow)	10298	15.4	44.0
	Dynamic Fuels (mixed fats)	7635	15.2	43.9
SIP	Amyris/Total	n/a	15.1	44.0
IPKA	Sasol	n/a	n/a	43.4
ATJ SPK	Gevo (isobutanol)	11498	15.4	43.9
	LanzaTech (ethanol)	12756	15.3	43.9
CHJ	ARA	8455	14.0	43.1
ATJ SKA	Swedish Biofuels	12924	14.4	43.4
	Byogy	7614	n/a	43.4
Hydroprocessed Depolymerized Cellulosic Jet (HDCJ)	KiOR	9818	11.8	41.6
Hydro-deoxygenated Synthetic Kerosene (HDO SK)	Virent/Shell	8535	14.4	43.0
SAK	Virent/Shell	n/a	10.2	40.7

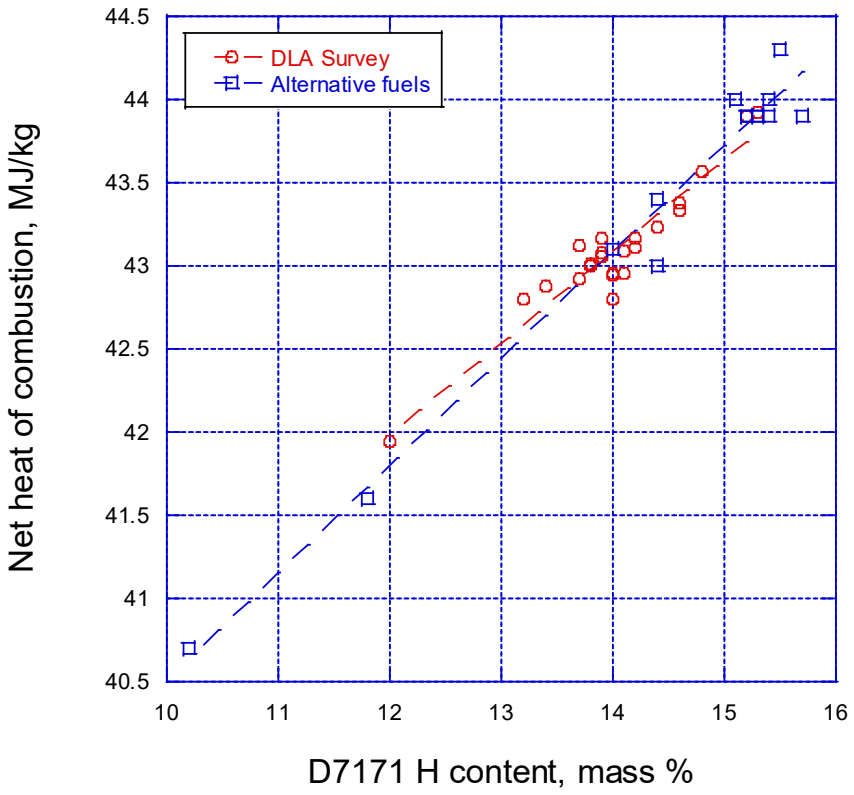

Figure 49 – correlation of H content of alternative fuels with heat of combustion (Table 14)

6.4 Estimation

Although not typically in recent Air Force use, ASTM D3343 (Standard Test Method for Estimation of Hydrogen Content of Aviation Fuels) can be used to estimate the hydrogen content of aviation fuels. The applicability of D3343 to alternative fuels is remains to be demonstrated. The calculation is done in terms of density, average boiling point, and aromatic content. Similarly (as stated above in this section), the net heat of combustion of aviation fuels can be estimated by ASTM D3338 (Standard Test Method for Estimation of Net Heat of Combustion of Aviation Fuels), although the author has little experience with that method. Similarly to D3343, in D3338 the net heat of combustion is estimated using density, aromatic content, and average boiling point. The applicability of D3338 to alternative fuels also remains to be shown.

6.5 Heat of formation

For some computer calculations, the heat of formation of various fuels is needed to calculate flame properties. As described in Reference 39, the heat of formation can be (back) calculated from the measured hydrogen content and measured heat of combustion.

$$C_aH_b + \left(a + \left(\frac{b}{4}\right)\right)O_2 \xrightarrow{yields} aCO_2 + \left(\frac{b}{2}\right)H_2O$$

$$Heat\ of\ Combustion\ \left(\frac{kcal}{mol}\right) = a(\Delta H_f CO_2) + \left(\frac{b}{2}\right)(\Delta H_f H_2O(gas)) - (\Delta H_f Fuel) - \left(a + \left(\frac{b}{4}\right)\right)(\Delta H_f O_2)$$

where the only unknown in the second equation is the heat of formation of the fuel (since b/a=H/C and the heat of formation of water and CO_2 are known). In this calculation below, the fuel H/C ratio is used to artificially define the fuel as (e.g.) $CH_{1.9818}$. This abstraction is used to initially (mis)define a mole of fuel to end up with the heat of formation in cal/g (as is typical in some calculations). Since a mole of fuel, or the fuel equivalent molecular weight, is an abstraction – typically heat of formation is reported in cal/g. However, an equivalent molecular weight by GCxGC or other means can be used to get heat of formation in terms of kcal/mol that is more realistic than defining the fuel as $CH_{1.9818}$. Such a calculation is performed in Table 15. Within the accuracies of the measured H content and heat of combustion, it appears the heat of formation of the three Category A fuels is essentially the same.

Table 15 – Heat of formation calculations

Fuel	wt% H (meas) SwRI D3701	H/C molar (calc from H content)	Mass heat of comb., MJ/kg (SwRI, meas D4809)	Mass heat of comb, kcal/g	Heat of formation (calc), cal/g	MW, GCxGC	Heat of formation, kcal/mol
A-1, POSF 10264	14.260	1.9818	43.24	-10335	-467.7	152	-71.1
A-2, POSF 10325	13.840	1.9141	43.06	-10292	-423.2	159	-67.3
A-3, POSF 10289	13.680	1.8885	42.88	-10249	-432.9	166	-71.9

1 calorie/gram = 4.184 Joules/gram = 1.8 BTU/lb

7. LOW TEMPERATURE PROPERTIES: VISCOSITY (AS F(T)), FREEZE POINT

In contrast to ground fuels, jet fuels have stringent low temperature requirements. These usually take the form of viscosity limits at temperatures of -20 °C or below and freeze point requirements. The freeze point of a multicomponent fuel like kerosene or jet fuel is not the simple solid-to-liquid phase change as a pure substance undergoes. As the temperature of jet fuel drops, paraffins begin to freeze out and the fuel becomes cloudier and more slushy, with the results that the fuel eventually will not pour and later freezes solid. This behavior has been discussed in detail in References 48, 49 and 50. There are several types of tests that are performed in this two-phase regime, such as cloud point, pour point, and freeze point. For this discussion, it is sufficient to state that the freeze point is determined by freezing the fuel solid, then gradually warming. The point where the last crystal of suspended solid (wax) disappears is the freeze point. Viscosity is probably the more critical property to control at low temperatures, but the freeze point remains in the specification also[48,49]. Currently, most jet fuel specifications have a viscosity limit of 8 cSt at -20 °C, but there is some movement toward a 12 cSt limit at -40 °C being imposed (as in ASTM D7566) to ensure adequate atomization of low temperature fuel (and adequate APU starting[57]). This 12 cSt limit at -40 °C is more stringent than the 8 cSt limit, corresponding more closely to 6.5 cSt at -20 °C. The use of additives to affect low temperature properties has been studied.[52,53,54]

Two types of viscosity can be measured. Kinematic viscosity (ν, units of mm^2/s or cSt) differs from dynamic viscosity (η, units of Pa-s, dyne-s/cm^2 [Poise], g/cm-s, or even lb/ft-h) by the density of the fuel (ρ):

$$\nu = \eta / \rho$$

The jet fuel specifications refer to kinematic viscosity, typically measured by ASTM D445 (Standard Test Method for Kinematic Viscosity of Transparent and Opaque Liquids and Calculation of Dynamic Viscosity), ASTM D2386 (Standard Test Method for Freezing Point of Aviation Fuels), or ASTM D5972 (Standard Test Method for Freezing Point of Aviation Fuels-Automatic Phase Transition Method). Viscosity is very temperature sensitive. Dynamic viscosity is often fitted as

$$\mu = Aexp(B/T)$$ [71,49]

often termed the Andrade equation. Typically, kinematic viscosity (ν) data is linearized with temperature using an ASTM D341 (Standard Practice for Viscosity-Temperature Charts for Liquid Petroleum Products)-type plot, where

$$\log[\log(\nu + 0.7)] = A - B \log T$$

In either case, viscosity increases exponentially as temperature is decreased. This ASTM linearization method for kinematic viscosity is used in the CRC Handbook[1] and has been shown to be accurate for a wide variety of fuels (including alternative fuels) and pure hydrocarbons[16]. The statistical distribution of viscosity (-20 °C) and freeze point from PQIS 2013 is shown in Figures 50 and 51, respectively.

One might expect viscosity and freeze point to be correlated, but (as shown in Figure 52), they are not as closely correlated as might be expected. Freeze point is driven primarily by the n-paraffin content, while viscosity is a complex function of all the hydrocarbon types in the fuel. One might expect freeze point to be proportional to final boiling point, since freeze point is controlled by high MW wax formation, but (as shown in Figure 53) the correlation is not all that great.

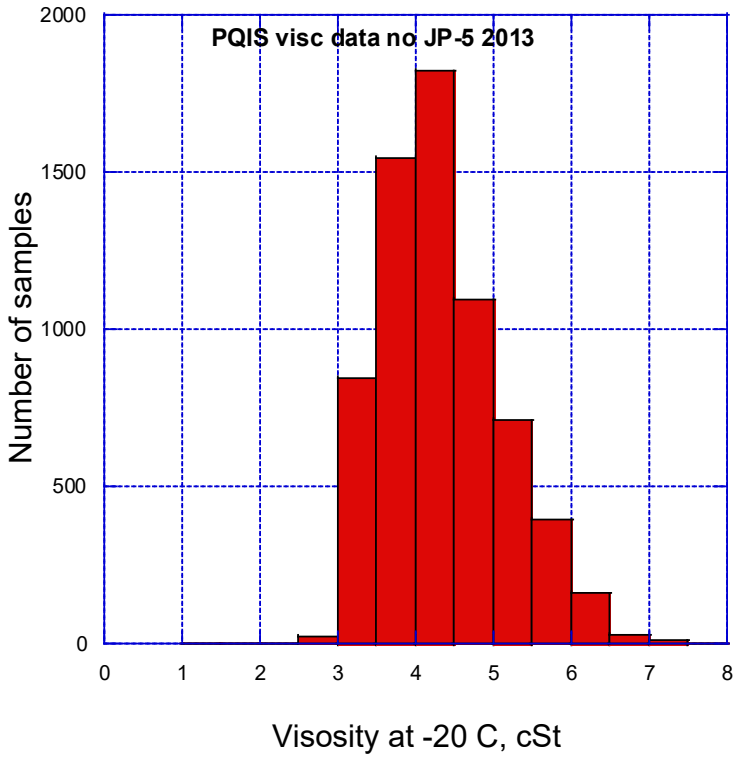

Figure 50 – PQIS 2013 viscosity data for Jet A/JP-8/Jet A-1

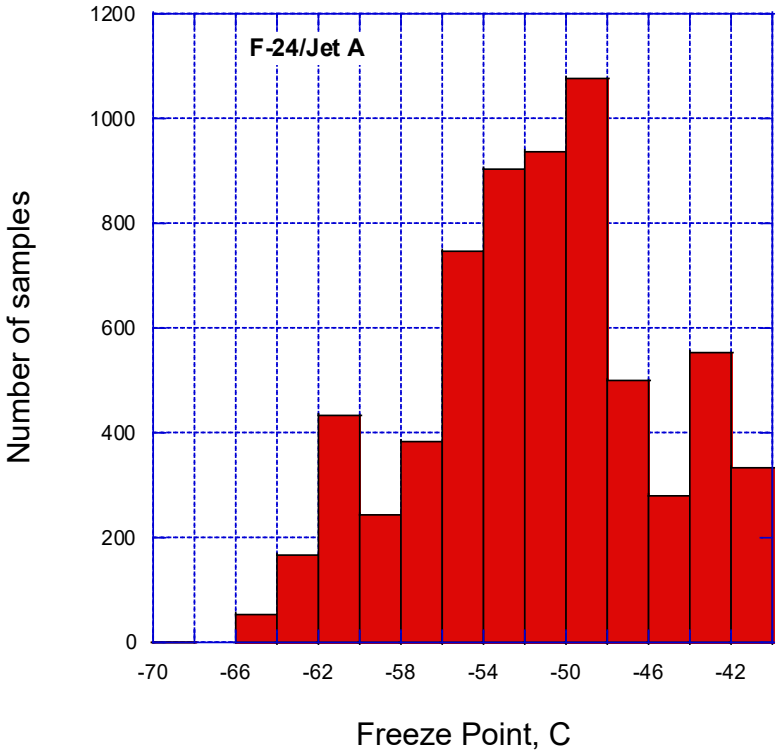

Figure 51 – 2013 PQIS data for Jet A freeze point

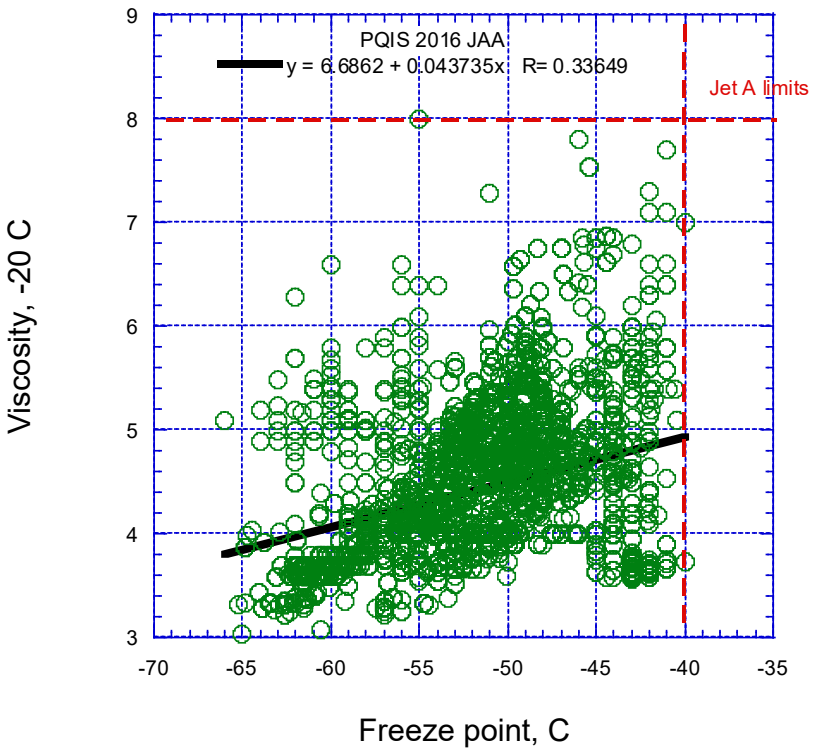

Figure 52 – Correlation of viscosity and freeze point

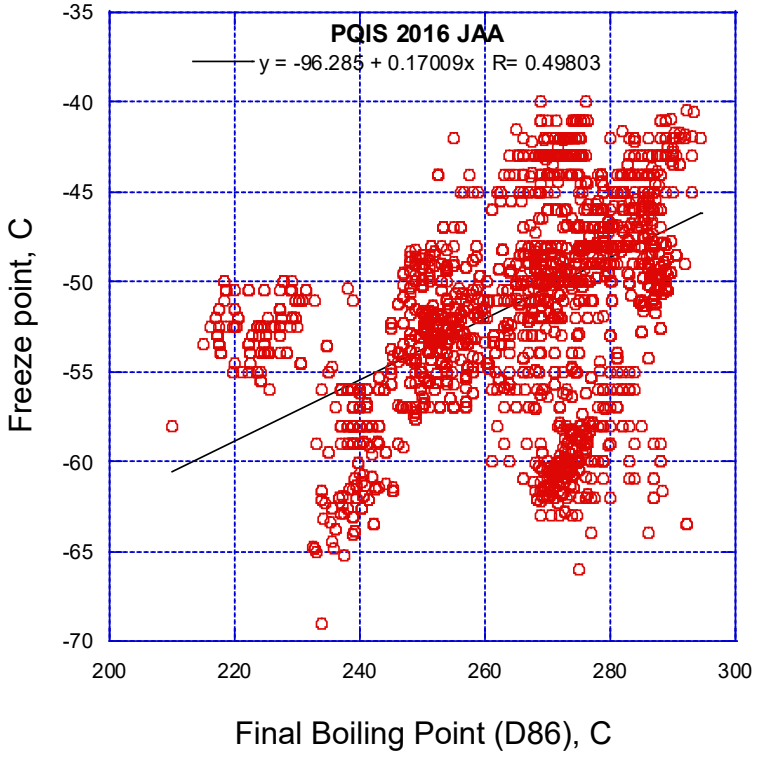

Figure 53 – Correlation of freeze point and final boiling point

Studies have examined replacing the freeze point with a flowability test[48]. One option is to use the Scanning Brookfield viscometer, ASTM D5133 (Standard Test Method for Low Temperature, Low Shear Rate, Viscosity/Temperature Dependence of Lubricating Oils Using a Temperature-Scanning Technique)[49]. Typical data is shown in Figure 54[58]. The curves tend to have a prominent knee where viscosity increases rapidly. This knee temperature correlates well with freeze point, as shown in Figure 55.

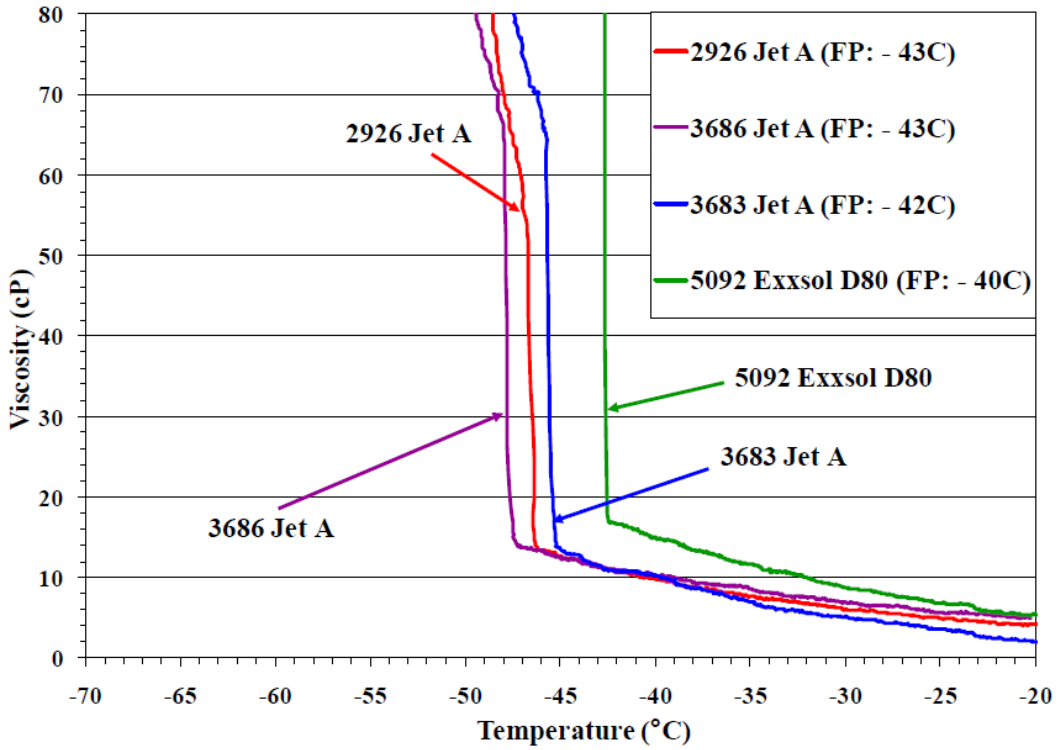

Figure 54 – Scanning Brookfield viscometer data for several jet fuels[58]

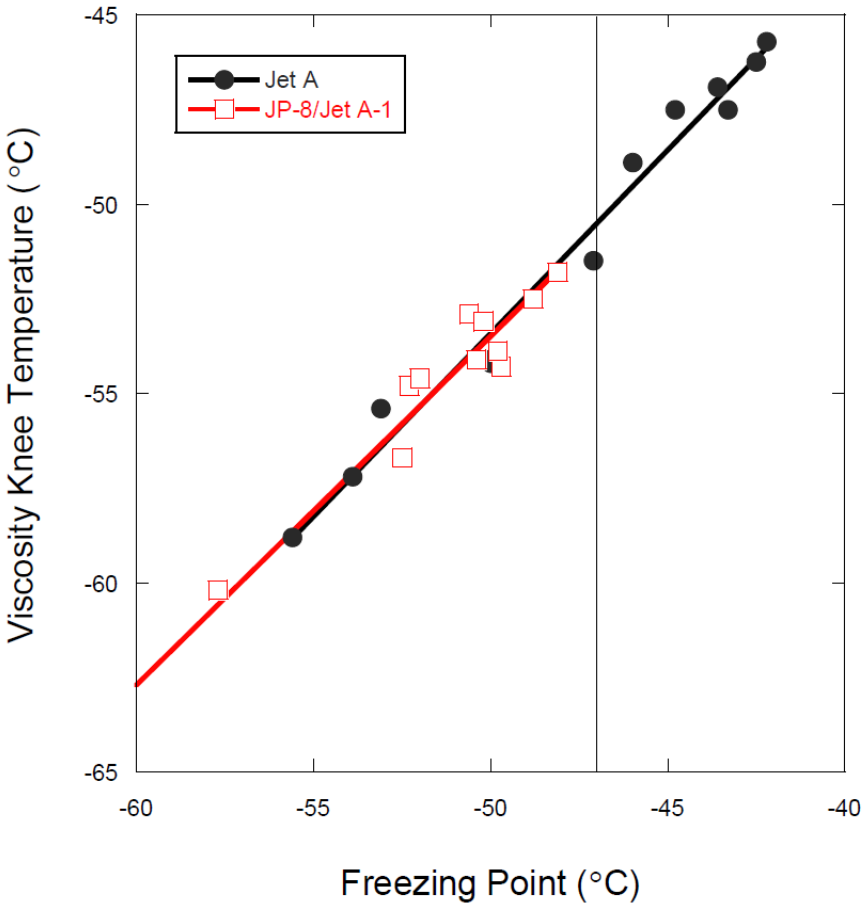

Figure 55 – Relationship of D5133 knee temperature and freeze point[49]

The kinematic viscosity behavior of the three Category A fuels is shown in Figure 56, plotted as in ASTM D371. The data is indeed linear on this type of plot. One of the aims of the "Category A" fuels was to cover the range of viscosities seen in practice, and the three fuels do cover this range well and correspond to the World Survey "max" and "min" lines, as well as the CRC Handbook average "Jet A" line.

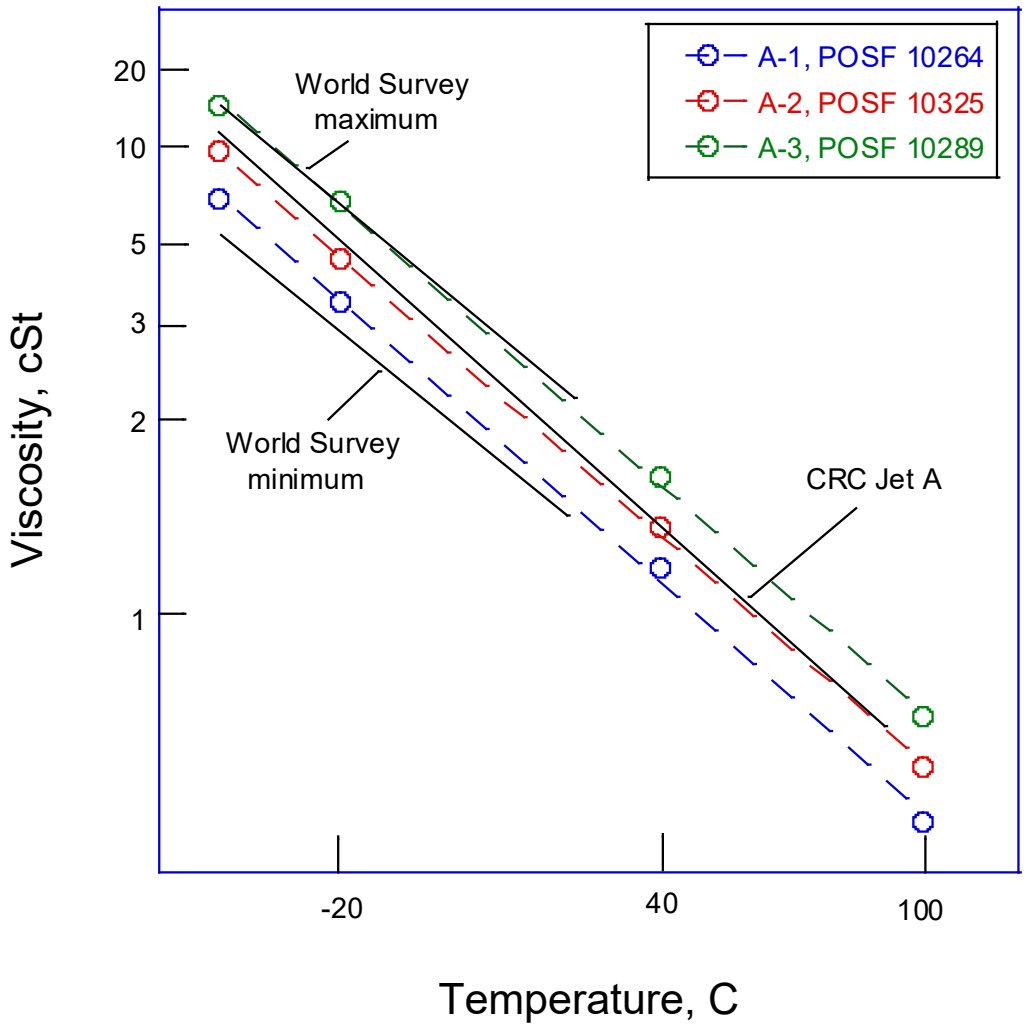

Figure 56 – Viscosity data for reference fuels

This linearity of viscosity with temperature on an ASTM D341 plot does not carry over to higher temperatures. As shown in Figures 57 and 58, nearing the critical temperature the viscosity becomes sensitive to pressure. This older data is apparently calculated, and is in wonderful English units, preserved for posterity in Figure 57 (subcritical T, up to 700 °F) and G-9 (T > 700 °F/370 °C). For reference, the data at 0 °F is roughly 12 lb/ft-hr, which translates to ~5 centiPoise at -18 °C (1 lb/ft-hr = 0.413 centiPoise = 0.413 milliPascal-second). For a jet fuel of density 0.8 g/cm^3 density, 5 cP translates roughly to 6.25 cSt, so these number are line with the measured data shown in Figure 56 at lower temperatures.

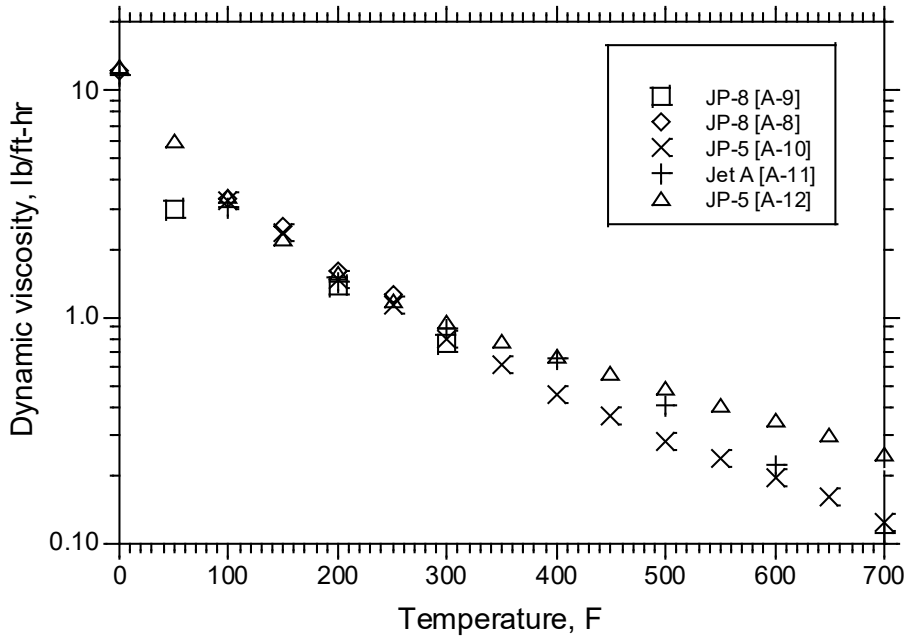

Figure 57 – Selected dynamic viscosity data to 700 °F (calculated)

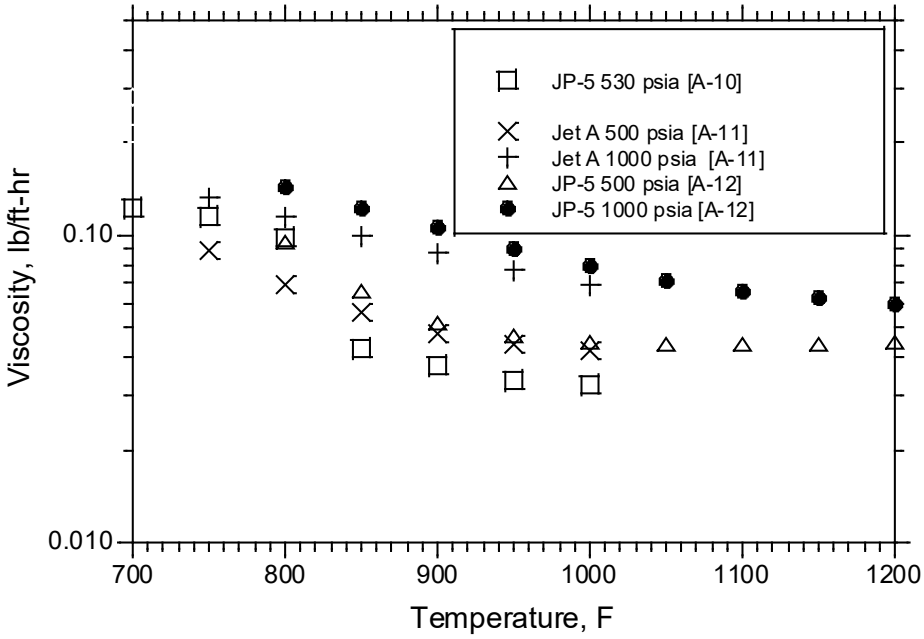

Figure 58 – Selected dynamic viscosity data 700 to 1200 °F (calculated)

7.1 Alternative fuels

Freeze point and low temperature viscosity data for selected alternative fuels is shown in Table 16. The various Research Reports also have kinematic viscosity versus temperature data, but it falls within the limits of Figure 54 so is not included. There is also literature data from NIST[51], Purdue[55,56], and the U.S. Naval Academy (dynamic viscosity)[76]. NIST's data is limited by an absence of data below 293 K. Purdue's papers show blending data for alternative fuels (spoiler alert – non-linear).

Table 16 – Selected low temperature data for alternative aviation fuels (data from AF reports and ASTM Research reports)

Fuel	Companies	POSF	Freeze point, °C	Viscosity, -20 °C (cSt)	Viscosity, -40 °C (cSt)
Synthetic Paraffinic Kerosene (SPK)	Sasol IPK	7629	<-61	3.4	6.4
	Shell SPK	5729	-54	2.6	n/a
	Syntroleum S-8	5018	-49	4.3	n/a
Hydroprocessed Esters and Fatty Acids (HEFA, aka HRJ)	UOP camelina	10301	-57	5.1	11.4
	UOP tallow	10298	-53	5.0	11.0
	Dynamic Fuels (mixed fats)	7635	-49	5.8	13.8
SIP	Amyris/Total	n/a	<-100	13.1-14.6	n/a
IPKA	Sasol	n/a	<-70	3.8	n/a
ATJ SPK	Gevo (isobutanol)	11498	-90	5.4	10.5
	LanzaTech (ethanol)	12756	<-89	4.2	8.7
CHJ	ARA	8455	-49	4.1	7.9
ATJ SKA	Swedish Biofuels	12924	<-61	3.4	7.3
	Byogy	7614	-77	5.0	n/a
Hydroprocessed Depolymerized Cellulosic Jet (HDCJ)	KiOR	7602	<-61	n/a	n/a
Hydro-deoxygenated Synthetic Kerosene (HDO SK)	Virent/Shell	8535	<-80	6.1	data
SAK	Virent/Shell	n/a	-77	1.9	n/a

8. DERIVED CETANE NUMBER/CETANE NUMBER

The cetane number of a diesel fuel (or a jet fuel) is a characteristic of its performance in a diesel engine, as typically characterized by ASTM D613 (Standard Test Method for Cetane Number of Diesel Fuel Oil). ASTM D6890 (Standard Test Method for Determination of Ignition Delay and Derived Cetane Number (DCN) of Diesel Fuel Oils by Combustion in a Constant Volume Chamber) is a simpler test method that produces an ignition delay in milliseconds, which is converted to a derived cetane number (DCN). The equation is

$$DCN = 4.460 + \left(\frac{186.6}{ID}\right)$$

with ignition delay (ID) in milliseconds. DCN correlates well with engine cetane[59], and is specified to cover the range from 33 to 64 DCN. Although specified for diesel fuel, DCN has been found to be relevant to jet fuel combustion in diesel engines, and has been found to correlate with lean blowout in gas turbine combustors under some conditions[61,62,63]. DCN data for jet fuel is available in Reference 7 with additional data being available as part of an ongoing DLA-funded survey program, as well as data from the ASTM jet-in-diesel task force [60]. The vast majority of DCN data falls between 39 and 50, as shown in Table 17 (from Reference 7) and Figure 59. Table 17 includes the NJFCP fuels, with A-1 (Sample No. 23), A-2 (Sample No. 22), and A-3 (Sample No. 24). Figure 59 includes the DLA survey data as well as the ASTM Task Force data. Another view of the DCN data is a box plot, which shows the spread of data around the median DCN of ~45 (Figure 61). The box shows the 25% of fuels on either side of the median, with the bars showing the range of data. The point at DCN 37.9 is labeled as an outlier by the software because it lies outside the acceptable range, defined as a value above or below the box by an amount that is greater than 1.5 times the thickness of the box. Figure 60 could be used to define the experience base of DCN for conventional fuels as a range of 39 to 50.

Table 17 – One set of DCN data[7]

Sample Name	Sample No.	Ignition Delay ms	Derived Cetane Number (DCN)
ATJ	1	21.6	15.2
ATJ/JP-8	2	6.0	34.6
HEFA (R-8)	3	3.4	59.1
HDCJ	5	10.1	24.0
HDCJ / JP-8	6	5.4	39.2
HRJ Camelina / JP-8	4	4.0	51.0
JP-8 Blend Stock	7	4.6	45.4
JP-8 - PADD 1	8	4.5	45.7
JP-8 - PADD 2	9	4.1	49.7
JP-8 - PADD 3	10	4.5	45.9
JP-8 - PADD 4	11	4.9	42.3
JP-8 - PADD 5	12	4.4	46.4
JP-8 - WPAFB	25	4.3	47.9
Jet A - FAME Sensitive	13	5.1	41.0
Jet A - PADD 1	14	4.5	45.7
Jet A - PADD 2	15	5.3	39.9
Jet A - PADD 3	16	4.1	50.1
Jet A - PADD 4	17	4.6	44.9
Jet A - PADD 5	18	4.7	43.8
Jet A - Nominal	22	4.3	48.3
Jet A - Best Case	23	4.2	48.8
JP-5 Supplier 1	19	4.6	44.7
JP-5 - Worst Case	24	5.4	39.2

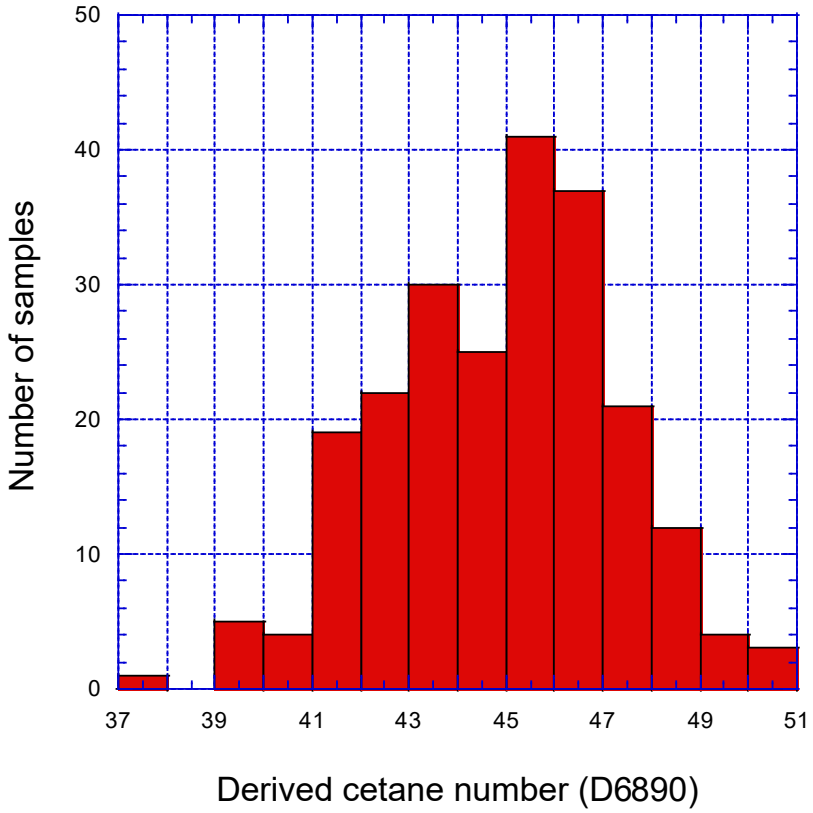

Figure 59 – Aggregated DCN data for conventional jet fuels (JP-8, Jet A, Jet A-1, JP-5)

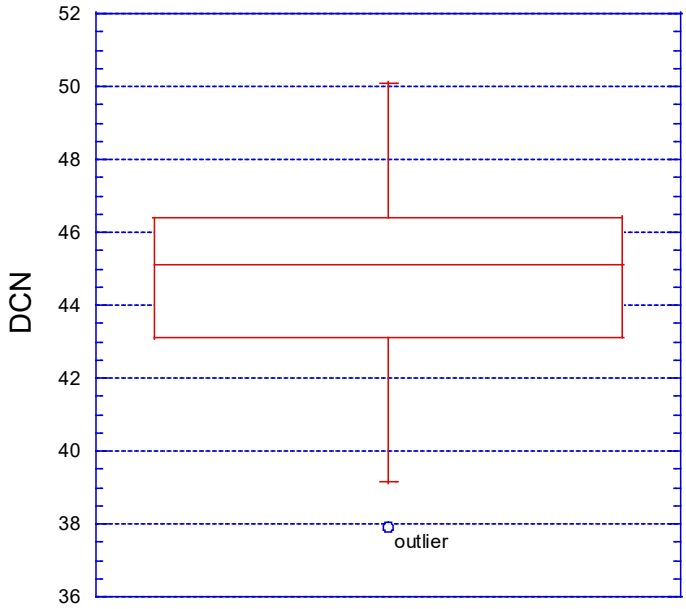

Figure 60 – Box plot for DCN data in Figure 59

8.1 Alternative fuels

The DCN for alternative fuels has been found to be much more variable than seen for conventional fuels. This is illustrated in Table 18 and Figure 61. In Figure 61, it can be seen that alternative fuels with DCNs outside of the typical range diverge from the D613 = D6890 line (noting the DCNs below 33 are outside of the specified range in D6890). The DCN of the Gevo ATJ fuel is notably low at 15 to 17 – too low to run on the D613 engine. Some limited blending studies have been done with the Gevo ATJ fuel and conventional fuels, with the results shown in Figure 62. Most of these blending results are courtesy of the U.S. Navy.

The DCN results in Table 18 are explainable from the fuel's composition. Normal paraffins and lightly branched iso-paraffins have high DCNs (short ignition delays) – so the alternative fuels that are predominantly lightly branched iso-paraffins like SPK and HEFA have relatively high DCNs. Highly branched iso-paraffins and aromatics have low DCNs/long ignition delays, thus Virent HDO SAK (>99% aromatics), KiOR HDCJ (~50% aromatics), and Gevo ATJ (>99% highly-branched C12 and C16 iso-paraffins) are notably low DCN entries in Table 18. A recent review of alternative aviation fuel combustion includes DCN and additional data such as flame speed.[119] ASTM D7170 DCN for some alternative fuels is also available.[120]

Table 18 – ASTM D6890 DCN results for alternative fuels (from Research Reports and other reports)

Fuel	Companies	DCN
Synthetic Paraffinic Kerosene (SPK)	Sasol IPK	31.5
	Shell SPK	59.6
	Syntroleum S-8	60.0
Hydroprocessed Esters and Fatty Acids (HEFA, aka HRJ)	HRJ-8 camelina	53.9
	Dynamic Fuels (mixed fats)	59.0
SIP	Amyris/Total	58.2
ATJ SPK	Gevo (isobutanol)	15-17
	LanzaTech (ethanol)	47.9
CHJ	ARA	49.9
ATJ SKA	Swedish Biofuels	43, 45
Hydroprocessed Depolymerized Cellulosic Jet (HDCJ)	KiOR	24.0
Hydro-deoxygenated Synthetic Kerosene (HDO SK)	Virent/Shell	43.1
HDO SAK	Virent/Shell	8.5

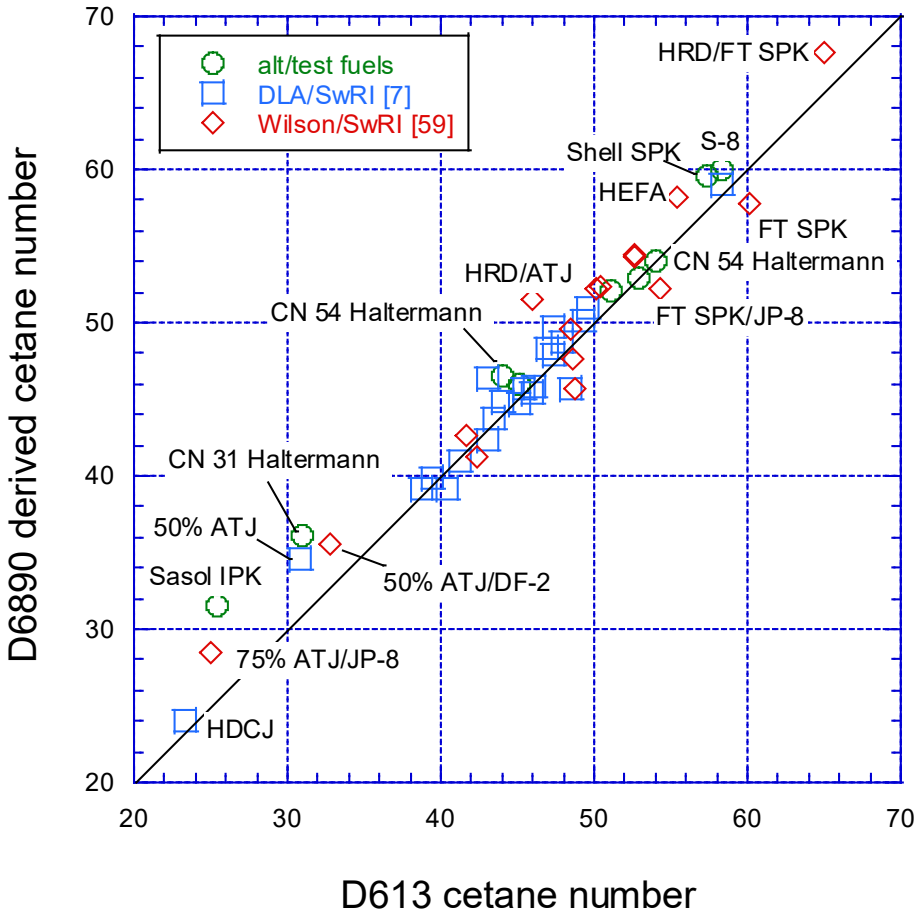

Figure 61 – Correlation of D613 cetane number and D6890 DCN from References 59 and 7

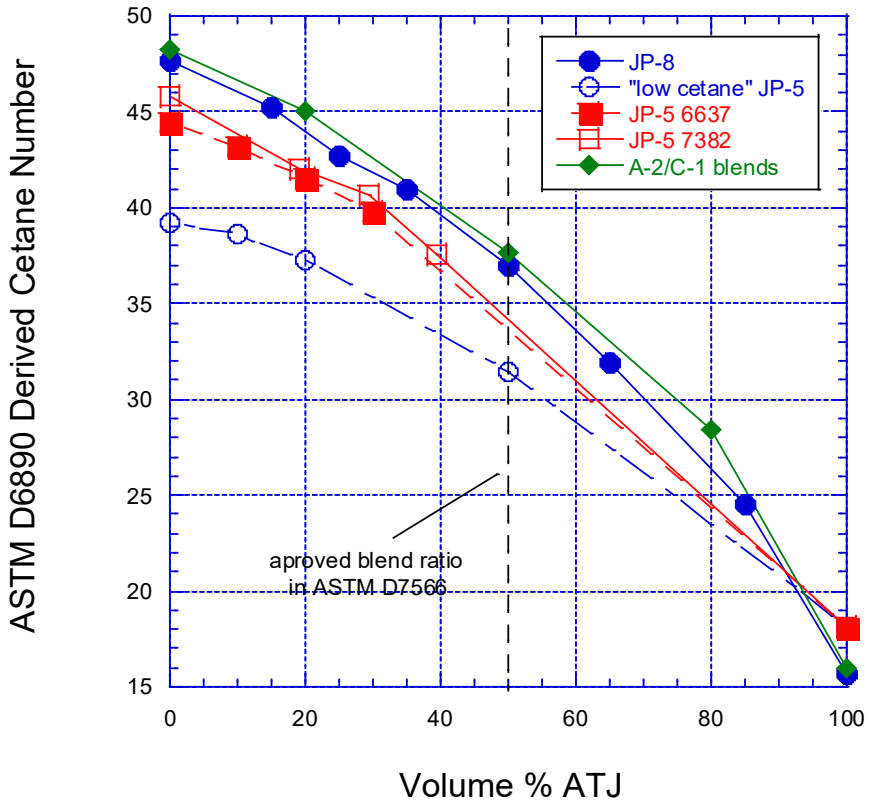

Figure 62 – DCN for blends of jet fuel with Gevo ATJ (most data courtesy of U. S. Navy)

8.2 Estimation

The most common estimation technique for cetane number is the ASTM D4737 cetane index. Cetane index has been found to be inaccurate for highly isoparaffinic alternative fuels. For example, the calculated cetane index for Sasol IPK has been reported to be 51, while the D613 cetane is 25 and the DCN is 31. Pande and Hardy presented a newer correlation using additional chemical measurements from NMR[64]. The simpler Procedure B (diesel fuels meeting the requirements for Specification D975, Grade No. 2-D S500) for calculated cetane index (CCI) from D4737 is reproduced below. Note that this correlation is specified for diesel fuel, not jet fuel. However, it uses readily available density and D86 distillation data as correlating parameters, so it is a reasonable option for estimating cetane number for conventional fuels in the absence of DCN data.

$$CCI = -399.90(D) + 0.1113(T_{10}) + 0.1212(T_{50}) + 0.0627(T_{90}) + 309.33$$

$CCI = Calculated\ Centane\ Index\ by\ Four\ Varible\ Equation$
$D = Density(g/mL) at\ 15℃, determined\ by\ Test\ Mthods\ D1298\ or\ D4052$
$T_{10} = 10\%\ recovery\ temperature(℃)\ determined\ by\ Test\ Method\ D86^{*}$
$T_{50} = 50\%\ recovery\ temperature(℃)\ determined\ by\ Test\ Method\ D86^{*}$
$T_{90} = 90\%\ recovery\ temperature(℃)\ determined\ by\ Test\ Method\ D86^{*}$
$^{*} = Must\ be\ corrected\ to\ standard\ barometric\ pressure$

9. ENTHALPY, HEAT CAPACITY, HEAT OF VAPORIZATION

The use of fuel as a coolant obviously could benefit from additional knowledge of its enthalpy-versus-temperature behavior. There are enthalpy diagrams for JP-4 and JP-5 in the CRC Handbook – but they are of somewhat murky attribution[1]. Since JP-4 and JP-5 were the primary fuels in the mid-to-late 1950s, it is believed that those charts date back to that time. Maxwell's book[6] includes an enthalpy plot for a hydrocarbon with a mean average boiling point of 400 °F (204 °C) and a characterization factor of 12, as shown in Figure 63. Per the earlier discussion in Section 3, these parameters are basically those for Jet A-1/Jet A fuels, so Figure 63 can be used to estimate Jet A/Jet A-1/JP-8 enthalpy. Note that Figure 63 includes both liquid and vapor data. For use as a coolant, the liquid-phase enthalpy (at pressure) is of most interest. Note also that enthalpy values depend on the reference state selected – in Figure 63, liquid enthalpy is defined as 0 at T=0 °F. Other sets of data define the zero point as 70 °F. One could either use the enthalpy directly or use heat capacity to calculate enthalpy change:

$$\Delta H = C_p \Delta T \; or \; \Delta H = \int_{T_1}^{T_2} C_p dT$$

As discussed below, heat capacity is a function of temperature, so these calculations are not necessarily simple. Riazi[4] can be consulted for details. For the purposes of this report, several sets of data for kerosene fuels will be presented. For example, UTRC's endothermic fuel program has measured the enthalpy of JP-7 and JP-8[67]. There is some relatively old data in the literature for several fuels, including one kerosene fuel that has properties very near typical average jet fuels[65]. In addition, ongoing CRC project AV-20-14 with the University of Delaware is re-measuring the enthalpy of a number of jet fuels in order to update the CRC Handbook[66]. The high pressure/liquid phase data from these references is compared in Figure 64. The data is pretty consistent to about 200 °C, where some divergence begins. Figure 65 shows the effect of pressure on (two-phase) enthalpy data. Note that at low pressure the fuel vaporizes, thus such a chart could be used to estimate the heat of vaporization. The two different data sets are not very consistent. Reference 66 is being updated with additional data as of early 2020.

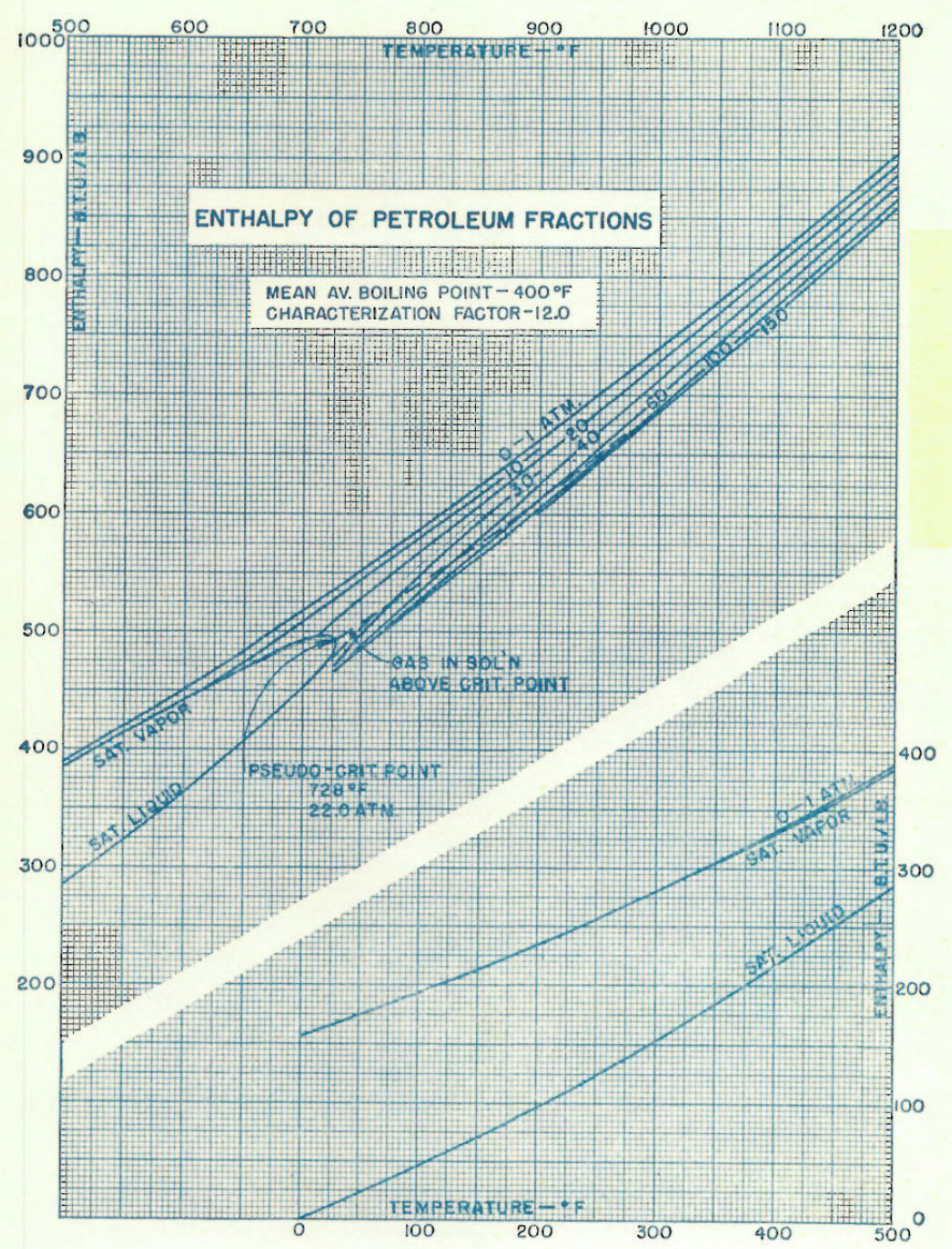

Figure 63 – Enthalpy diagram for a petroleum fraction

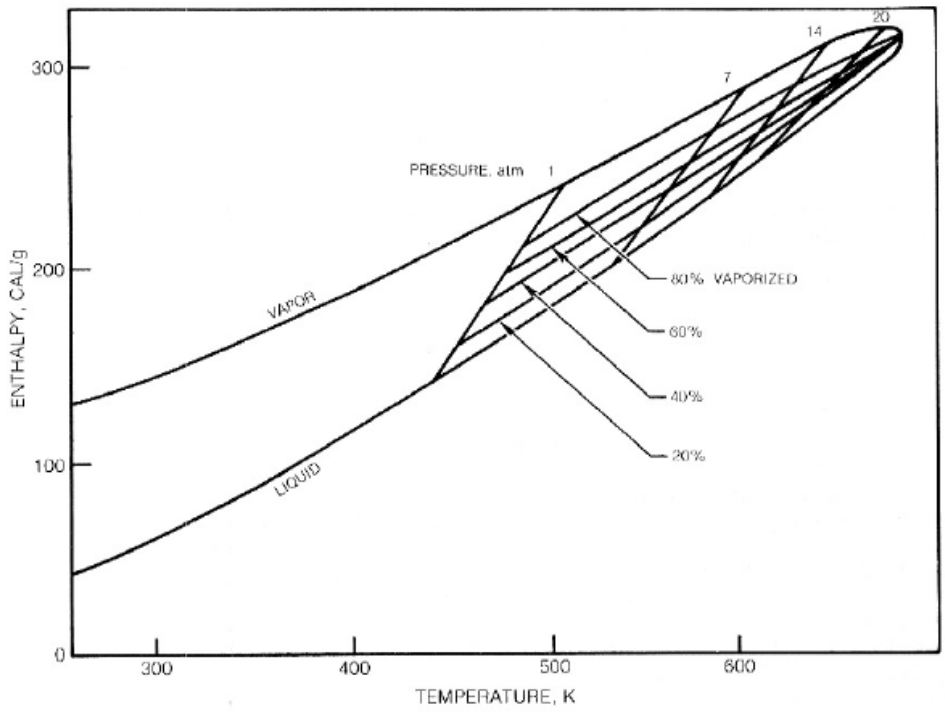

Figure 64 – Enthalpy diagram from Szetela et al.[69], calculated from API Technical Data Book.

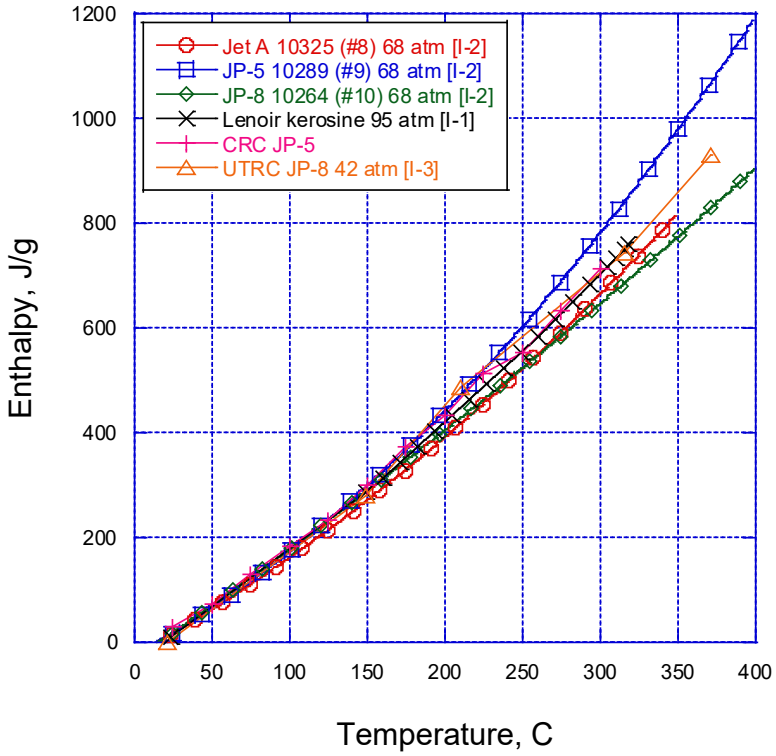

Figure 65 – Liquid enthalpy as a function of temperature for several fuels

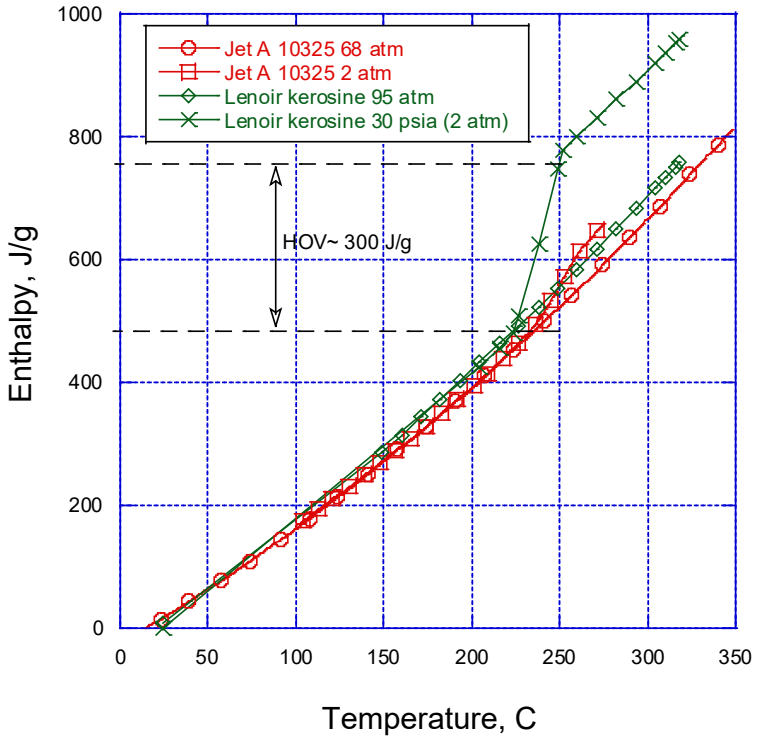

Figure 66 – Pressure effect on enthalpy[65,66].

9.1 Heat of Vaporization (HOV)

The heat of vaporization is relevant to jet fuel behavior in combustors. Note one difference between jet fuels and pure components – for a pure component, the vaporization occurs at one temperature, so the heat of vaporization is straightforward to define. For multicomponent jet fuels that vaporize over 100 to 150 °C (the range from initial to final boiling point), the heat of vaporization is less well defined since some of the enthalpy change in going from liquid to fully vaporized fuel includes the enthalpy change of heating the vaporized light ends to the final boiling point. The CRC Handbook has a chart of heat of vaporization as a function of temperature that seems problematic to interpret. These complications aside, there are data sets and correlations that can be used to compare to the ~300 J/g heat of vaporization in Figure 65[65]. Nelson[5] has a chart for HOV that yields HOV~115 BTU/lb (267 kJ/kg). The CRC Handbook[1] gives HOV ~ 275 kJ/kg at 208 °C (118 BTU/lb), using 208 C as the equivalent normal boiling point (nbp) of an average jet fuel such as the A-2 fuel. Riazi[4] has equation for HOV (p. 327, reproduced below) that yields and HOV~ 258 J/g at 208 °C.

$$\Delta H_{vap}(nbp) = 37.32315(T_b^{1.12086})(SG^{0.00977089})$$

Lefebvre[68] has

$$\Delta H_{vap}(nbp) = (360 - 0.39T[in\ K])/SG$$

yielding a HOV value of 307 kJ/kg. Sauerbrunn[66] measured HOV on ~20 fuels – for a subset of 10 Jet A-1 fuels, the result was HOV = 308 ± 10 J/g at a peak vaporization temperature of 191 ± 7 °C. Given the scatter in the data, it is reasonable to estimate the heat of vaporization of jet fuel as (roughly) 300 J/g.

9.2 Heat capacity

Heat capacity (C_p) is not a specification property (in contrast to density and viscosity), but is a fit-for-purpose property and was measured at SwRI for the three Category A fuels using ASTM E1269. The results are shown in Figure 67. There is some spread in the data, similar to the spread shown in the CRC Handbook[1], which shows differences among fuels, probably due to density differences. Esclapez[36] has fit the A-2 C_p data as 0.00428* T [K] + 0.723 [C_p in kJ/kg-K].

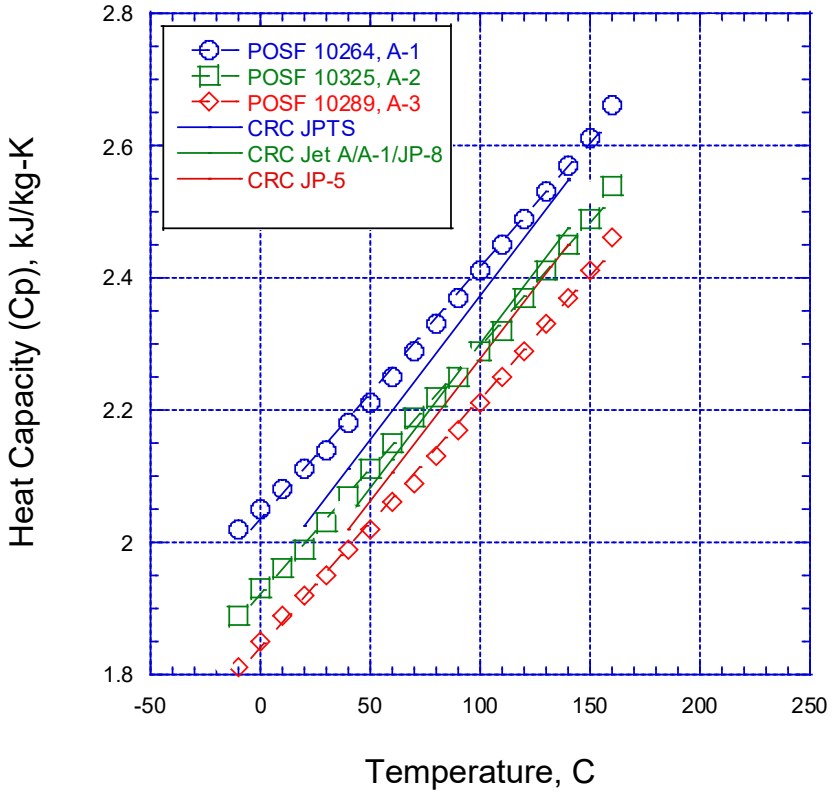

Figure 67 – Category A heat capacity data compared to CRC Handbook

Some older references include heat capacity (Cp) over a wide range of temperatures, calculated using equations of state or using correlations[9,10,11,12]. That data is fairly consistent for the liquid phase up to ~ 500 °F (260 °C). The data at temperatures about the critical temperature (~700 °F) is more scattered. The data is shown in Figures 68 and 69 in its original units (where 1.0 kJ/kg-K = 0.239 BTU/lb_m-F).

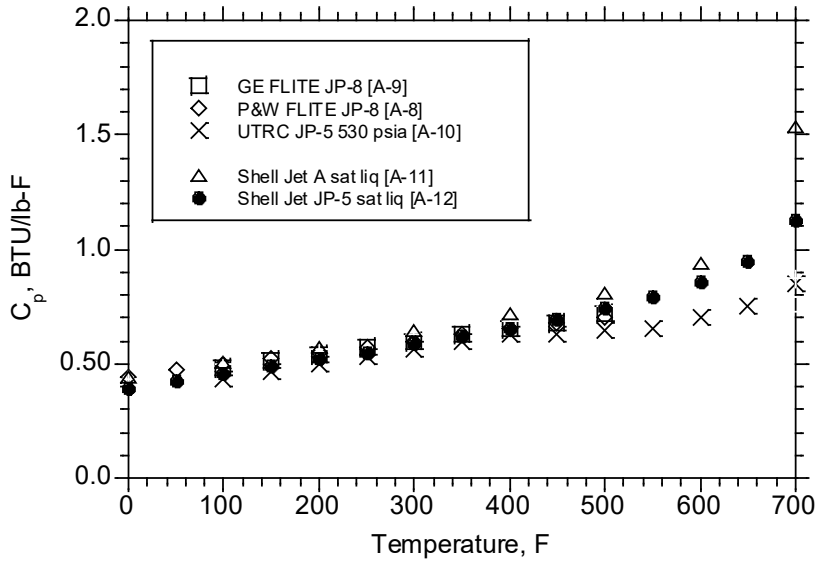

Figure 68 – High temperature heat capacity data (up to 700 °F)

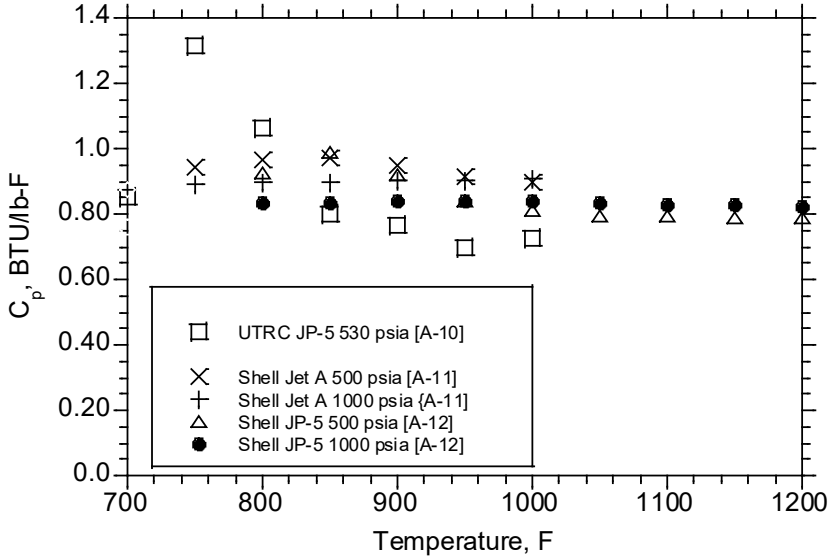

Figure 69 – High temperature heat capacity data (700 to 1200 °F)

Lefebvre[68] includes equations for liquid phase and vapor phase heat capacities:

$$C_p = \frac{\left(0.76 + 0.00335T(in\ K)\right)}{relative\ density} \times 0.5(kJ/kg\ K)$$

$$Vapor\ C_p = (0.136 + 0.0012T)(4 - dr)(dr = relative\ density)$$

9.3 Alternative fuels

The heat capacity at constant pressure has been measured for a number of fuels at SwRI. Since heat capacity is related to enthalpy through

$$\Delta H = C_p \Delta T$$

One could get an estimate of heat capacity from ΔH/ΔT in Figure I-2 using 100 °C and 200 °C points, resulting in Cp = ΔH/ΔT =(420-180 J/g)/(200-100 °C) = 2.4 J/g-C = 2.4 kJ/kg-K. Thus, at 150 °C, the heat capacity of jet fuel should be roughly 2.4 kJ/kg-K. As shown in Figure 70, the SwRI data is roughly consistent with that value. The spread in heat capacities for the various fuels in Figure 69 seems unwarranted given the similarities in composition for the various alternative fuel blends. In any case, the current data is roughly consistent with earlier data.

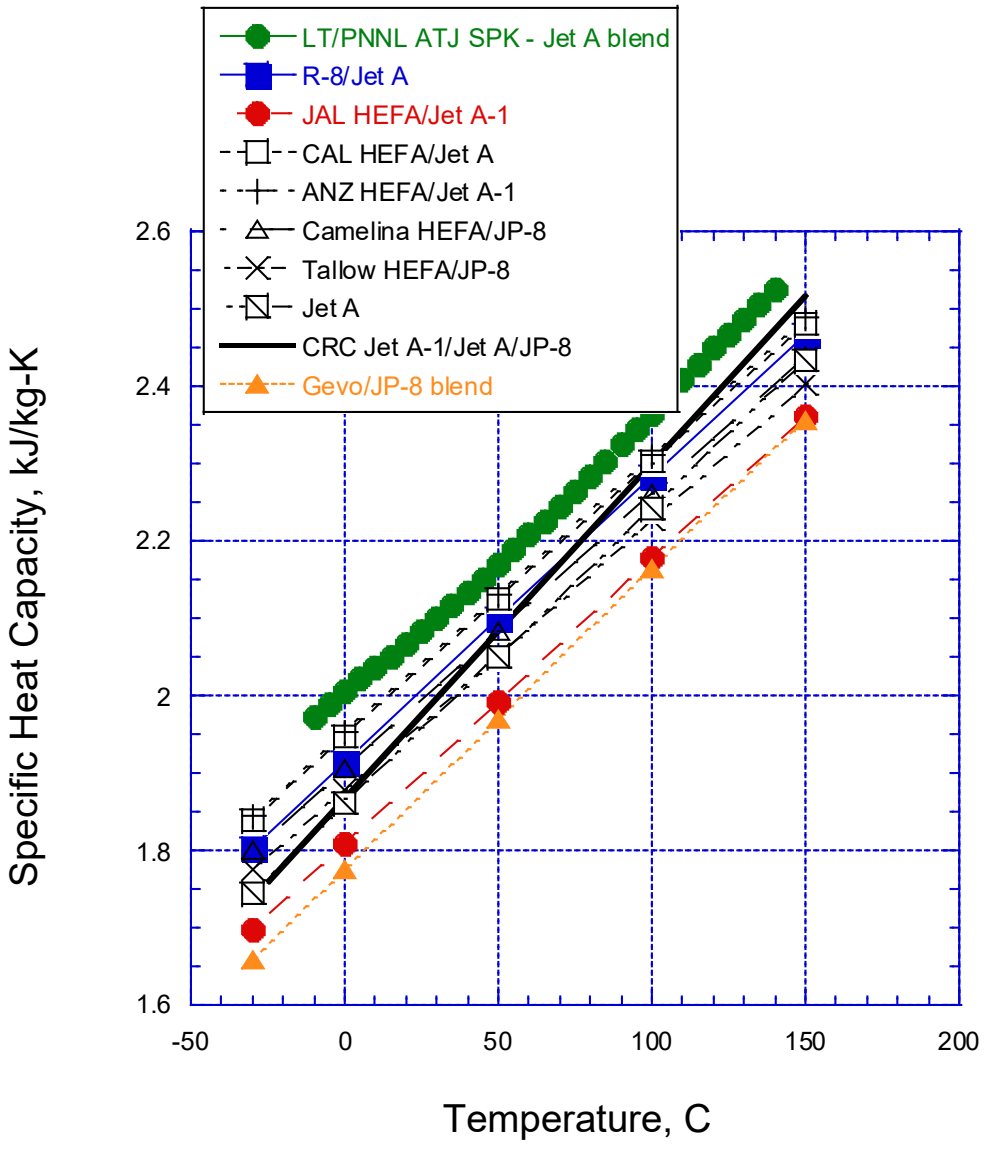

Figure 70 – Heat capacity data for several alternative fuel blends

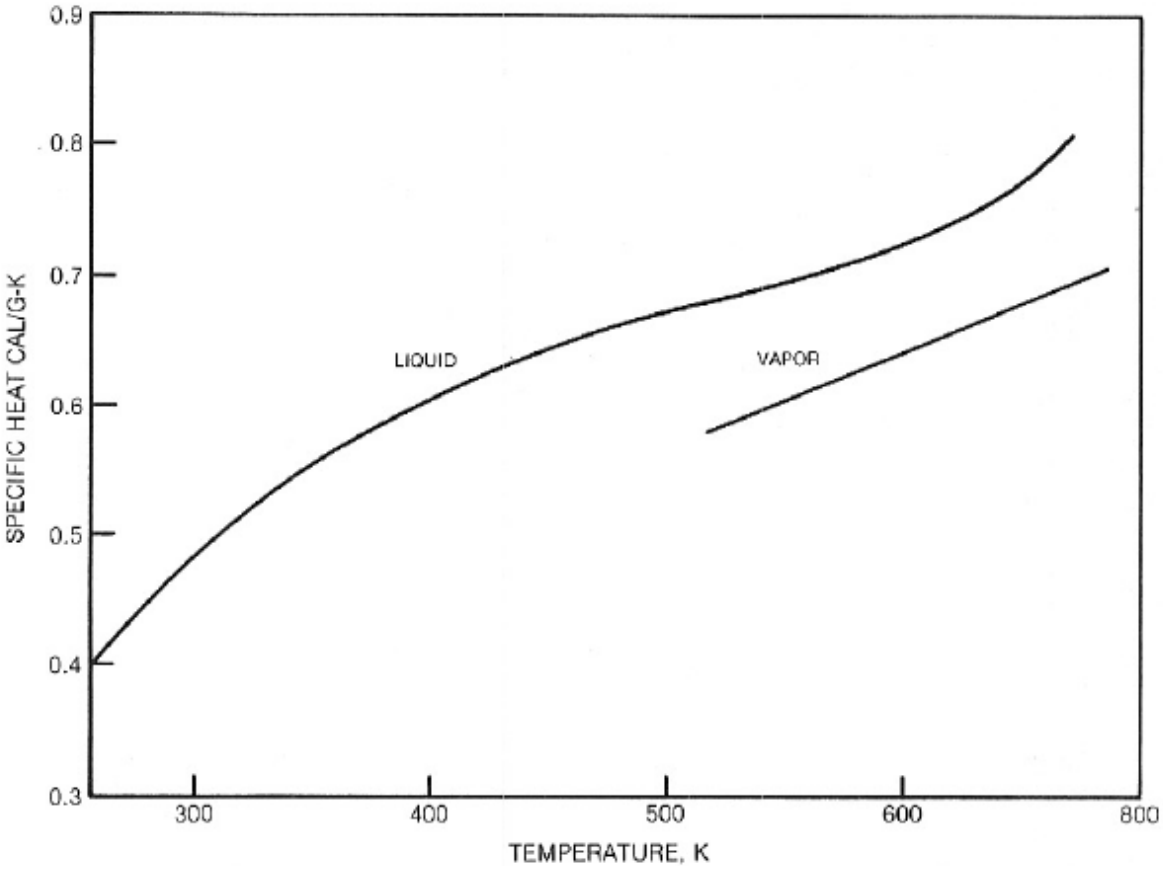

Figure 71 – General jet fuel heat capacity diagram[69]

10. SPEED OF SOUND, BULK MODULUS

Bulk modulus is a measure of the compressibility of a fluid with changes in pressure. Bulk modulus can affect ignition timing in diesel engines[70], and is relevant for fuel-draulic systems that use fuel as a hydraulic fluid. A good discussion of the bulk modulus is presented in the latest edition of the CRC Handbook[1]. Although most fuel gauging systems rely on the dielectric constant/permittivity (discussed in Section 13), some newer gauging systems use ultrasonic systems that rely on the speed of sound[71]. The pairing of the two properties in this section may seem odd, but one type of bulk modulus (adiabatic bulk modulus) can be calculated directly from the speed of sound(c) and the density(ρ), so the data for both speed of sound and bulk modulus(K) is collected here (at no additional charge!).

$$c = \sqrt{\frac{\mathrm{K}}{\rho}}$$

10.1 Speed of Sound – Conventional Fuels

Note that there are several datasets of different types described in this section. SwRI developed a high-pressure instrument to measure density and speed of sound (and thus bulk modulus) as a function of pressures up to about 5000 psia (34 MPa) at 35 and 75 °C[78,80,81]. As described for alternative fuels below, SwRI also has published data at atmospheric pressure and a fixed temperature[77]. The CRC World Fuel Survey presents data on speed of sound as a function of temperature (-40 °C to 70 °C), and includes speed of sound plotted as a function of density[2]. The speed of sound for all conventional fuels is very similar over that temperature range, as shown in Figure 72[2]. The World Survey fit the various fuels types separately for speed of sound versus temperature, leading to the equations in Table 19. However, the lines are almost coincident. In contrast to dielectric constant, plotting speed of sound as a function of density causes the data for the various fuel types to separate into separate lines, indicating that density is not the only primary factor controlling speed of sound. Several NIST papers present speed of sound data used to create equations of state[72,73,74,75]. Speed of sound is not included in the CRC Handbook of Fuel Properties[1], although bulk modulus as a function of temperature is included, with of constant pressure up to 28 MPa. For estimation purposes, it is probably adequate to use the jet fuel class to approximate the speed of sound as a function of temperature.

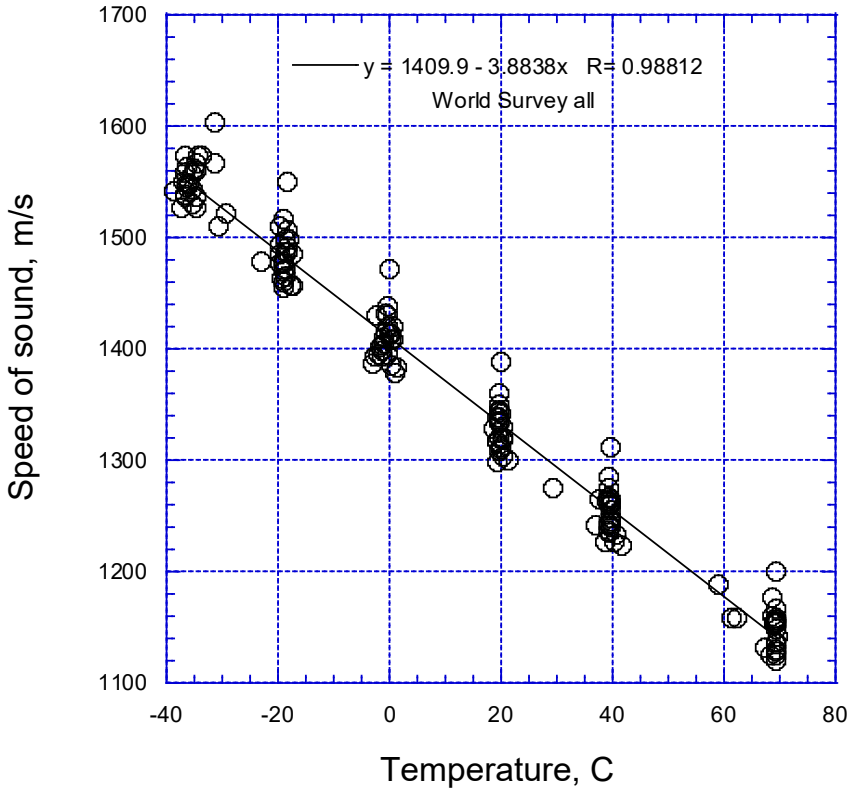

Figure 72 – Speed of sound as a function of temperature from World Survey

Table 19 – Speed of sound versus temperature equations from World Survey

Summary-Velocity of Sound (V_{OS}) in m/s Versus Temperature in °C		
Fuel	Linear Fit Equation	Regression Fit Value(R^2)
Jet A	$V_{OS} = -3.8850T + 1413.7$	0.9860
Jet A-1	$V_{OS} = -3.9106T + 1402.3$	0.9779
JP-5	$V_{OS} = -3.8276T + 1413.0$	0.9985
JP-8	$V_{OS} = -3.8678T + 1399.4$	0.9658

SwRI's speed of sound data for the three reference jet fuels is shown in Tables 20, 21, and 22 as a function of pressure for two temperatures[7]. This data allows one to show the speed of sound as a function of pressure, as shown in Figure 73 (apologies for the mixed units, straight from the original data in Tables 21 to 23). There is a clear separation amongst the fuels apparently related to density, in contrast to the World Survey. Note, however, that the magnitude of variation in speed of sound is not large – a 3000 psi increase in pressure increases speed of sound by roughly 100 m/s (<10%). The speed of sound data are roughly linear with pressure – noting that speed of sound measurements through a high-pressure cell are difficult[78].

Table 20 – SwRI high-pressure data below for Jet A/POSF 10325/A-2[7]

Temperature	Pressure	Density	SOS	Bulk Modulus
°C	psi	g/cm^3	m/s	psi
34.7	75	0.7836	1263.8	181,526
34.7	447	0.7859	1269.6	183,725
34.7	1601	0.7927	1320.7	200,557
34.7	2173	0.7950	1338.2	206,475
34.7	2889	0.7973	1362.9	214,786
34.7	4205	0.8042	1410.0	231,890
34.7	4901	0.8087	1436.2	241,943
74.9	266	0.7538	1123.5	138,013
74.9	762	0.7607	1143.0	144,147
74.9	1182	0.7630	1162.2	149,461
74.9	1868	0.7675	1197.2	159,567
74.9	2688	0.7698	1230.0	168,932
74.9	3394	0.7744	1255.2	176,951
74.9	3871	0.7790	1269.4	182,046
74.9	4996	0.7836	1305.3	193,636

Table 21 – SwRI high-pressure data below for JP-8/POSF 10264/A-1

Temperature	Pressure	Density	SOS	Bulk Modulus
°C	psi	g/cm^3	m/s	psi
34.5	323	0.7630	1245.1	171,560
34.5	762	0.7653	1259.2	175,979
34.5	1544	0.7675	1290.0	185,255
34.5	2059	0.7698	1310.6	191,783
34.5	2679	0.7744	1334.1	199,913
34.5	3366	0.7790	1352.6	206,695
34.7	4357	0.7813	1392.2	219,619
34.7	4958	0.7836	1425.0	230,762
74.9	352	0.7332	1099.0	128,444
74.9	991	0.7378	1128.6	136,289
74.9	1534	0.7424	1156.6	144,037
74.9	2421	0.7469	1196.3	155,050
74.9	3194	0.7492	1228.7	164,068
74.9	3871	0.7538	1255.3	172,282
74.9	4806	0.7607	1291.1	183,921
74.9	5530	0.7630	1310.3	189,982

Table 22 – SwRI high-pressure data below for JP-5/POSF 10289/A-3

Temperature	Pressure	Density	SOS	Bulk Modulus
°C	psi	g/cm^3	m/s	psi
34.7	222	0.8136	1294.9	197,860
34.7	603	0.8136	1308.9	202,171
34.7	1328	0.8182	1326.2	208,715
34.7	2282	0.8228	1366.8	222,934
34.7	3274	0.8274	1395.7	233,767
34.7	4380	0.8296	1432.4	246,894
34.7	4761	0.8319	1445.9	252,260
75.2	298	0.7839	1148.4	149,945
75.2	909	0.7862	1166.3	155,104
75.2	1557	0.7930	1193.7	163,904
75.2	2282	0.7953	1223.4	172,658
75.2	3350	0.7999	1264.3	185,449
75.2	3999	0.8045	1294.9	195,638
75.2	4761	0.8090	1311.1	201,697

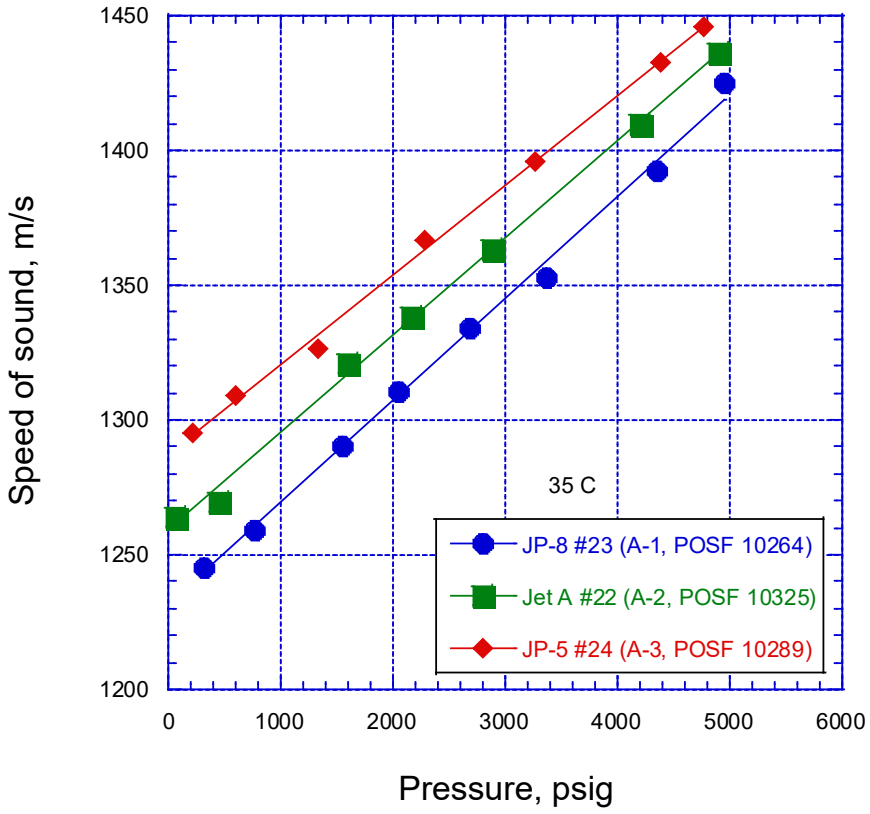

Figure 73 – Speed of sound as a function of pressure at 35 °C[7]

NIST speed of sound data[72,73,74,75] is pretty consistent with the World Survey data and SwRI atmospheric pressure data, as shown in Figure 74. World Survey fuel 043 is a JP-8 fuel that seems to be an outlier in Figure 74 (and 72) – it has no obvious properties that are outside the norm, so it isn't clear why the speed of sound of this fuel is relatively high. Again, though, the data appears to indicate that (to a first approximation) jet fuel speed of sound is independent of conventional fuel type and decreases linearly with temperature between -40 and 80 °C.

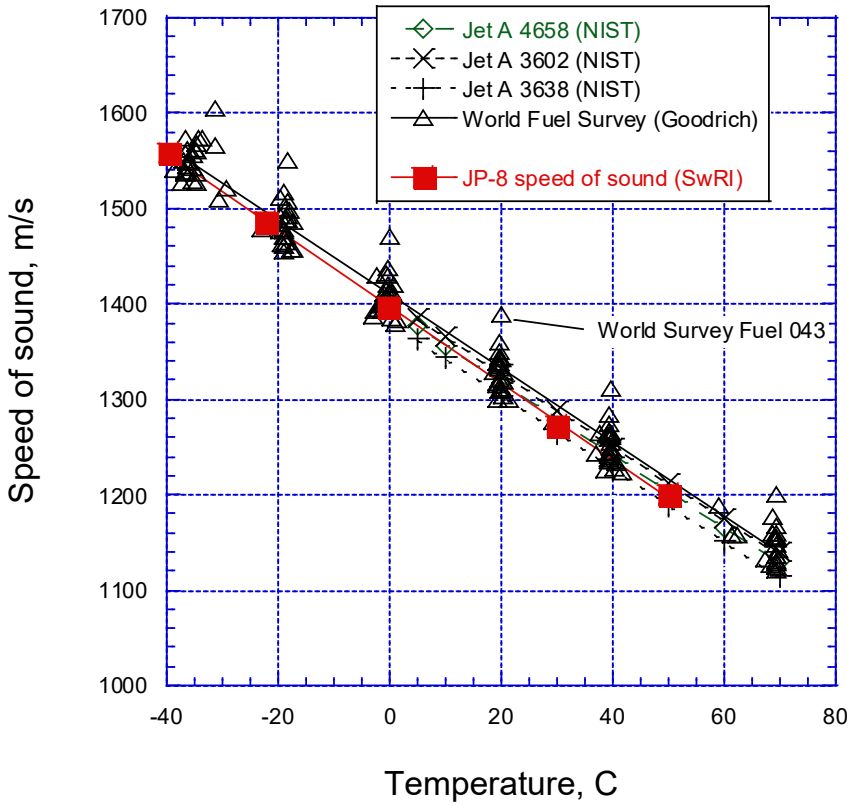

Figure 74 – Comparison of speed of sound

10.2 Bulk Modulus – Conventional Fuels

The adiabatic bulk modulus (K, Pa) is calculated from the density (ρ, kg/m^3)) and speed of sound (c, m/s):

$$K = \rho c^2$$

There are bulk modulus data presented (without citing the data source) in the CRC Handbook[1]. Bulk modulus data is also presented in a DLA-funded survey of fuels[7], where Tables 19 to 21 were excerpted. The CRC Handbook data is presented in Figure 75. Note that showing a single line for bulk modulus at a given pressure for Jet A/Jet A-1/JP-8/JP-5 in Figure 73 supports to some extent independence of the speed of sound (and thus bulk modulus) from fuel type shown in the World Survey results for speed of sound. There should still be a density effect, but to this first approximation all jet fuel types are assumed to have the same density. This is verifiable – from PQIS 2013, the weighted mean densities are Jet A – 0.8048, Jet A-1 – 0.7963, JP-8 – 0.7999, JP-5 – 0.8092. For 2016, the weighted mean densities were 0.8067, 0.7985, 0.7977, 0.8101, respectively. So, assuming the densities of all of these kerosene fuels is the same introduces errors on the order of 1% - good enough for initial estimates of speed of sound and bulk modulus. The bulk modulus equations are shown in Table 23. One might expect that

bulk modulus would be linear with temperature, since its component density and speed of sound are linear with temperature – but Figure 75 indicates otherwise.

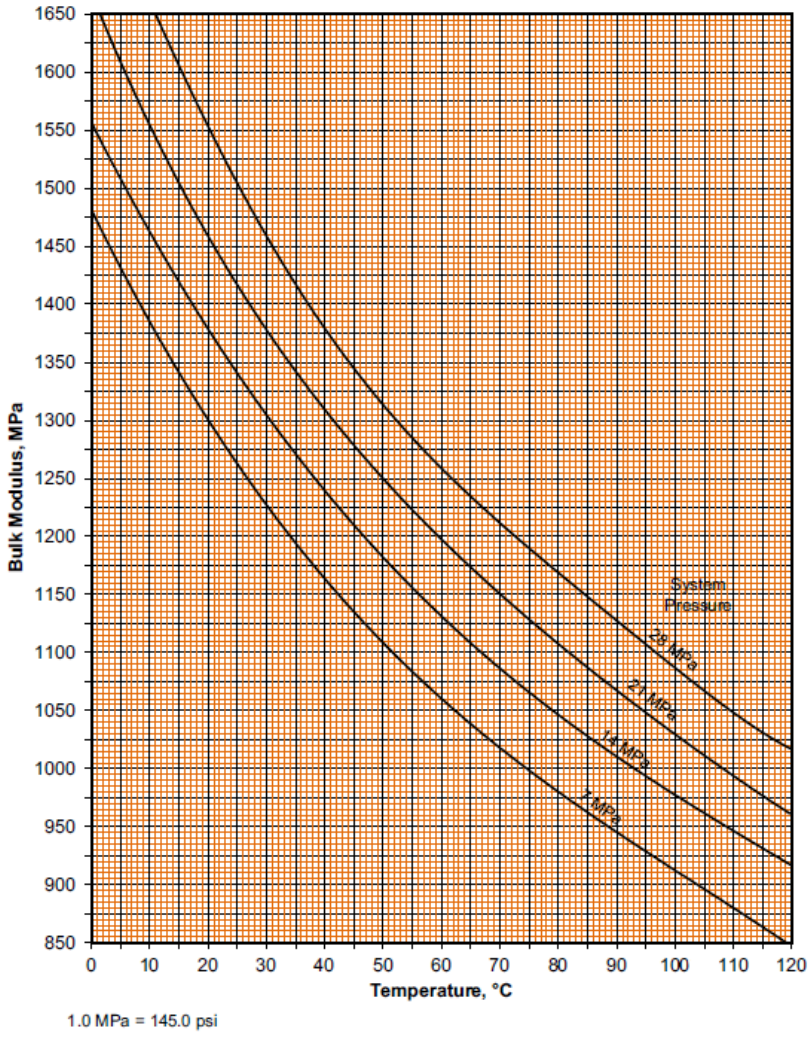

Figure 75 – Bulk modulus as a function of temperature taken from CRC Handbook[1]

Table 23 – Bulk modulus relations as a function of temperature taken from CRC Handbook[1]

x = Temperature, °C y = Bulk Modulus, MPa

System Pressure	*Equation*
28 MPa	y = 6.959×10–8 x5 – 2.086×10–5 x4 + 1.884×10–3 x3 – 4.786×10–4 x2 – 11.80 x + 1778
21 MPa	y = 1.630×10–6 x4 – 6.596×10–4 x3 + 1.101×10–1 x2 – 12.44 x + 1669
14 MPa	y = –1.595×10–4 x3 + 5.802×10–2 x2 – 10.00 x + 1557
7 MPa	y = –2.192×10–4 x3 + 6.836×10–2 x2 – 10.34 x + 1482

The data in Tables 19 to 21[7] and published NIST data[72,73,74,75] can also be used to examine the effect of pressure on density. As shown in Figure 76, a linear fit of the data from NIST shows that density is indeed linear with pressure. The SwRI and NIST data appears somewhat inconsistent at lower pressure.

Note that Figure 14 says the density of Jet A/POSF 10325 is about ~0.786 at 37 °C (310 K) at atmospheric pressure, so the SwRI data at low pressure appears to have some bias. As shown in Figure 77, the SwRI bulk modulus data as a function of pressure for the three reference fuels shows similar trends to those seen in Figure 73 for speed of sound.

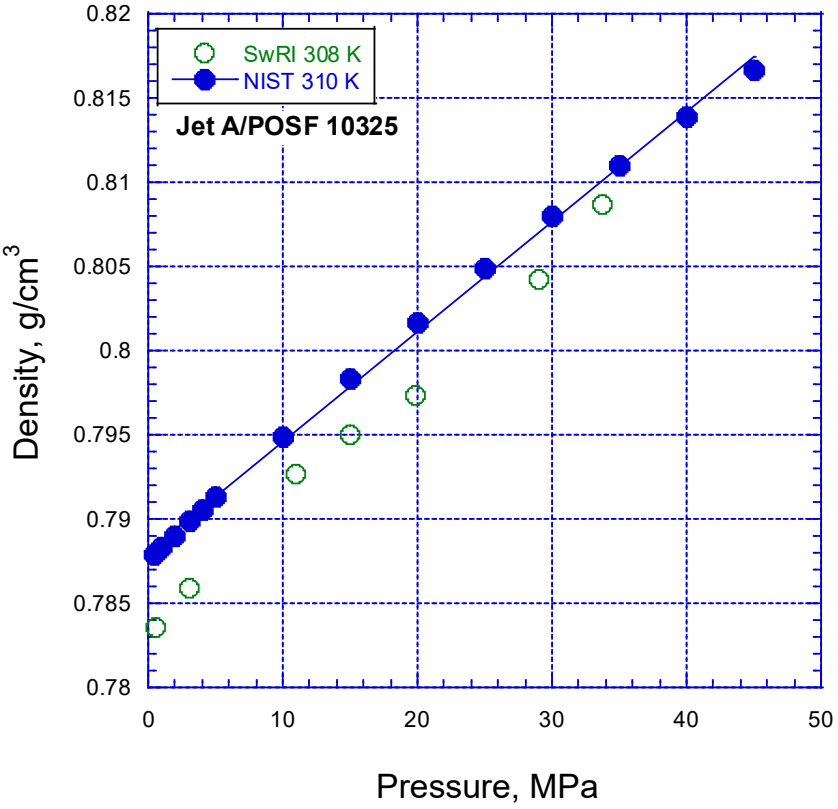

Figure 76 – Density as a function of pressure for Jet A/POSF 10325.

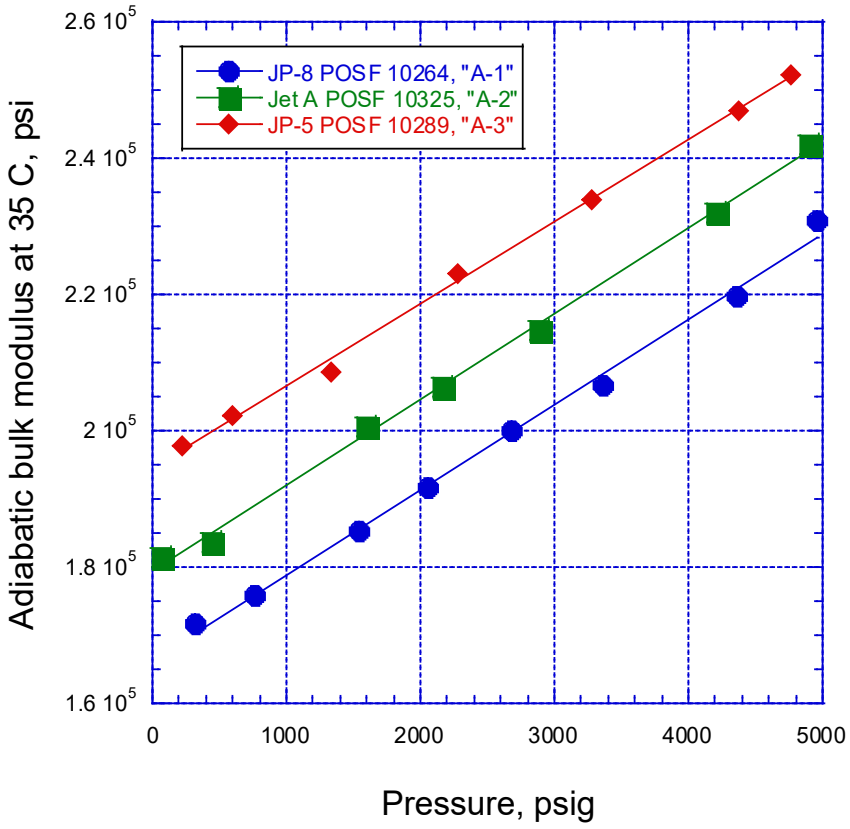

Figure 77 – Density as a function of pressure for Jet A/POSF 10325, JP-8/POSF 10264, and JP-5/POSF 10289 (compare to Figure 73 for speed of sound).

Some idea of the magnitude of the differences expected between the bulk modulus of fuels can be gleaned from the Category A fuel data from SwRI in Tables 21, 22, and 23[7] and in Figure 77. Given the discrete nature of the temperatures (35 and 75 °C), it is difficult to compare data for the three fuels at the same density, but it can be seen that lower densities show consistently lower speeds of sound and lower bulk moduli. The effect of density on bulk modulus is discussed further for a wider range of fuels below in the alternative fuel discussion.

10.3 Alternative fuels – Speed of Sound and Bulk Modulus

Data for speed of sound and bulk modulus is available for most of the alternative fuels evaluated from 2006 to the present time[87]. Recently data as a function of pressure has become available[78,80]. As shown in Table 24, the speeds of sound and bulk moduli track with density in this data at atmospheric pressure. More detailed data is available in the Research Reports for the various fuels as a function of pressure in addition to high-pressure density data available in References 72, 74, 75, and 79. An example is shown in Figure 78, where several alternative fuel blends fall within the envelope of the Category A fuels. There is some odd behavior at low pressure, and the speed of sound of two alternative fuel blends could be expected to be lower than that for the A-1 fuels since their density is lower, but this initial data says otherwise. The speed of sound and bulk modulus data for alternative fuels[72,73,74,75,76,87] bears further analysis, but at this point it appears that the alternative fuels and blends should have speeds of sound and bulk moduli similar to that of conventional jet fuels of the same density. But the presence of data sets where density varies with composition (at a fixed T, P) and data

where the density varies with pressure (as above), allows one to attempt to see if the bulk modulus data is best characterized by the density of the fuel. When plotted as a function of density (Figure 79), various alternative fuels and blends in Table 24 track well with density, but the density trends are not coincident with those from fuels where density is varied with pressure. So, density is certainly not the only important parameter. This has been verified at AFRL with a bulk modulus rig similar to that at SwRI. In Figure 80, the bulk modulus for two fuels is shown at two temperatures. The bulk modulus data for the two conventional fuels does not collapse into a single line when plotted versus density. Speed of sound for alternative fuels is linear with temperature[72,73,74,75].

Table 24 – Atmospheric pressure bulk modulus data.[77]

Sample Description	Speed of Sound (m/s) @ 30 °C	Density (g/cm3) @ 30 °C	Isentropic Bulk Modulus (psi) @ 30 °C
HRJ8 (R-8 w/ JP-8 Additives)	1247	0.7503	169,283
R-8/JP-8 50/50	1267	0.7721	179,717
Sasol IPK	1212	0.7497	159,690
Neste Oil NExBTL BioJet	1275	0.7603	179,293
Rentech FT SPK w/ JP-* Additives	1246	0.7512	169,015
HRJ (Tallow)	1241	0.7463	166,620
3HRJ (Camelina)	1220	0.7391	159,600
TS-1	1256	0.7497	171,479
HRJ (Tallow)/JP-8 50/50	1258	0.7697	176,642
HRJ (Camelina)/JP-8 50/50	1247	0.7661	172,710
Shell FT SPK	1205	0.7247	152,657
JP-8	1284	0.8016	191,712
Jet A	1262	0.7873	181,872
Premium Ultra-Low Sulfur Diesel	1329	0.8241	220,966
GEVO	1181	0.7455	150,769
GEVO/JP-8 50/50	1231	0.7701	169,372
Cyclohexane	1228.43(lit 1228.72)	--	--
Cyclohexane	1229.38(lit 1228.72)	--	--
Cyclohexane	1228.47(lit 1228.72)	--	--
Cyclohexane	1228.44(lit 1228.72)	--	--

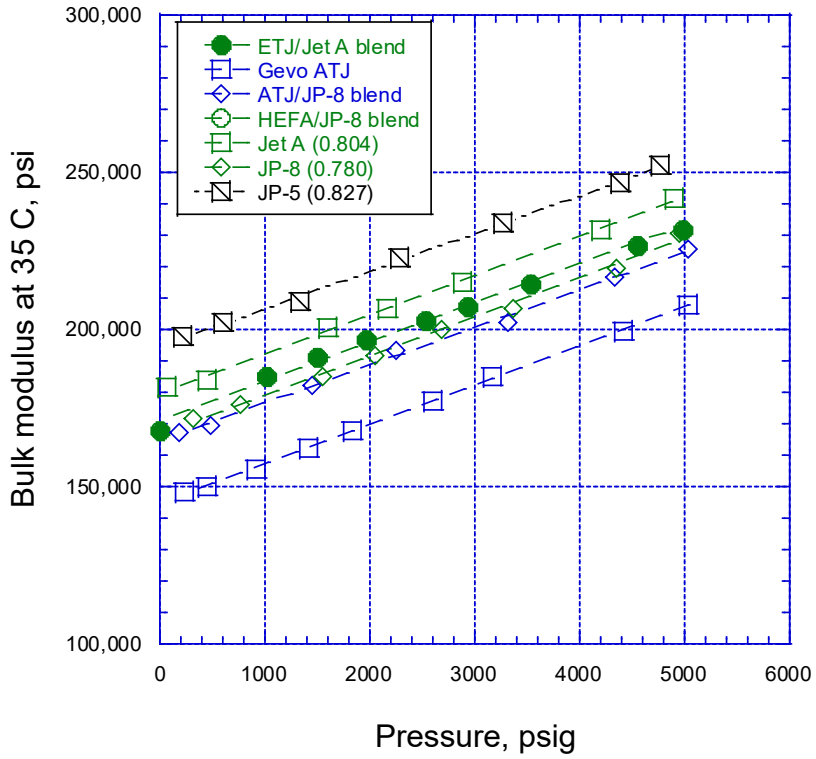

Figure 78 – bulk modulus as a function of pressure (mostly from Reference 7)

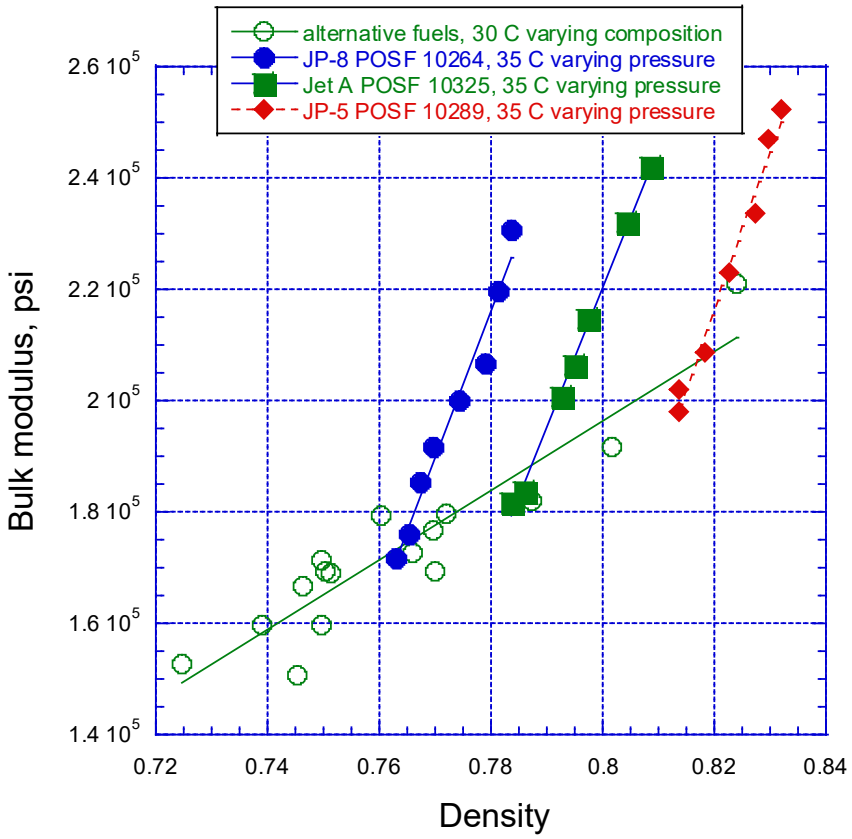

Figure 79 – Bulk modulus as a function of density for Category A fuels

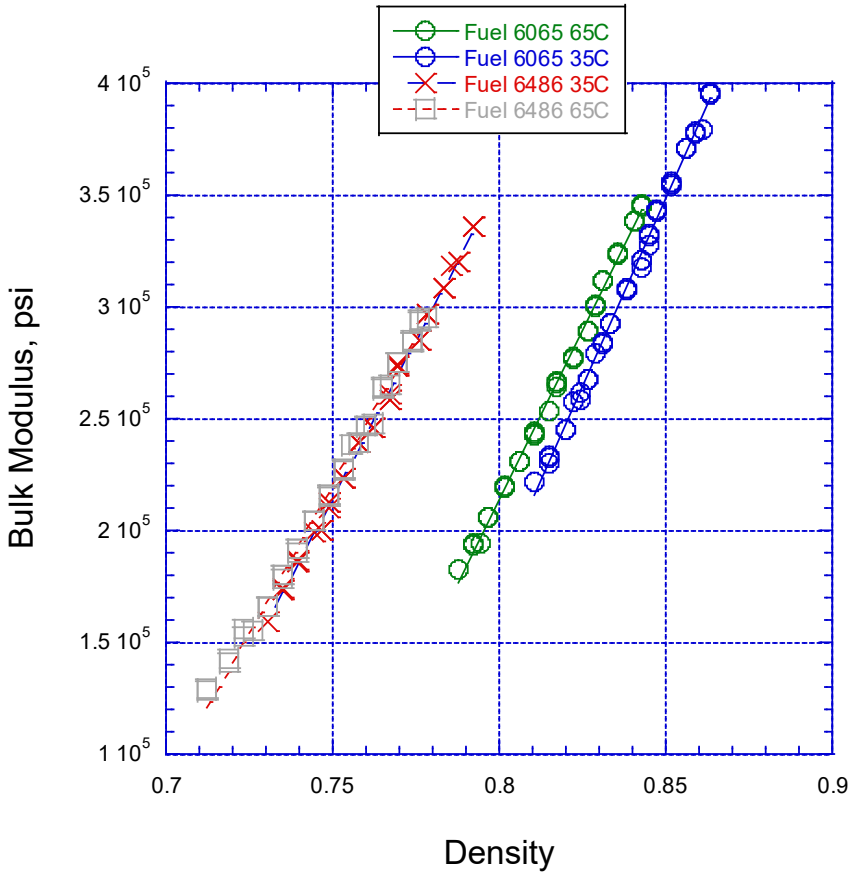

Figure 80 – Bulk modulus versus density for two conventional fuels[81]

Focusing on just the alternative fuels at 30 °C and atmospheric pressure, Figure 81 shows the data with most of the fuels labeled. Highly branched isoparaffinic fuels (Sasol IPK and Gevo ATJ, labeled in blue) seem fall off the trend line a bit – an observation perhaps deserving of further study. In any case, bulk modulus for jet fuels is not a simple function of density or fuel type/composition. Thus, no estimation techniques are presented.

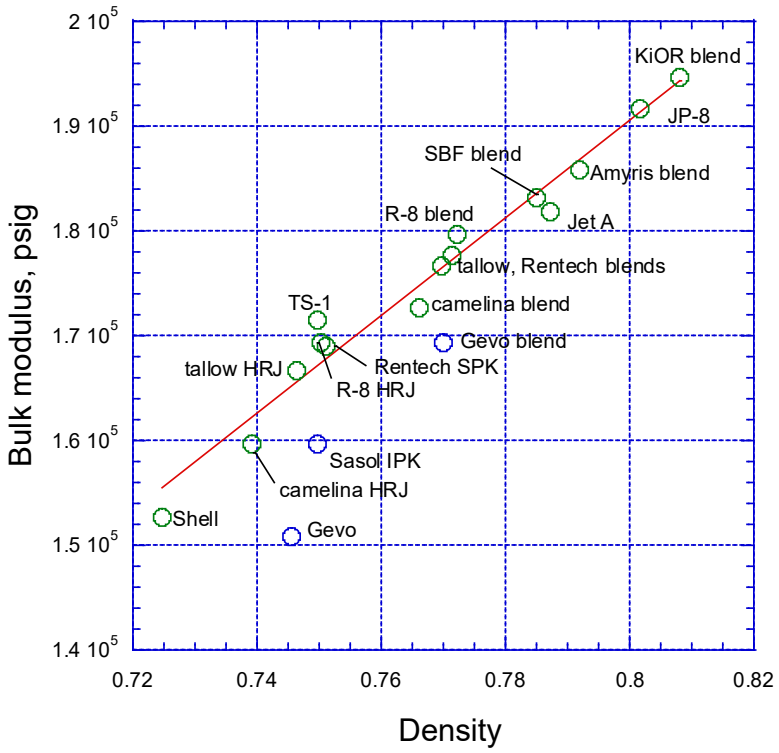

Figure 81 – Atmospheric pressure bulk modulus for various alternative fuels at 30 ℃ as a function of density[77]

11. THERMAL CONDUCTIVITY

The CRC Handbook shows a single line for thermal conductivity versus temperature – for all jet fuels. That is fine as far as it goes – but the line has shifted over the years in the Handbook, and the source of the data is not really known. Several historical data sources were found from 1974 and 1991[82,83,84], but the data is inconsistent. Recent data has been obtained from SwRI for several jet fuels and blends. All of this data is summarized in Figure 82. Reference 82 used a hot wire transient apparatus. Reference 83 used ASTM D2717-95 (Standard Test Method for Thermal Conductivity of Liquids). SwRI technique is cited below[87]:

> "Since most of the literature data for thermal conductivity of liquids is based on hot wire data (referencing ASTM D2717), we sought to acquire an instrument that would provide comparable measurements. One such instrument is the Transient Hot Wire (THW) Liquid Thermal Conductivity Meter from ThermTest, Inc. This instrument uses small test volumes and rapid test times to limit the effects of convection. Verification checks using hydrocarbon standards showed a <2% deviation from literature values across a wide temperature range. The upper temperature limit was generally restricted to less than 50% of the boiling point to avoid non-linear behavior.
>
> In 2014, a method for the use of the THW with liquids was established under ASTM D7896-14."

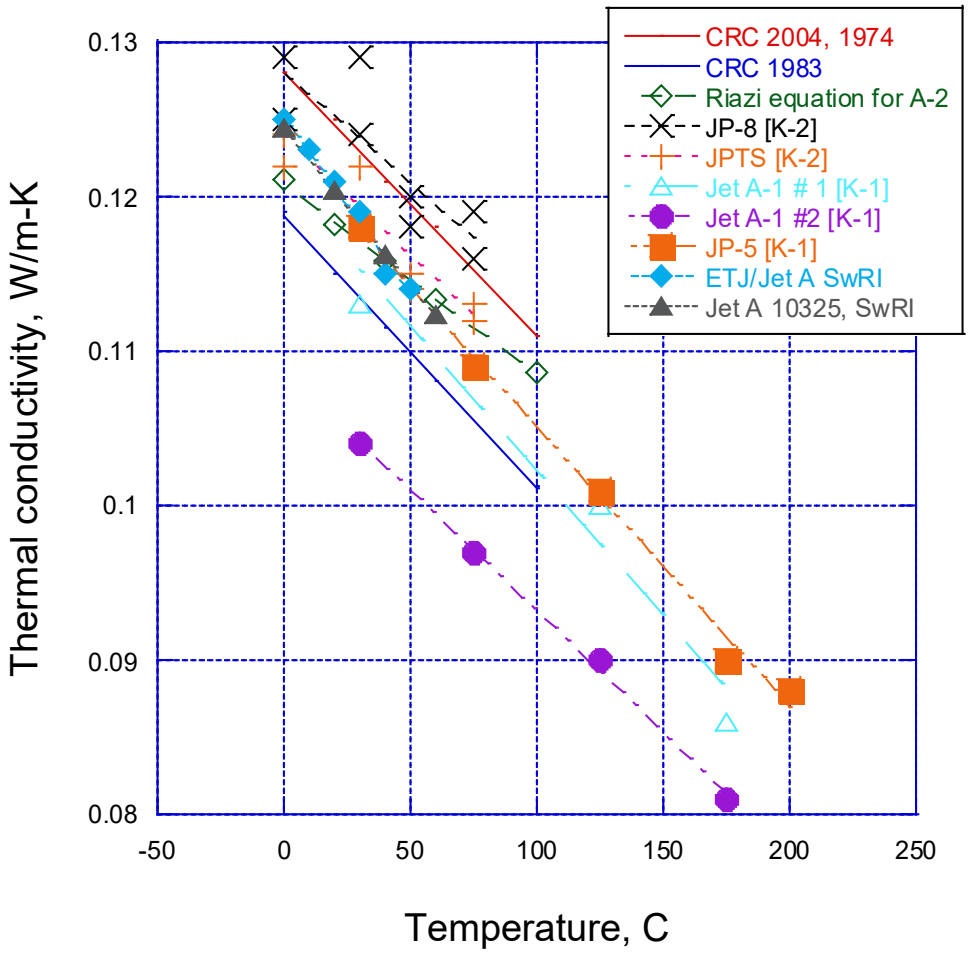

Figure 82 – Experimental and tabulated thermal conductivity data.

ETJ is ethanol-to-jet.

Although the data sets are very inconsistent, they typically show linear decreases in thermal conductivity with temperature, with the preponderance of data falling between the two CRC Handbook lines shown. The CRC Handbook (2012) cites

$$k = 0.1283 - 0.0001738T \ (k \ in \ W/m\ K, T \ in \ C)$$

This equation yields results close to the 1974 Handbook line. Riazi[4] presents an equation for thermal conductivity that basically splits the difference between the two CRC lines (Figure 83) when the values for the A-2 fuel are plugged into the equation.

$$k = 10^{-2}(0.11594T_b^{0.7534}SG^{0.5478} - 2.2989T_b^{0.2983}SG^{0.0094}) \times \left(\frac{1.8T - 460}{300}\right) + 2.2989 \times 10^{-2}\ T_b^{0.2983}SG^{0.0094}$$

where T_b and T are in K and k (thermal conductivity) is in W/m-K. Lefebvre[68] includes a simpler equation:

$$k = \frac{0.134 - 0.000063T}{SG} (T \ in \ K)$$

which yields a thermal conductivity of 0.115 for A-2 at 15 °C, somewhat lower than most of the data in Figure 82. Using the most recent data from SwRI as a benchmark, it seems like the latest calculation method and the most recent data indicate neither CRC Handbook line is very representative of actual fuels. Thermal conductivity appears to be a problematic property. Apparently, knowing its value accurately is not necessary for succcessful aircraft operation.

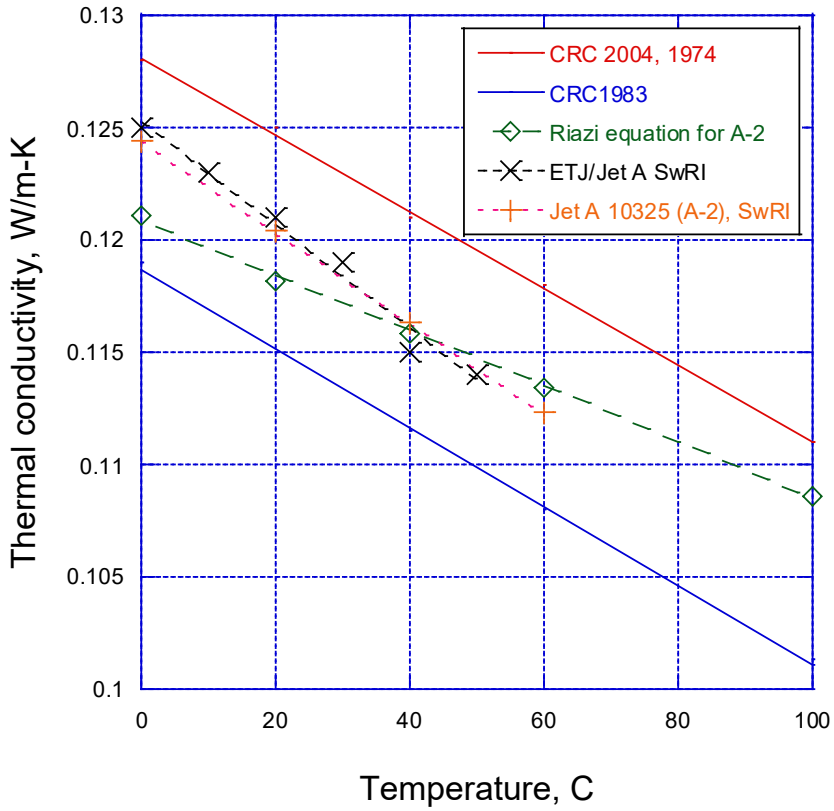

Figure 83 – Thermal conductivity as a function of temperature.

Higher temperature thermal conductivity data (calculations) is available[8,9,10,11,12,13]. The data is shown in Figures 84 (subcritical) and 85 (supercritical). The data is shown in its original English units (1 W/m-K = 0.578 BTU/ft-hr-F), and is apparently calculated. The data is only somewhat consistent with the later CRC line at low temperatures – so higher temperature data is very suspect, especially since the two sets of data with varying pressures show opposite trends with pressure. Caveat emptor.

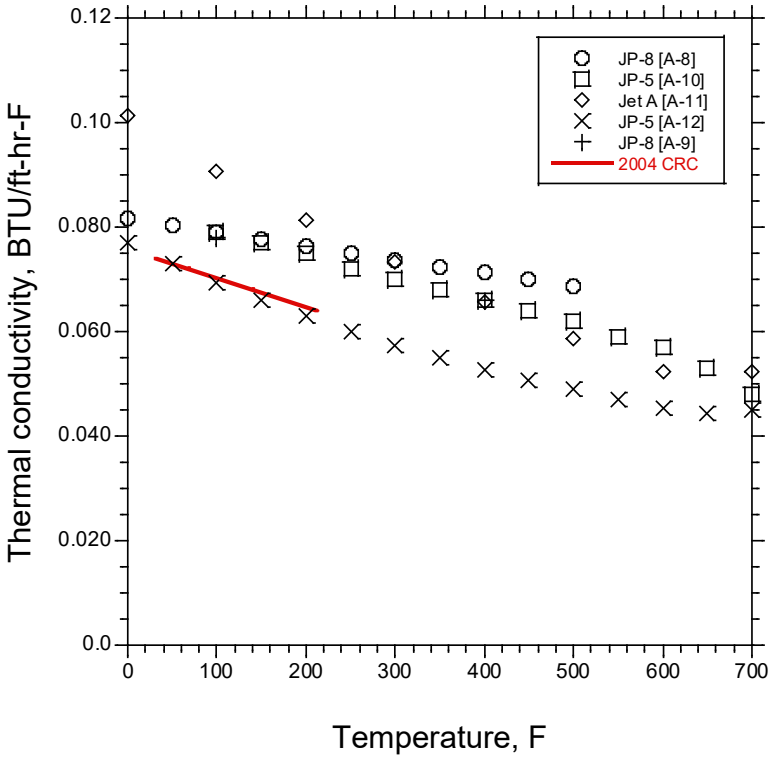

Figure 84 – High temperature (subcritical) thermal conductivity data (calculated).

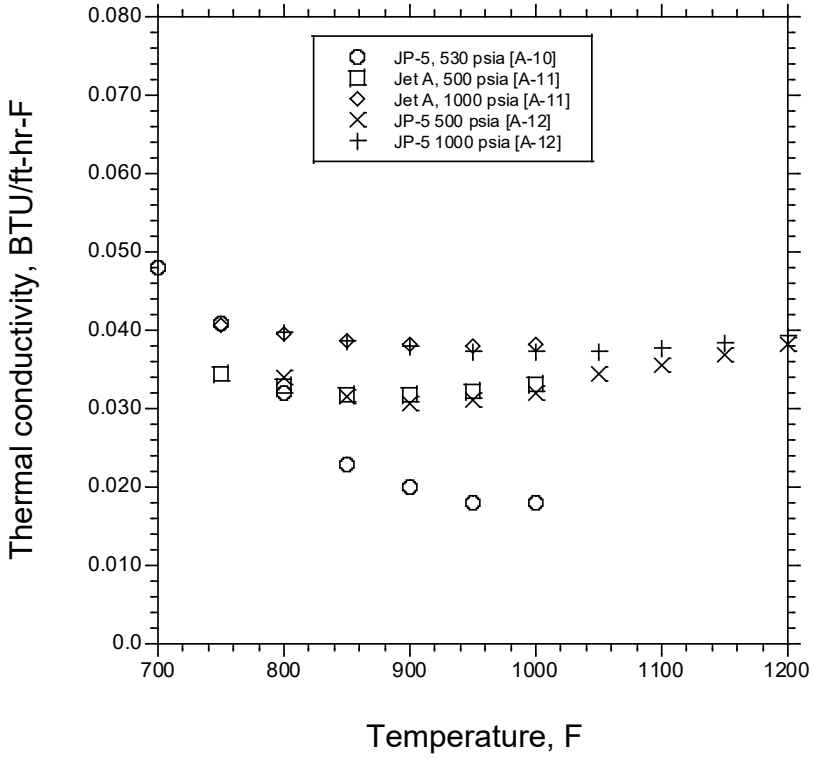

Figure 85 – High temperature (supercritical) thermal conductivity data (calculated)

12. SURFACE TENSION

As a non-specification property, surface tension is a relatively-rarely-measured property that is relevant to fuel atomization in gas turbine combustors (as are viscosity and density). However, "All of these [combustion-related] properties are controlled by the current jet fuel specifications except surface tension, which varies only slightly among kerosene fuels and is of little consequence."[88] Note that surface tension refers to a fuel/air interface, while interfacial tension typically refers to a fuel/water interface. For interfacial tension values (somewhat higher than surface tension), see Reference 85. There are a number of somewhat-inconsistent data sets for surface tension of jet fuels. For the Category A fuels and most alternative fuel blends, there is current surface tension data from SwRI using ASTM D1331A (Standard Test Methods for Surface and Interfacial Tension of Solutions of Paints, Solvents, Solutions of Surface-Active Agents, and Related Materials). This data does not match well with the CRC Handbook data[1] (1983/2004 Handbook line is lower, later Handbook lines are higher) or with the World Survey data using D971 (Standard Test Method for Interfacial Tension of Oil Against Water by the Ring Method)[2]. To quote the 2012 Handbook: "The surface tension values from the original NACA TN 3276 handbook, as well as previous versions of the CRC Handbook of Aviation Fuel Properties, used the Ramsey-Shields Eötvös correlation to generate surface tension values." The 2012 Handbook references new surface tension data from NRL: "Surface tensions of aviation fuels were measured as a function of temperature using an automated tensiometer to perform the bubble pressure method." The World Survey cites D971 measurements, which seems a bit odd since D971 is an interfacial tension method. Quoting the World Survey:

> "ASTM D 971, "Standard Test Method for Interfacial Tension of Oil Against Water by the Ring Method" was the test method used by SwRI to determine the surface tension for fuel samples. This method is typically used for mineral oils. However, because a standard test method for the surface tension of aviation fuels does not exist, it is occasionally used for this purpose. Surface tension in this method is a function of the force required for a platinum ring to be pulled through a fuel/water interface, the densities of the fuel and water, and the dimensions of the ring."

More recent measurements by UDRI[85] and the U.S. Naval Academy[89,90] use variations of the pendant drop method where surface tension is calculated from droplet shape measurements. This data has been reported to be consistent with the (new/2012) CRC Handbook data. Although the absolute values of surface tension obtained by these various techniques does show some variation, there are some consistencies

1) Surface tension decreases very linearly between roughly -40 °C and +100 °C
2) Amongst a group of jet fuels, variations in surface tension appear to correlate with density, with higher-density fuels having higher surface tensions.
3) There may be secondary effect of fuel hydrocarbon type[85].

Thus, comparing the absolute values of the surface tensions from the various techniques would require comparing fuels of the same density and composition. The data sets don't allow that, although SwRI and UDRI have both measured the surface tension of the same JP-5 fuel (POSF 10289), while the World Survey shows surface tension for a JP-5 fuel of similar density at 22 °C (Fuel 039). Comparing these four data sets yields Figure 86. One can see that for similar fuels with similar densities, there is still an offset between the data sets, apparently due to differences in the methods. The discussion that follows will evaluate some aspects of the various data sets to glean further insights.

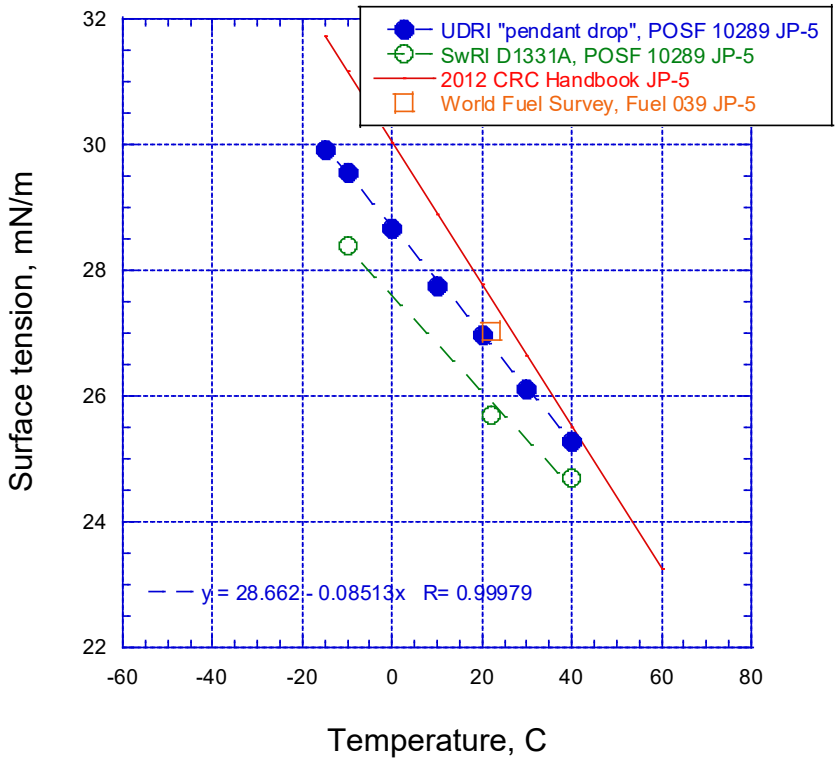

Figure 86 – Comparison of JP-5 surface tension as a function of temperature for the UDRI pendant drop method[85], the SwRI D1331A method[87], the World Fuel Survey D971 method[2], and the 2012 CRC Handbook JP-5 line[1].

As mentioned previously (and also mentioned in the cited references), density appears to be a significant correlating parameter. The CRC Handbook handles this by separating fuels by class (and thus density: JP-TS having a lower surface tension (and density) than Jet A/Jet A-1/JP-8, which have lower surface tensions and density than JP-5. The World Survey includes mostly Jet A/Jet A-1, although the lowest density fuel in the Survey (the Sasol synthetic jet fuel) also has the lowest thermal conductivity. One might (vainly) hope that plotting surface tension as a function of density might collapse all of the data onto a single line, as was done previously for some of the other properties. As can be seen from Figure 87, there is definitely a correlation with density, but there is significant scatter. The scatter may be due to the test method, or may be due to another factor such as composition.

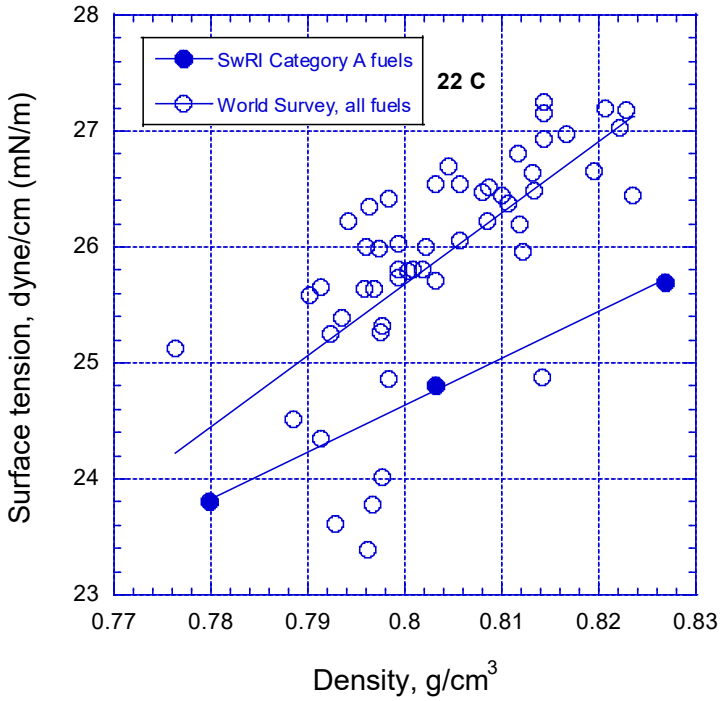

Figure 87 – Surface tension (22 ℃) vs. density data (15 ℃) for various fuels from the World Survey[2]

Some clues as to the impact of composition as the secondary factor can be gained from pure component surface tension data[86]. If one plots pure component surface tension data as a function of density (Figure 88[86]), the linear trend of Figure 87 is reproduced. Also evident is a disconnect between the n-paraffins and the cycloparaffins/aromatics in terms of the slope of the surface tension – density line. This chemical class difference may help to explain some of the scatter in Figure 87. However, the smaller UDRI data set shows less variation when surface tension is plotted as a function of density, as will be discussed below in the alternative fuels section (Figure 89).

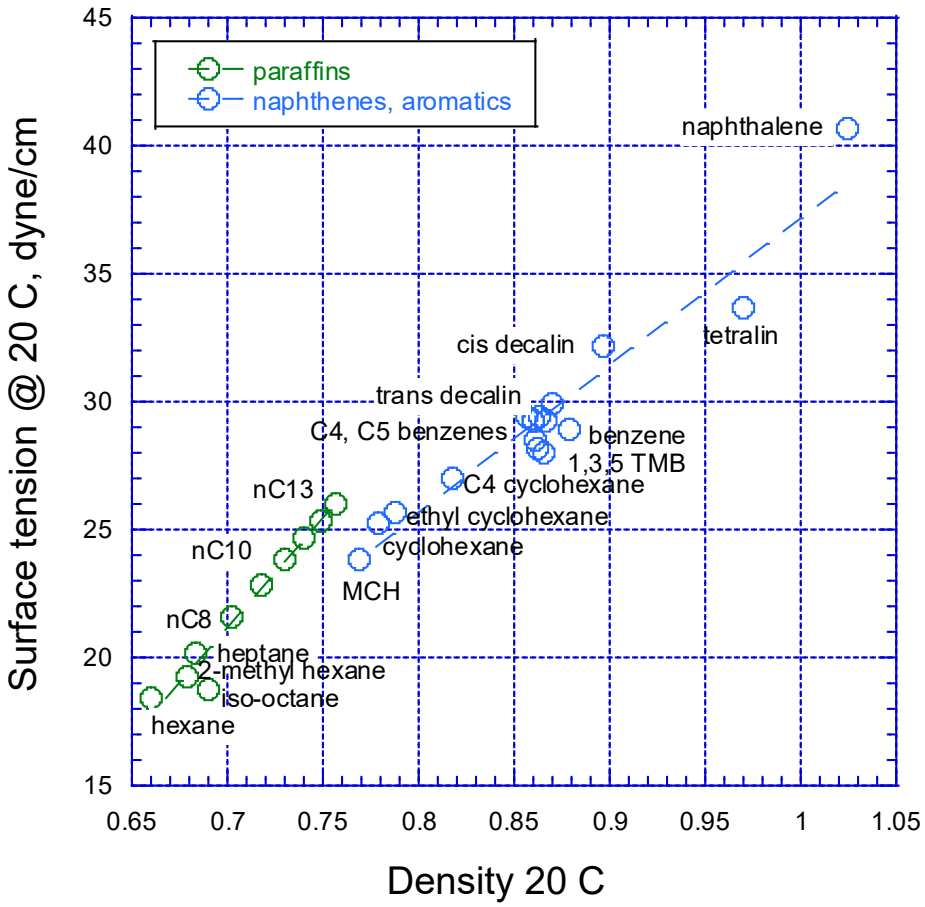

Figure 88 – Pure component surface tension data[86]

12.1 Alternative fuels

The surface tension data for certification of alternative fuel blends (reminder - acronym decoder in Table 4) was generally measured at SwRI using ASTM D1331[77,87,16]. In general, the surface tension for the blends as a function of temperature was very linear, and consistent with conventional fuels of the same density. UDRI has acquired surface tension data for a number of neat alternative fuels and other fuels[85 and unpublished]. As shown in Figure 89, over a wide range of density (much wider than permitted in the jet fuel specification), surface tension at a given temperature is well represented by a linear correlation with density (at the specification temperature of 15 °C).

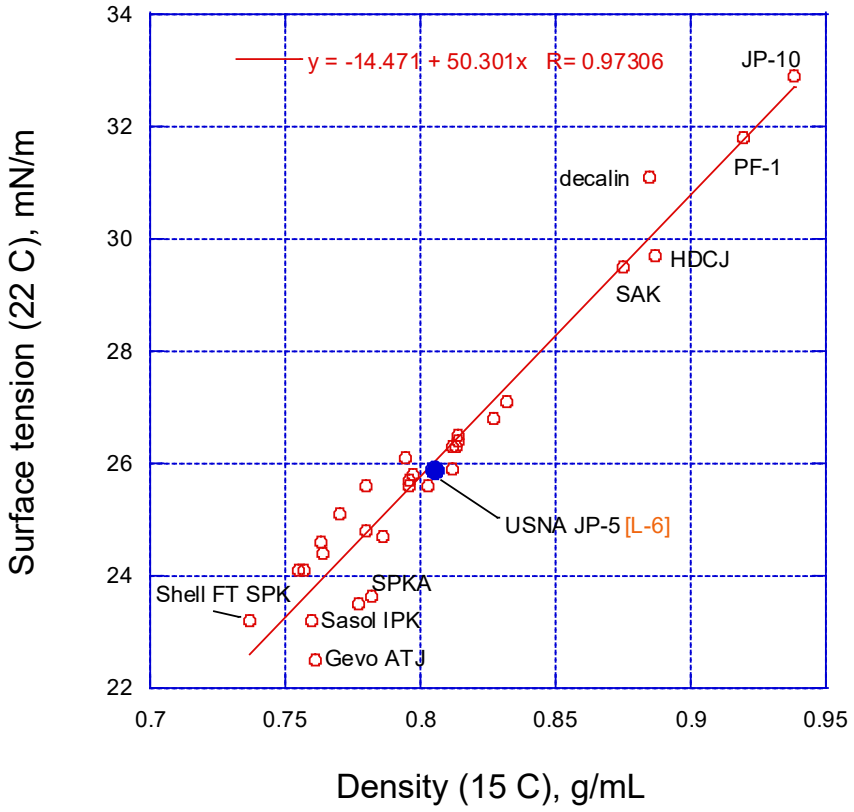

Figure 89 – Surface tension as a function of temperature.

12.2 Estimation

The most straightforward way to estimate surface tension for a fuel with a known density is to use Figure 89 to estimate the surface tension at 22 °C, then use the slope of the line in Figure 86 to correct for temperature. This should be more accurate than using the equations in the CRC Handbook. If one wanted to calculate the surface tension, Riazi[4] (p. 359) has a surface tension equation as a function of reduced temperature ($T_r = T/T_c$) and K_w (Watson K factor).

$$\sigma = \frac{673.7(1 - T_r)^{1.232}}{K_W}$$

K_w is inversely proportional to density (as mentioned earlier), but also includes a boiling point term which brings in the paraffinicity of the fuel. Using this equation for the Category A fuels produces a surface tension significantly higher than any of the measured data (e.g., POSF 10289 JP-5 is predicted to have a surface tension of ~29 mN/m (or dyne/cm) at 22 °C, well above the values shown in Figure 86[14]). Lefebvre[68] shows a graph of surface tension versus T that is consistent with the earlier CRC Handbook data and thus is low compared to current measurements), and references Barnett and Hibbard[15] – the source for the early Handbook data.

13. DIELECTRIC CONSTANT

As mentioned earlier, fuel dielectric constant/permittivity is an important property for most fuel gauges[71,91,92]. There is data for dielectric constant versus temperature in the CRC Handbook[1] and in the CRC World Survey[2]. Riazi states that the dielectric constant is the square of the refractive index for simple molecules, although this relationship breaks down for more complex species[4]. Since refractive index is directly related to density, it is no surprise that dielectric constant measurements are usually presented as a function of density. The World Survey dielectric constant measurements were made by Goodrich, whereas most of the measurements made on alternative fuels and blends were made by SwRI (with Goodrich's instrument). There has been some industry dis-satisfaction with the results for alternative fuels, although eventually all the alternative fuel blends undergoing approval were judged to have acceptable dielectric constant values. This is discussed in more detail in the alternative fuel section below. Goodrich has also looked at the effect of the JP-8+100 additive (a strong surfactant) on dielectric constant and found the additive to have a negligible effect on dielectric constant and fuel gauging[93].

The World Survey data shows some interesting trends. When plotted versus density, the dielectric constant data roughly collapses onto a single curve, although three fuels stand out a bit (Figure 90). Those three fuels are the highest density fuels in the survey, and also have the highest cycloparaffin content by GCxGC. For fuel 020, 111, and 211, the cycloparaffin contents are 63.2, 50.8, and 57.5 mass%, respectively. The next highest cycloparaffin content in the Survey was 45%. The slopes of the lines are similar, but the three fuels appear to be displaced in terms of dielectric constant. Thus, density is the primary correlating factor, but cycloparaffin content appears to also be important. Although ASTM D4054 implies that alternative fuels only need to fall within the scatter of the World Survey data to be acceptable, some in industry are more interested in the slope of the dielectric constant-versus-density line, although their data review process has not been completely disclosed.

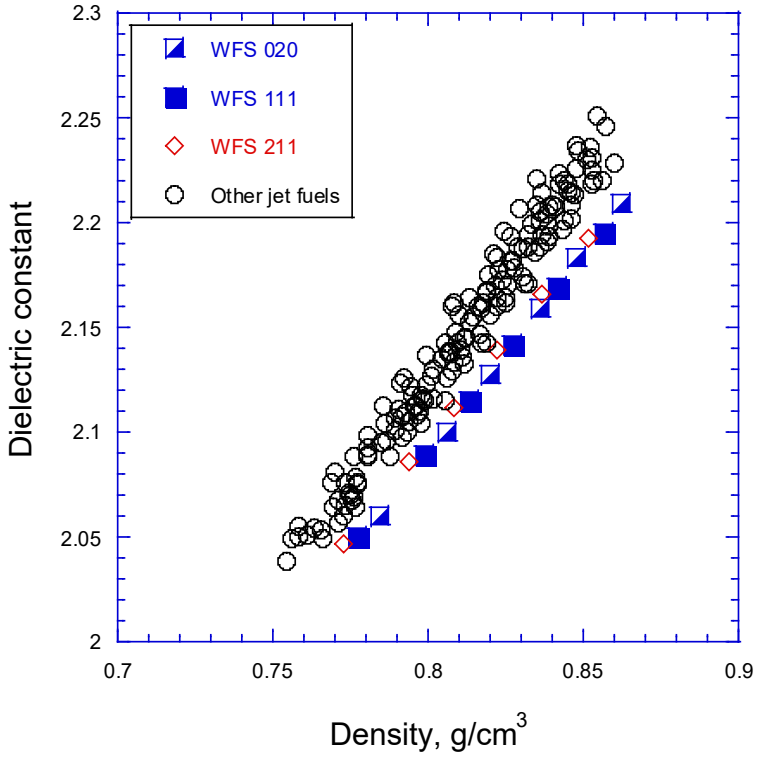

Figure 90 – Dielectric constant versus density for World Survey.

Airbus has presented a somewhat different picture of how dielectric constant affects fuel gauging[71,92]. The basis of this assessment is the Clausius-Mossati relationship:

$$D = (K-1) / [A + B(K-1)]$$

where D is the fuel density, K is the dielectric constant, and A and B are constants, with the A for Jet A being reported as 1.0 ± 10% and B being 0.3658[71]. The relevance to fuel gauging assessment can be seen by rearranging:

$$(K-1)/D = A + B(K-1)$$

Thus, if one plots (K-1)/D versus K-1, a least squares fit can give A and B.

Thus, Airbus assesses the dielectric constant (aka permittivity) behavior on a plot of (K-1)/D versus K-1, replotted as Figure 91. There are two sets of data in Figure 91, the usual World Survey data[2] and a similar data set from ARINC[95]. To generate the best-fit line, the data sets are taken as a whole. Taking each individual fuel set as a separate line and averaging the slopes produces a similar "best fit" line for the World Survey fuels. The best-fit equations are what is used in the fuel gauging software to predict density and fuel load. The best fit for the CRC data is very close to published values for A and B[71].

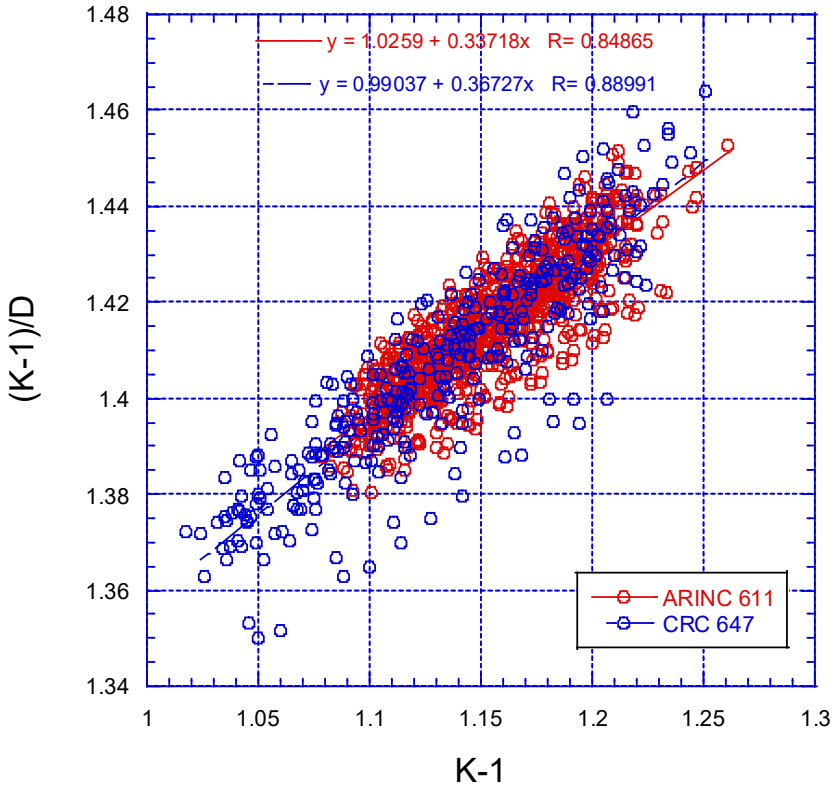

Figure 91 – Dielectric constant data plotted as Clausius-Mossati relationship

An error analysis of the effect of new dielectric constant data on fuel gauging can be done by fixing B and using dielectric constant and density data at 20 °C, for example, to fix A. Then density at -40 °C, for example, can be predicted using this relationship and compared to measured density data[71,92,94]. The difference between calculated and estimated value is expected to be < 1.2% for effective fuel gauging. For fuels with slopes of (K-1)/D vs K-1 very different from standard fuels, this criterion will not be met.

13.1 Alternative fuels

Alternative fuel dielectric constant measurements by SwRI produced the type of results shown in Figure 93. One can see that the alternative fuels blends fall within the scatter of the World Survey data, although there appears that the slope of the lines might be slightly lower for alternative fuels. This has become an issue. If one plots the slope of these lines for various alternative fuels (from SwRI measurements) and includes the World Survey slopes, Figure 94 is produced. Although the scatter is large, one can see that the SwRI slopes are consistently less than those in the World Survey, even though the same equipment is being used. Thus far, industry seems to believe that this is an instrument issue, rather than an alternative fuel composition issue. However, it has been a deterrent to alternative fuel approvals. Plotting the data in the Clausius-Mossati manner leads to a similar conclusion: the B for the SwRI measurements is measurably less than that for the CRC World Survey and ARINC data sets. However, it should be noted that conventional fuels have similar slopes to alternative fuels in the SwRI data sets, indicating the slope difference is instrument-related, rather than fuel composition-related.

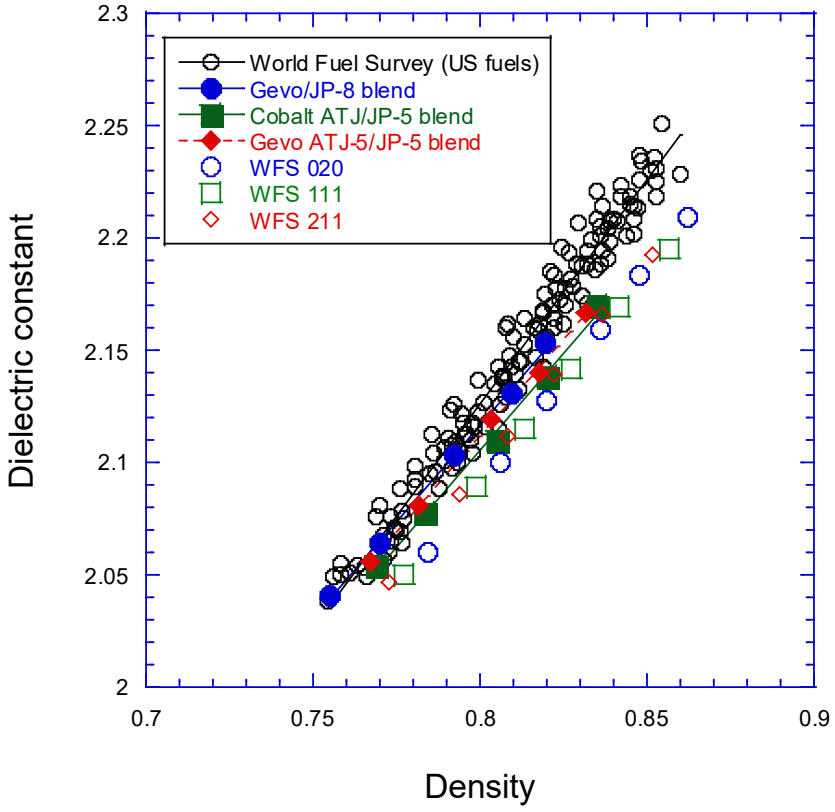

Figure 93 – Dielectric versus density for various fuels.

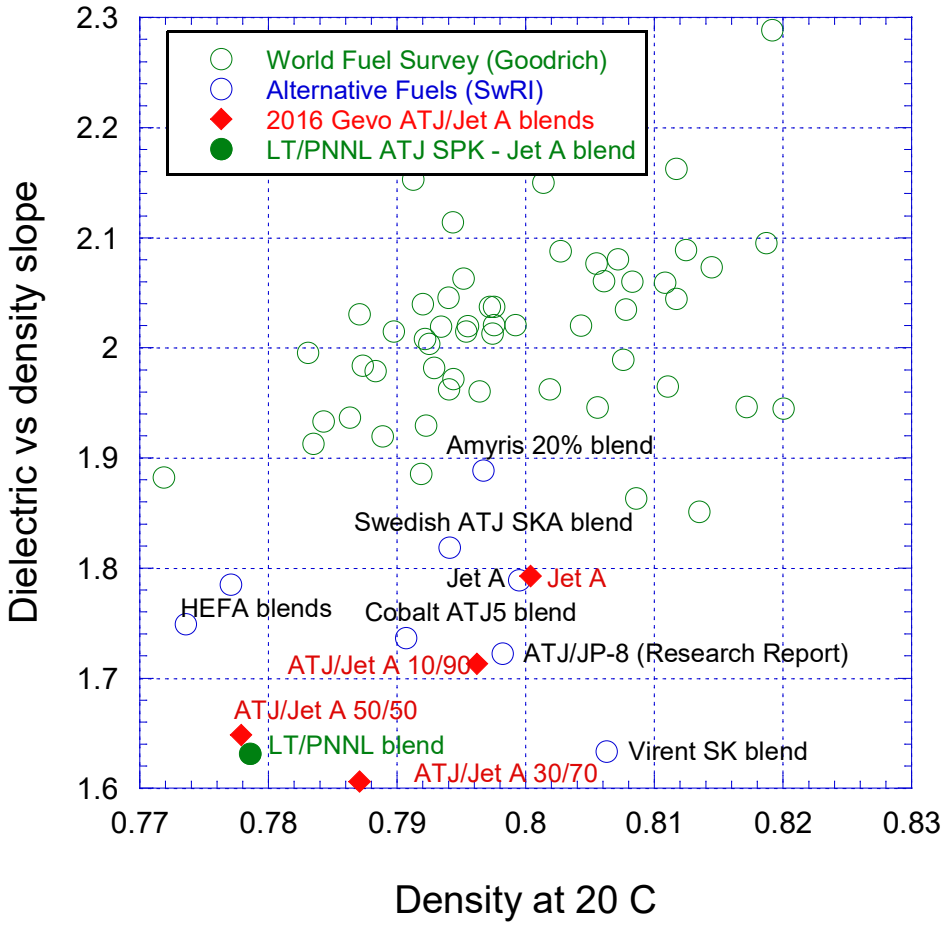

Figure 94 – Slope of dielectric constant-versus-density lines (e.g., Figure 93) for various fuels

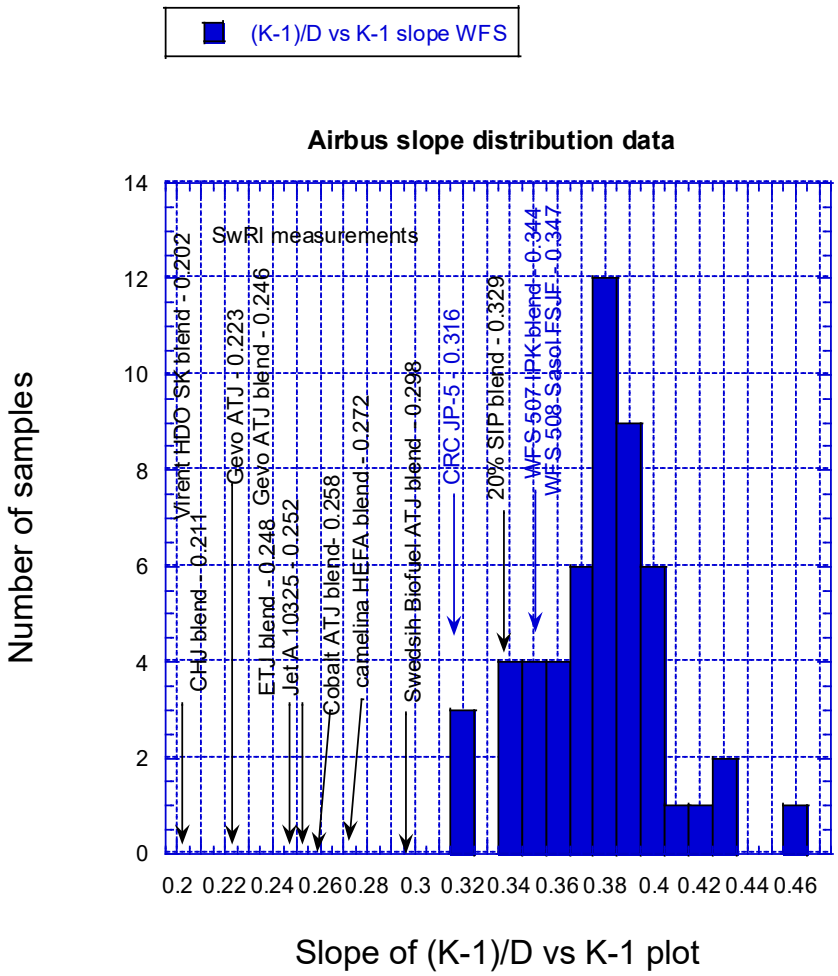

Figure 95 – Statistical distribution of slopes in Clausius-Mossati plot

14. DISSOLVED GASES

Liquid fuel exposed to air rapidly picks up dissolved oxygen and nitrogen (and a bit of argon and CO_2). As it says in the CRC Handbook, "The solubility of gases in fuels is important in the design of fuel systems and their components. High evolution of gases resulting from decreased atmospheric pressure during climb can cause fuel to foam out of the tank vents. When pumping fuel, gas phase separation can occur leading to vapor lock or cavitation problems"[1]. The dissolved oxygen in jet fuel (~70 to 80 ppm mass at ambient pressure and temperature) is crucial to thermal instability[96]. The CRC Handbook[1] has equations and charts for the solubility of oxygen, nitrogen, air, and CO_2 as a function of temperature. The data is presented as Ostwald coefficient (volume of gas dissolved in one volume of solvent, gas volume measured at conditions of solution) and Bunsen coefficient (solubility of gas, expressed as the gas volume reduced to 273 °K (32 °F) and 1 atm, dissolved by one volume of liquid at the specified temperature and 1 atm). These coefficients are typically calculated using ASTM D2779 (Standard Test Method for Estimation of Solubility of Gases in Petroleum Liquids) or D3827 (Standard Test Method for Estimation of Solubility of Gases in Petroleum and Other Organic Liquids).

In thermal stability tests with jet fuels where the oxygen content was monitored, an on-line method was developed to get an accurate measurement without exposing the fuel to atmospheric oxygen[97,98,99]. For alternative fuels, direct measurements were made of dissolved gases in air-saturated fuel at ambient temperature and pressure to ensure that alternative fuels and blends fell within experience for dissolved gas content. As expected from ASTM D2779, the results typically tracked with fuel density, as shown in Figure 96[100,101]. These UDRI measurements are consistent with other literature data[15,102,1] when converted to Ostwald coefficient, as shown in Figure 97. The more recent versions of the CRC Handbook have some inconsistencies with the 1983 version, with the equations and charts showing significant higher air solubilities. It isn't clear if the oxygen solubility refers to an oxygen dissolved in fuel exposed to air or to 100% oxygen. However, the chart for air solubility in the most recent Handbook has Ostwald coefficients about 50% higher than the 1983 chart.

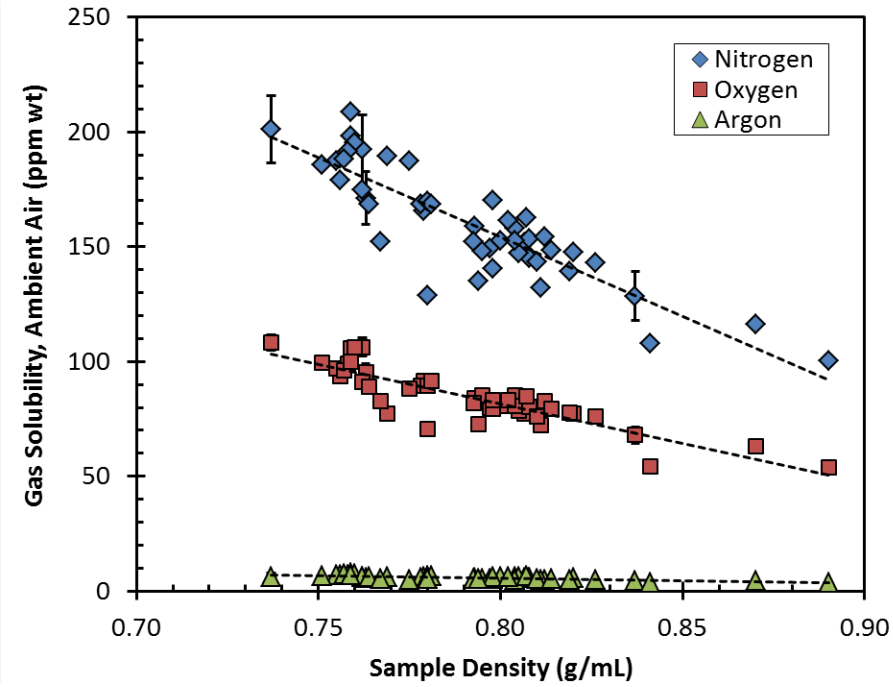

Figure 96 – Dissolved gases in jet fuels as a function of density[100].

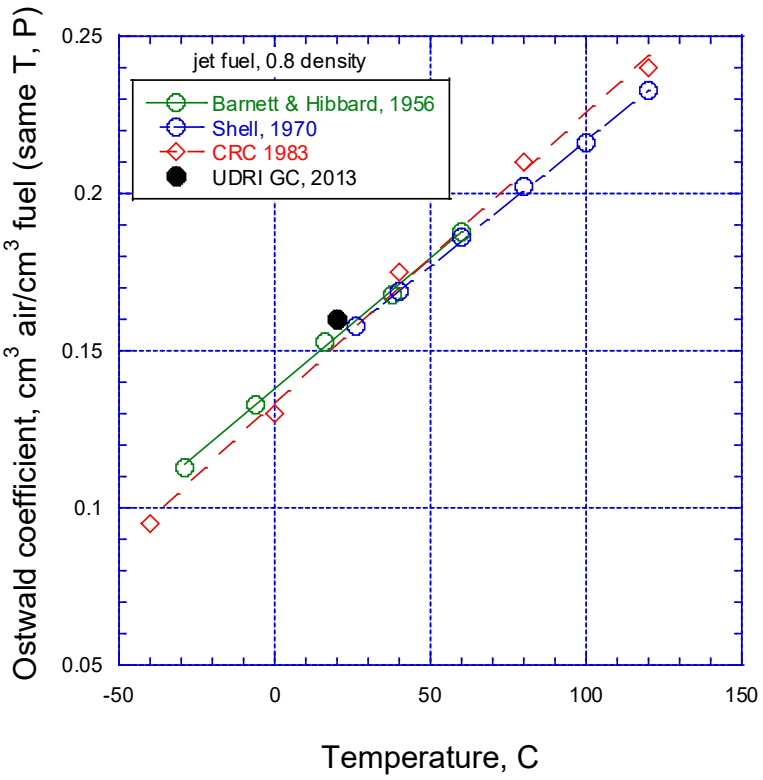

Figure 97 – Comparison of Ostwald coefficients for air for literature data and for Data in Figure 96 converted to Ostwald coefficient.

14.1 Alternative fuels

Perhaps not surprisingly, alternative fuels have air solubilities consistent with their densities, as shown in Figure 98[100]. The data shown as air is the sum of the separate N_2, O_2, and argon measurements in Figure 96. The consistent falling below the line of F-76 (marine diesel fuel) remains to be explained.

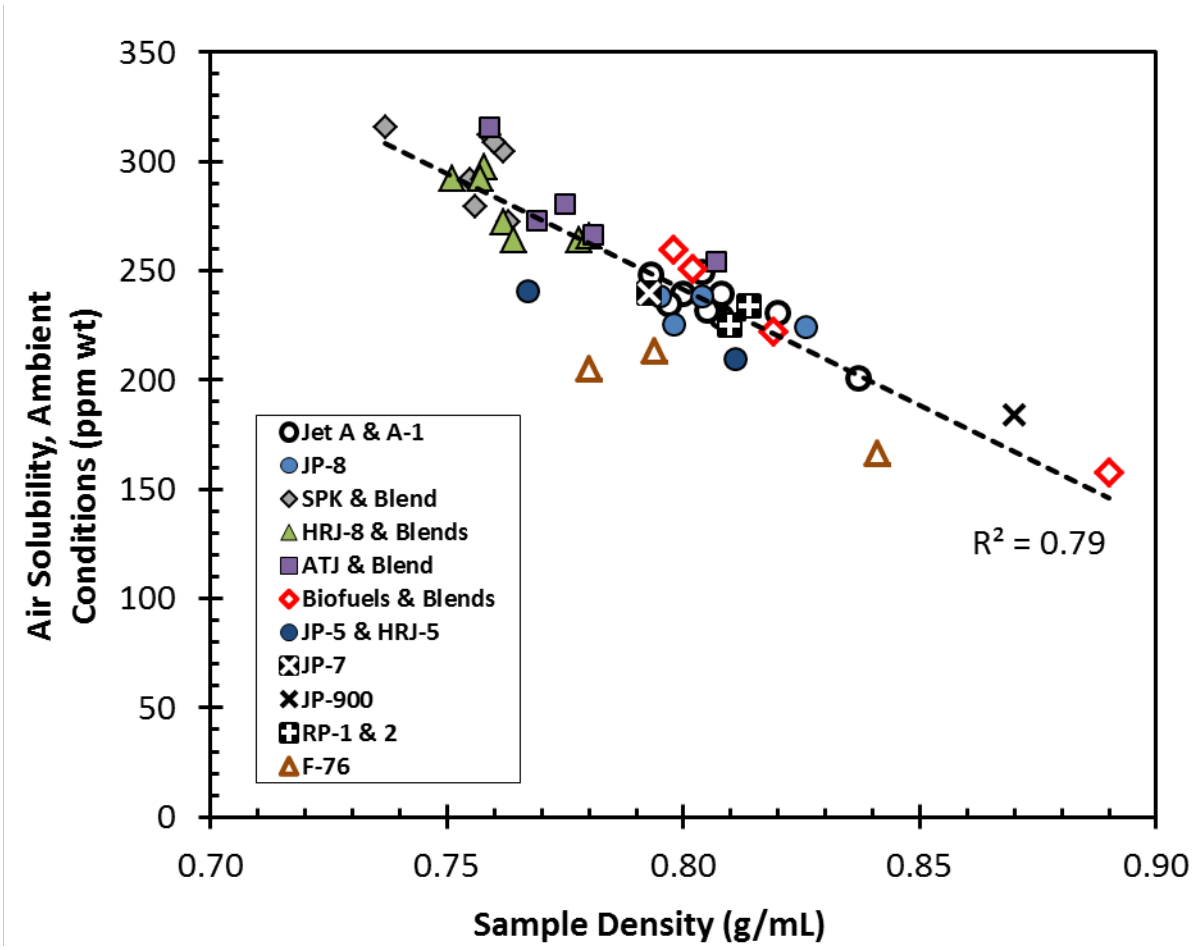

Figure 98 – Air solubility of various fuels, blend stocks, and blends under ambient conditions[100].

15. LUBRICITY

Lubricity, at least in the context of jet fuel, is the lubricating quality of jet fuel during use in fuel controls, fuel pumps, and other fuel system components. ASTM D1655-18 states:

> "Aircraft/engine fuel system components and fuel control units rely on the fuel to lubricate their sliding parts. The effectiveness of a jet fuel as a lubricant in such equipment is referred to as its *lubricity*. Differences in fuel system component design and materials result in varying degrees of equipment sensitivity to fuel lubricity. Similarly, jet fuels vary in their level of lubricity. In-service problems experienced have ranged in severity from reductions in pump flow to unexpected mechanical failure leading to in-flight engine shutdown."

A thorough discussion of this is beyond the scope of this report (and the capability of the author) – a good place to start are several CRC reports[103,107,109]. Military issues with fuel lubricity led to the development and use of a corrosion inhibitor/lubricity additive in the JP-8 and JP-5 specifications[104, 105,108, 116]. The additives are permitted (not mandated) in ASTM D1655. Various types of test devices have been used to characterize jet fuel (and diesel fuel) lubricity[117]. The various test methods include ASTM D5001 (Standard Test Method for Measurement of Lubricity of Aviation Turbine Fuels by the Ball-on-Cylinder Lubricity Evaluator (BOCLE)[113]), ASTM D6078 (Standard Test Method for Evaluating Lubricity of Diesel Fuels by the Scuffing Load Ball-on-Cylinder Lubricity Evaluator (SLBOCLE)[115]), and ASTM D6079 (Standard Test Method for Evaluating Lubricity of Diesel Fuels by the High-Frequency Reciprocating Rig (HFRR)[114]). The jet fuel lubricity limit is not in the required section of the specification, but rather is in the Appendix in Section X1.10.3, where acceptable lubricity is defined as an ASTM D5001 (BOCLE) wear scar diameter (WSD) on <0.85 mm for aviation fuels.

15.1 Alternative Fuels

Alternative/synthetic fuels in their un-additized state were expected to have poor lubricity given their similarity to the severely hydroprocessed jet fuels described in ASTM D1655 (and some would cite their lack of aromatics [106]). As shown in Table 25, alternative fuels typically did have lower lubricity in their non-additized state than after the addition of CI/LI additive[110]. The main reason the data is sketchy is that lubricity testing usually became a focus only on the final fuel blend, rather than the neat alternative fuel. One of the fit-for-purpose tests listed in ASTM D4054 (Standard Practice for Evaluation of New Aviation Turbine Fuels and Fuel Additives) involves clay treating the alternative fuel (blend) and then measuring lubricity (wear scar diameter or WSD) as CI/LI is added. Typical results are shown in Figure 99. CI/LI additive was always found to be effective in reducing the BOCLE WSD in alternative fuel blends. Note that the clay-treating increases the wear scar diameter (worsens the lubricity) for the ETJ/Jet A blend, as expected.

Aircraft fuel pump endurance testing[111,112] with unadditized alternative fuels demonstrated that hardened aircraft fuel pumps could last 1000 hours even in the absence of CI/LI. This was not the case for ground vehicle fuel pumps (e.g., [121]). AF- and Army-funded testing demonstrated dramatic life reductions with low-lubricity alternative fuels (Table 26). HFRR and SLBOCLE testing of alternative fuel blends gave results consistent with conventional fuels, including a lack of response to CI/LI additive.

Table 25 – Lubricity results for alternative fuels with and without CI/LI.

Fuel	Companies	POSF	D5001 WSD w/o CI/LI	D5001 WSD w/ CI/LI
Synthetic Paraffinic Kerosene (SPK)	Sasol IPK	7629	n/a	0.60, 0.62
	Shell SPK	5729	n/a	0.70
	Syntroleum S-8	5018	n/a	0.56, 0.60
Hydroprocessed Esters and Fatty Acids (HEFA, aka HRJ)	UOP camelina	10301	n/a	0.54, 0.61
	UOP tallow	10298	0.82	n/a
	Dynamic Fuels (mixed fats)	7635	0.72	n/a
ATJ SPK	Gevo (isobutanol)	11498	0.80, 0.78	n/a
CHJ	ARA	8455	0.52	n/a

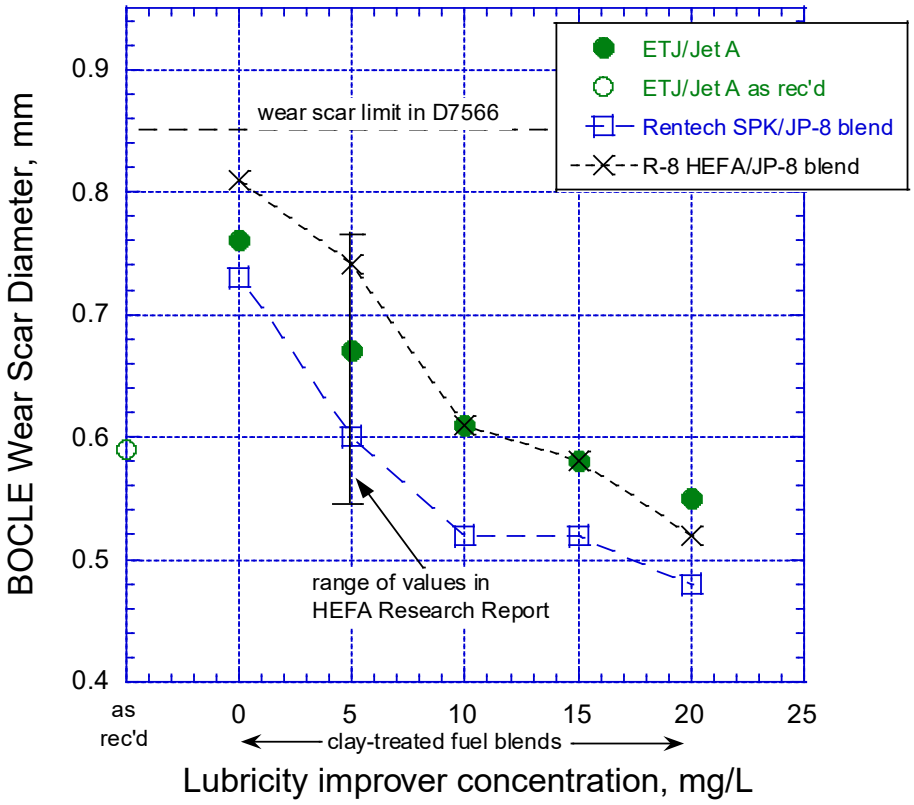

Figure 99 – Typical alternative fuel blend response to CI/LI additive

Table 26 – Effect of lubricity additive (and BOCLE wear scar) on diesel engine pump life.

Fuel	ASTM D5001 WSD, mm	Stanadyne pump life, hrs	Observations
R-8 HEFA + 22.5 ppm DCI-4A	0.6	500	"R-8 fuel with 22.5-ppm DCI-4A CI/LI additive was slightly more erratic in fuel delivery throughout the 500-hour test"
R-8 HEFA/Jet A 50/50 blend + 22.5 ppm DCI-4A		500	"R-8/Jet-A fuel blend with 22.5-ppm DCI-4A CI/LI additive had slightly less component wear, and slightly better 500-hour delivery performance."
R-8 HEFA + 8.5 ppm DCI-4A	0.75	500	"Although the 0.75-mm BOCLE wear scar R-8 fuel completed 500-hours of operation there was performance degradation of the fuel injection pumps, such that engine peak torque would be decreased, the engine peak power would be decreased, and with the cranking speed delivery at zero, an engine would be unable to start with these pumps. This additive treatment level for R-8 fuel would not be recommended for diesel engine use."
R-8 HEFA + 2.75 ppm DCI-4A	0.85	183	"The 0.83-mm BOCLE wear scar R-8 fuel completed only 183-hours of operation due to substantial over-fuelling by the fuel injection pumps, such that exhaust black smoke would increase at all conditions, the cranking speed delivery increase would cause white smoke, possibly too rich to ignite, and half of the fuel injectors exhibited performance degradation that would impact engine operation and emissions. This additive treatment level for R-8 fuel is ineffectual in providing proper diesel engine rotary fuel injection pump wear protection"
R-8 HEFA (neat)	0.87	25	"Initial tests with R-8 HRJ [HEFA] fuels revealed severe wear and extreme life reduction of rotary fuel injection pumps for diesel engines. The untreated R-8 HRJ fuel caused performance degrading wear on rotary fuel injection pumps within 25-hours of operation on the untreated fuel."

16. SUMMARY

If the reader has suffered through this report to this point, he or she will have noticed that the (author's) understanding of several physical properties is relatively inadequate. Specification properties are typically well-behaved and follow expected trends, such as density, viscosity, (measured) net heat of combustion, distillation, flash point, freeze point, H content. However, there are issues with a number of properties:

1) Surface tension – the various test methods appear to show variations outside of the reproducibility of the methods. The methods based on droplet shape appear to be the most consistent and are recommended.

2) Dielectric constant – the differences in the slope of the dielectric constant-versus-density line appears to differ between the benchmark World Survey data and the more recent SwRI measurements. An adequate explanation is not yet apparent. On the positive side, it appears that jet fuels that meet the density/viscosity/flash point/freeze point/distillation limits (including all alternative fuel blends approved through 2019) will have dielectric constants within the range that allows adequate fuel gauging.

3) Speed of sound, bulk modulus – the speed of sound and bulk modulus data is relatively consistent and indicates that density is the primary correlating factor. However, there appears to be a secondary effect of fuel composition that is not adequately understood.

4) Enthalpy, heat of vaporization – data at high pressure seems consistent between historical data and current data being obtained through CRC. That does not appear to be the case for enthalpy of vaporization in multiphase systems.

5) Thermal conductivity – the current approach of assuming all jet fuels fall onto a single line for thermal conductivity versus temperature appears adequate, although the variations between the various test methods have not been adequately explained.

17. REFERENCES

1 Coordinating Research Council, “Handbook of Aviation Fuel Properties,” CRC Report 530 (1983), CRC Report 635 (2004), CRC Report 663 (2012).

2 Hadaller, O. J., & Johnson, J. M., “World Fuel Sampling Program,” Coordinating Research Council Report 647, 2006. (often termed the CRC World Fuel Survey or just “World Fuel Survey” in this report)

3 Defense Logistics Agency (DLA), “Petroleum Quality Information System (PQIS)”, annual reports through 2013, public release; reports 2016 and later DoD only (Distribution E).

4 Riazi, M. R., Characterization and Properties of Petroleum Fractions, ASTM Stock Number: MNL50, ASTM, West Conshohocken, PA, 2005.

5 Nelson, W. L., Petroleum Refinery Engineering, McGraw-Hill, New York, 1958.

6 Maxwell, J. B., Data Book on Hydrocarbons – Application to Process Engineering,” Van Nostrand, NY, 1950.

7 Edwards, T, Hutzler, S, et al., “TRI-SERVICE JET FUEL CHARACTERIZATION FOR DOD APPLICATIONS; Compositional Analysis – Task 1; Fit-For-Purpose and Trace Impurity Evaluations -Task 2 & 3,” SwRI Project 08.17149.36.100, May 2015. Appendices B and C in Bartsch, T. et al., “Engineering Research and Technical Analyses of Advanced Airbreathing Propulsion Fuels,” AFRL-RQ-WP-TR-2015-0017, December 2014.

8 Bucknell, R. L., “Fuels and Lubricants Influence on Turbine Engine Design and Performance (FLITE),” AFAPL-TR-73-52, Vol. II, Jun. 1973. (“FLITE”) (also JP-4,5,7 data)

9 Sumey, I. E., “Fuels and Lubricants Influence on Turbine Engine Design and Performance (FLITE),” AFAPL-TR-73-54, Vol. II, Nov. 1974. (“FLITE”) (also JP-4,5,7 data)

10 TeVelde, J. A., Glickstein, M., “Heat Transfer and Thermal Stability of Alternative Aircraft Fuels – Vol. 1,” NAPC-PE-87C, Nov. 1983 (“UTRC JP-5”)

11 Faith, L. E., et al., “Heat Sink Capability of Jet A Fuel – Heat Transfer and Coking Studies,” NASA CR-72951, July 1971 (“Shell Jet A”).

12 Nixon, A. C., et al., “Vaporizing and Endothermic Fuel for Advanced Engine Application – Part III – Studies of Thermal and Catalytic Reactions, Thermal Stability, and Combustion Properties of Hydrocarbon Fuels,” AFAPL-TR-67-114, Part III. Vol. II, February 1970. (Limited Distribution) (“Shell JP-5”)

13 MacFarlane, W. R., and Wiese, D. E., "Fuel Options for High Mach Propulsion, Vol. II, Fuel Properties," WRDC-TR-90-2090, Oct. 1990.

14 Edwards, T., “Reference Jet Fuels for Combustion Testing,” AIAA 2017-0146, January 2017.

15 Barnett, H. C., and Hibbard, R. R., “Properties of Aircraft Fuels,” NACA TN 3276, August 1956.

16 Moses, C., “Review of Bulk Physical Properties of Synthesized Hydrocarbon: Kerosenes and Blends,” AFRL-RQ-WP-TR-2017-0091, June 2017.

17 Martel, C. R., “Military Jet Fuels, 1944-1987,” Air Force Wright Aeronautical Lab., Rept. AFWAL-TR-87-2062, Nov. 1987.

18 Dukek, W. G., et al., “Milestones in Aviation Fuels,” AIAA 69-779, 1969.

19 Chevron, “Diesel Fuels Technical Review,” 2007 (https://www.chevron.com/-/media/chevron/operations/documents/diesel-fuel-tech-review.pdf) and “Motor Gasolines Technical Review,” 2009.

20 Moses, C., “Comparative Evaluation of Semi-Synthetic Jet Fuels,” final report for CRC Project No. AV-2-04a, September 2008.

21 Moses, C., “Comparative Evaluation of Semi-Synthetic Jet Fuels - Addendum: Further Analysis of Hydrocarbons and Trace Materials To Support Dxxxx,” final report for CRC Project No. AV-2-04a, April 2009. (DXXXX later became D7566).

22 The Boeing Company, UOP, & United States Air Force Research Laboratory. (2011). Evaluation of Bio-Derived Synthetic Paraffinic Kerosenes (Bio-SPKs). West Conshohocken, PA: ASTM International Research Report D02-1723.
23 Edwards, T., Johnston, G. et al., "Evaluation of Alcohol to Jet Synthetic Paraffinic Kerosenes (ATJ SPK)," ASTM Research Report D02-1828, 2016.
24 Edwards, T., "USAF Jet Fuel Research 1987-2019," AFRL-RQ-WP-TR-2019-0103, June 2019.
25 Vozka, P., Kilaz, G., "A review of aviation turbine fuel chemical composition-property relations," Fuel 268 (2020) 117391.
26 Szetela E. J., TeVelde, J. A., "External Fuel Vaporization Study Phase II Final Report," NASA CR 165513, Nov. 1981
27 Prok, G. M., Seng, G. T., "Initial Characterization of an Experimental Referee Broadened-Specification (ERBS) Aviation Turbine Fuel," NASA TM 81440, Jan. 1980.
28 Yu, J., Eser, S., "Determination of Critical Properties (T_c, P_c) of Some Jet Fuels," Ind. Eng. Chem. Res., Vol. 34, pp. 404-409, 1995.
29 Riazi, M. R. and Daubert, T. E., "Analytical Correlations Interconvert Distillation Curve Types," *Oil & Gas Journal*, Vol. 84, 1986, August 25, pp. 50–57.
30 Bruno, T. J., "Improvements in the Measurement of Distillation Curves. Part 1: A Composition-Explicit Approach," Ind. Eng. Chem. Res. 2006, 45, 4371−4380.
31 Smith, B. L.; Bruno, T. J. Improvements in the Measurement of Distillation Curves: Part 4. Application to the Aviation Turbine Fuel Jet-A. Ind. Eng. Chem. Res. 2007, 46, 310−320.
32 Jessica L. Burger and Thomas J. Bruno, "Application of the Advanced Distillation Curve Method to the Variability of Jet Fuels," Energy Fuels 2012, 26, 3661−3671.
33 Bruno, T. J., Smith, B. L., "Evaluation of the physicochemical authenticity of aviation kerosene surrogate mixtures Part I: Analysis of volatility with the advanced distillation curve," Energy Fuels, Vol. 24, pp. 4266−76, 2010.
34 Edwards, T., ""Kerosene" Fuels for Aerospace Propulsion – Composition and Properties," AIAA Paper 2002-3874, 2002. Note that an unfortunate typo in this paper attributes the composition data to "ASTM D2784".
35 Shi, X., et al., "Quantitative composition-property relationship of aviation hydrocarbon fuel based on comprehensive two-dimensional gas chromatography with mass spectrometry and flame ionization detector," Fuel 200 (2017) 395–406.
36 Esclapez, L. et al., "Fuel effects on lean blow-out in a realistic gas turbine combustor," Combustion and Flame 181 (2017) 82–99.
37 West, Z., unpublished refractive index measurements on DLA survey fuels [A-7]
38 Lovestead, T. M., Burger, J. L., Schneider, N., Bruno, T. J., "Comprehensive Assessment of Composition and Thermochemical Variability of Three Prototype Gas Turbine Fuels by GC/QToF-MS and the Advanced Distillation-Curve Method as a Basis of Comparison for Novel Fuel Development," Energy & Fuels, Vol 30, pp. 10029−10044, 2016.
39 D2789 − 95 (Reapproved 2016), "Standard Test Method for Hydrocarbon Types in Low Olefinic Gasoline by Mass Spectrometry."
40 Shafer, L., Striebich, R., Gomach, J., Edwards, T., "Chemical Class Composition of Commercial Jet Fuels and Other Specialty Kerosene Fuels," AIAA Paper 2006-7972, November 2006.
41 Striebich,R. C., Shafer, L. M., Adams, R. K., West, Z. J., DeWitt, M. J., Zabarnick, S., "Hydrocarbon Group-Type Analysis of Petroleum-Derived and Synthetic Fuels Using Two-Dimensional Gas Chromatography," *Energy & Fuels*, Vol. 28, pp. 5696−5706, 2014.
42 Striebich, R. C., et al., "Hydrocarbon Group-Type Analysis of Current and Future Aviation Fuels: Comparing ASTM D2425 to GCxGC," Proceedings of the 12th International Conference on the Stability, Handling, and Use of Liquid Fuels," Sarasota FL, 2011.

43 Dryer, F. L., et al., “System and method for the determination of mixture averaged molecular weight of complex mixtures,” patent 9,410,876, published August 9, 2016.
44 Wang, Y., et al., “A new method of estimating derived cetane number for hydrocarbon fuels,” Fuel, Vol. 241, pp. 319-326, 2019.
45 Wang, Y., et al., “On estimating physical and chemical properties of hydrocarbon fuels using mid-infrared FTRI spectra and regularized linear models,” Fuel 255 (2019) 115715.
46 Won, S. H., Carpenter, D., Nates, S. , Dryer, F. L., “Derived Cetane Number as Chemical Potential Indicator for Near-Limit Combustion Behaviors in Ga Turbine Applications,” ASME PowerEnergy 2018-7414, June 2018.
47 Vozka, P. et al., “Middle distillates hydrogen content via GCxGC-FID,” Talanta 186 (2018) 140–146.
48 Rickard, G., “Develop an Aviation Fuel Cold Flowability Test to Replace Freezing Point Measurement,” Final Report for CRC Report AV-11-09, October 2010.
49 Zabarnick, S., West, Z. J., Shafer, L. M., and Cook, R., “Studies of Scanning Brookfield Viscometry as a Replacement for Freezing Point in Aviation Fuel Specifications,” Final Report for CRC Project Number AV-16-11, October 2013.
50 The Effects of Operating Jet Fuels Below the Specification Freeze Point Temperature Limit. S Zabarnick & J Ervin, Federal Aviation Administration, DOT/FAA/AR-09/50, January 2010.
51 Fortin, T. J., Laesecke, A., “Viscosity Measurements of Aviation Turbine Fuels,” Energy & Fuels, Vol. 29, pp. 5495-5506, 2015.
52 Atkins, D., Ervin, J. S., “Experimental Studies of Jet Fuel Viscosity at Low Temperatures, Using a Rotational Viscometer and an Optical Cell,” Energy & Fuels, Vol. 19, pp. 1935-1947, 2005.
53 Atkins, D., Ervin, J. S., Freezing of Jet Fuel within a Buoyancy-Driven Flow in a Rectangular Optical Cell,” Energy & Fuels, Vol. 15, pp. 1233-1240, 2001.
54 Ervin, J. S., Zabarnick, S., et al., “Development of an Advanced Jet Fuel with Improved Low Temperature Flow Performance – The JP-8+100LT Program,” U.S. Air Force Research Laboratory Report, AFRL-RZ-WP-TR-2011-2054, 2011.
55 Vozka, P., et al., “Impact of HEFA Feedstocks on Fuel Composition and Properties in Blends with Jet A,” Energy & Fuels, Vol. 32, pp. 11595-11606, 2018.
56 Vozka, P., et al., “Impact of Alternative Fuel Blending Components on Fuel Composition and Properties in Blends with Jet A,” Energy & Fuels, Vol. 33, pp. 3275-3285, 2019.
57 Culbertson, B., Williams, R. W., “Alternative Aviation Fuels for Use in Military Auxiliary Power Units (APUs) and Engines,” AFRL-RQ-WP-TR-2017-0047, March 2017.
58 Steve Zabarnick, Linda Shafer, Zach West, Rhonda Cook, Matt DeWitt, and Ted Williams, “Low-Temperature Additive Performance in Jet A Fuels,” AFRL-RQ-WP-TR-2013-0093, April 2013.
59 George Wilson, G. R., “Comparison of ASTM D613 and ASTM D6890 Final Report,” TFLRF No. FR 467, April 2016.
60 P. Wells, R. Gaughan, “Jet for Diesel Task Force,” ASTM – June 2011, Baltimore, MD and December 2011 New Orleans, LA.
61 Colket, M. et al., “An Overview of the National Jet Fuel Combustion Program,” AIAA 2016-0177, Jan. 2016.
62 Heyne, J. S. et al., “Year 2 of the National Jet Fuels Combustion Program: Moving Towards a Streamlined Alternative Jet Fuels Qualification and Certification Process,” AIAA 2017-0145, Jan 2017.
63 Heyne, J.S. et al., “Year 3 of the National Jet Fuels Combustion Program: Practical and Scientific Impacts,” AIAA-2018-1667, Jan 2018.
64 Pande, S. G., Hardy, D. R., “Cetane Number Predictions of a Trial Index Based on Compositional Analysis,” Energy & Fuels, Vol. 3(3), pp. 308-312, 1989.

65 Lenoir, J. M. and Hipkin, H. G., “Measured Enthalpies of Eight Hydrocarbon Fractions,” Journal of Chemical and Engineering Data, Vol. 18, No. 2, 1973, pp. 195–202.
66 Sauerbrunn, S., “Determination of Heat of Vaporization and Creating Enthalpy Diagrams for Several Common Jet Fuels,” final report for CRC project AV-20-14, April 2019.
67 Huang, H., Spadaccini, L. J., Sobel, D., “Endothermic Heat Sink of Jet Fuels for Scramjet Cooling,” AIAA Paper 2002-3871, July 2002.
68 Lefebvre, A., “Gas Turbine Combustion,” Hemisphere Publishing Corp., New York, 1983. Note that the chapter on gas turbine fuels was removed in later editions in favor of an expanded chapter on emissions – a clear case of editorial malpractice.
69 Szetela, E. J., Chiapetta, L., “External Fuel Vaporization Study, Phase 1 Report,” NASA CR 159850, 1980.
70 Andre´ L. Boehman, David Morris, and James Szybist, “The Impact of the Bulk Modulus of Diesel Fuels on Fuel Injection Timing,” Energy & Fuels 2004, 18, 1877-1882.
71 Aircraft Fuel Systems Roy Langton, Chuck Clark, Martin Hewitt and Lonnie Richards, 2009 John Wiley & Sons, Ltd. ISBN: 978-0-470-05708-7
72 Comparison of Jet Fuels by Measurements of Density and Speed of Sound of a Flightline JP-8, Stephanie L. Outcalt,* Arno Laesecke, and Karin J. Brumback, Energy Fuels 2010, 24, 5573–5578.
73 Outcalt, S. L., et al., “Density and Speed of Sound Measurements of Jet A and S-8 Aviation Turbine Fuels,” Energy & Fuels Vol. 23, pp. 1626-1633, 2009.
74 Outcalt, S. L., Fortin, T., “Density and Speed of Sound Measurements of Two Synthetic Aviation Turbine Fuels,” J Chem Engr Data, Vol. 56, pp. 3201-3207, 2011.
75 Outcalt, S. L., Fortin, T. J., “Density and Speed of Sound Measurements of Four Bio-Derived Aviation Fuels,” J Chem Engr Data, Vol. 57, pp. 2869-2877, 2012.
76 Luning Prak, D. J., et al., “Density, Viscosity, Speed of Sound, and Bulk Modulus of Methyl Alkanes, Dimethyl Alkanes, and Hydrotreated Renewable Jet Fuels,” Journal of Chemical & Engineering Data, Vol. 58, pp. 2065-2075, 2013.
77 Bessee, G. R., et al., “Advanced Propulsion Fuels Research and Development Support to AFRL/RQTF,” AFRL-RQ-WP-TM-2013-0010, December 2012 (Table E-10, page 404).
78 Hutzler, S. A., “Isentropic Bulk Modulus: Development of a Federal Test Method, Interim Report,” TFLRF No. 465, Contract No. W56HZV-09-C-0100 (WD19 and WD21-Task 2.1), January 2016.
79 Outcalt, S. L., “Compressed-Liquid Densities of Three “Reference” Turbine Fuels,” Energy Fuels 2016, 30, 10783−10788.
80 Hutzler, S., “Development of a Test Rig for Measuring Isentropic Bulk Modulus,” TFLRF Report No. 438, January 2013 (ADA589020).
81 Griesenbrock, M., unpublished bulk modulus data, 2015.
82 Hodgson, F. N., Scribner, W. G., Kemmer, A. M., “Environmental Degradation of Fuels, Fluids, and Related Materials for Aircraft,” AFAPL-TR-74-8, Vol. I, pp. 3-5, 1974.
83 Biddle, T. B., et al., “Properties of Aircraft Fuels and Related Materials,” Pratt & Whitney, WL-TR-91-2036, July 1991 (pp. 43-59).
84 Hodgson, F. N., Tobias, J. D., “Analysis of Aircraft Fuels and Related Materials,” Monsanto, AFAPL-TR-79-2016, March 1979.
85 West, Z. J., et al., “Investigation of Water Interactions with Petroleum-Derived and Synthetic Aviation Turbine Fuels,” Energy & Fuels 2018, 32, 1166−1178.
86 Jasper, J. J., “The Surface Tension of Pure Liquid Compounds,” Journal of Physical and Chemical Reference Data 1, 841 (1972).
87 Hutzler, S. A. et al., “Fit-For-Purpose (FFP) and Dynamic Seal Testing of Alternative Aviation Fuels,” AFRL-RQ-WP-TR-2014-0226, Aug 2014 (DTIC ADA612275).

88 Moses, C., “Effects of Fuel Properties on Combustion Parameters in Gas Turbine Engines,” Naval Fuels & Lubricants CFT Report 441/18-017, 14 February 2018.
89 Luning Prak, D. J., et al., “Density, Viscosity, Speed of Sound, Bulk Modulus, Surface Tension, and Flash Point of Binary Mixtures of n-Dodecane with 2,2,4,6,6-Pentamethylheptane or 2,2,4,4,6,8,8-Heptamethylnonane,” J. Chem. Eng. Data 2014, 59, 1334−1346.
90 Luning Prak, D. J., et al., “Densities, Viscosities, Speeds of Sound, Bulk Moduli, Surface Tensions, and Flash Points of Quaternary Mixtures of n-Dodecane (1), n-Butylcyclohexane (2), n-Butylbenzene (3), and 2,2,4,4,6,8,8- Heptamethylnonane (4) at 0.1 MPa as Potential Surrogate Mixtures for Military Jet Fuel, JP-5,” J. Chem. Eng. Data 2019, 64, 1725−1745.
91 Parmenter, D., “Assessing Gauging Performance of Synthetic Fuels,” Coordinating Research Council Aviation Meetings, May 2, 2013, Savannah GA.
92 Moses, C., “Concern About Density-Dielectric Correlation in Synthesized Kerosenes,” Coordinating Research Council Aviation Meetings, May 2, 2013, Savannah GA.
93 Kline, B. R., “JP-8+100 Fuel Study Covering the Parameters: Temperature, Density, Dielectric Constant, Velocity of Sound and Electrical Conductivity and the Effects of JP-8+100 Fuel on Fuel Gauging System Performance,” WL-TR-95-2158, Sept. 1995 (Limited Distribution D).
94 Belieres, J. P., “Updates on Dielectric Constant, Measurements and Impact on airplanes FQIS,” Coordinating Research Council Aviation Meetings, May 5, 2011, Seattle, WA.
95 ARINC 611, “Guidance for the Design and Installation of Fuel Quantity Systems,” 1999.
96 Hazlett, R. N., Thermal Oxidation Stability of Aviation Turbine Fuels, ASTM Monograph 1, American Society for Testing and Materials, Philadelphia, PA, 1991.
97 Rubey, W., et al., “In Line Gas Chromatographic Measurement of Trace Oxygen and Other Dissolved Gases in Flowing High Pressure Thermally Stressed Jet Fuel,” ACS Division of Petroleum Chemistry Preprints, Vol 37(2), pp. 371-376, 1992.
98 Striebich, R. C., Rubey, W., “Analytical Method for the Detection of Dissolved Oxygen,” ACS Division of Petroleum Chemistry Preprints, Vol 39(1), pp. 47-50, 1994.
99 Rubey, W. A., et al., “Gas Chromatographic Measurement of Trace Oxygen and Other Dissolved Gases in Thermally Stressed Jet Fuel,” Journal of Chromatographic Science, Vol. 33, August 1995.
100 West, Z., “Technical Memorandum - Dissolved Gas Solubility in Various Jet Fuels. II.,” 26 Nov 2012.
101 West, Z., “UDRI Method FC-M-103: Dissolved Gas Determination in Jet Fuel via GC-MS,” UDR-TR-2019-113.
102 Ross, K., Thompson, G. H., “The Solubility of Air in Aviation Turbine Fuel,” Shell Report K.186, 1970.
103 Rickard, G., Brook, P., “Aviation Turbine Fuel Lubricity - A Review,” CRC Report AV-14-11, August 2014.
104 Qualified Product List of Products Qualified Under Performance Specification QPL-25017,” 2010-09-03.
105 MIL-PRF-25017H w/Amendment 1, 04 August 2011, Performance Specification Inhibitor, Corrosion / Lubricity Improver, Fuel Soluble (NATO S-1747).
106 Hsieh, P. Y., Widegren, J. A., et al., “Direct Measurement of Trace Polycyclic Aromatic Hydrocarbons in Diesel Fuel with 1H and 13C NMR Spectroscopy: Effect of PAH Content on Fuel Lubricity,” Energy& Fuels, Energy Fuels, Vol. 29, pp. 4289−4297, 2015.
107 Proceedings of the CRC Fuel Lubricity Workshop, April 22, 1996.
108 Biddle, T. B., Edwards. W. H., “Evaluation of Corrosion Inhibitors as Lubricity Improvers,” AFWAL-TR-88-2036, July 1988.
109 Aviation Fuel Lubricity Evaluation, CRC Report 560, July 1988.
110 Frame, E., Alvarez, R., “Synthetic Fuel Lubricity Evaluations,” TFLRF Interim Report 367, September 2003.
111 Sympson, J., “T700 Biofuel Low Lubricity Endurance,” AFRL-RQ-WP-TR-2014-0243, Sep. 2014.

112 Kent, B., McCarthy, T., Medearis, G., Sympson, J. and Walker, J. “Low Lubricity Testing of T700 Main Fuel Pump,” AFRL-RQ-WP-TR-2017-0147, Nov. 2017.
113 ASTM D5001, “Standard Test Method for Measurement of Lubricity of Aviation Turbine Fuels by the Ball-on-Cylinder Lubricity Evaluator (BOCLE).”
114 ASTM D6079, “Test Method for Evaluating Lubricity of Diesel Fuels by the High-Frequency Reciprocating Rig (HFRR).”
115 ASTM D607, “Test Method for Evaluating Lubricity of Diesel Fuels by the Scuffing Load Ball-on-Cylinder Lubricity Evaluator (SLBOCLE).”
116 Turgeon, R., Lim, E., “F-76 Lubricity Improver Additive Evaluation,” NF&LCFT REPORT 441/13-007, 16 September 2013. AD 618817
117 McKay, B. J., Villahermosa, L. A., Kline, K. S., Muzzell, P. A., Stavinoha, L. L., “Bench-top Lubricity Evaluator Correlation with Military Rotary Fuel Injection Pump Test Rig,” SAE 2005-01-3899, Oct 2005, TARDEC 15283, ADA571036.
118 Yang, J. Xin, Z. et al, “An overview on performance characteristics of bio-jet fuels,” Fuel, Vol. 237, pp. 916–936, 2019.
119 Zhang, C., Hui, X., et al, “Recent development in studies of alternative jet fuel combustion: Progress, challenges, and opportunities,” Renewable and Sustainable Energy Reviews, Vol. 54, pp. 120-138, 2016).
120 Hui, X., Kumar, K., et al, “Experimental studies on the combustion characteristics of alternative jet fuels,” Fuel, Vol. 98, pp. 176-182, 2012.
121 Yost, D. M., Brandt, A. C., Hansen, G., “Engine and Pump Studies Utilizing JP-8 and Alcohol-to-Jet (ATJ) Blends,” AFRL-RQ-WP-TR-2014-0231, Aug 2014 (DTIC ADA613897).

APPENDIX – HISTORICAL HIGH TEMPERATURE PROPERTY DATA

The tables that follow are extracted from historical reports references in Section 1, to save the reader the trouble of extracting the data (although the reports are well worth reading). Most of this higher temperature data comes from calculations – these could be reproduced from modern programs such as NIST's REFPROP program.

[8] Bucknell, R. L., "Fuels and Lubricants Influence on Turbine Engine Design and Performance (FLITE)," AFAPL-TR-73-52, Vol. II, Jun. 1973. ("FLITE") (also JP-4,5,7 data)

[9] Sumey, I. E., "Fuels and Lubricants Influence on Turbine Engine Design and Performance (FLITE)," AFAPL-TR-73-54, Vol. II, Nov. 1974. ("FLITE") (also JP-4,5,7 data)

[10] TeVelde, J. A., Glickstein, M., "Heat Transfer and Thermal Stability of Alternative Aircraft Fuels – Vol. 1," NAPC-PE-87C, Nov. 1983 ("UTRC JP-5")

[11] Faith, L. E., et al., "Heat Sink Capability of Jet A Fuel – Heat Transfer and Coking Studies," NASA CR-72951, July 1971 ("Shell Jet A").

[12] Nixon, A. C., et al., "Vaporizing and Endothermic Fuel for Advanced Engine Application – Part III – Studies of Thermal and Catalytic Reactions, Thermal Stability, and Combustion Properties of Hydrocarbon Fuels," AFAPL-TR-67-114, Part III. Vol. II, February 1970. (Limited Distribution) ("Shell JP-5")

[13] MacFarlane, W. R., and Wiese, D. E., "Fuel Options for High Mach Propulsion, Vol. II, Fuel Properties," WRDC-TR-90-2090, Oct. 1990. (has JP-7 properties, not included here)

APPENDIX IV

FUEL AND LUBRICANT PROPERTIES

Fuel and lubricant properties are shown in tables XXXVI through XLVII.

A. FUEL PROPERTIES

Table XXXVI. Jet Engine Fuels Specific Gravity-Temperature Relationship

Temperature, °F	JP-4	JP-5	JP-6	JP-7	JP-8 and JET A-1
0	0.7860	0.8530	0.7970*	0.8200*	0.8440
50	0.7665	0.8300	0.7810*	0.7990*	0.8225
100	0.7455	0.8110	0.7660	0.7795	0.8050
150	0.7230	0.7900	0.7500	0.7610	0.7855
200	0.6990	0.7700	0.7270	0.7420	0.7665
250	0.6765	0.7500	0.7050	0.7225	0.7490
300	0.6490	0.7295*	0.6835	0.7020	0.7300
350	0.6300*	0.7090*	0.6575*	0.6760	0.7105
400	0.6100*	0.6890*	0.6310*	0.6560	--
450	--	0.6685*	0.6065*	0.6290	--
500	--	0.6480	0.5820*	0.6010	--

*Extrapolated Values.

Table XXXVII. Jet Engine Fuels Viscosity-Temperature Relationship

Temperature, °F	Viscosity, centistokes				
	JP-4	JP-5	JP-6	JP-7	JP-8 and JET A-1
-40	4.4	19.0	--	--	16.28
-30	3.59	13.7	--	10.45	12.01
0	2.4	7.5	2.0	7.0	6.00
77	1.18	2.25	1.25	2.20	2.16
100	1.00	1.95	1.15	1.73	1.71
150	0.84	1.30	0.95	1.35	1.33
200	0.62	0.92	0.81	0.87	0.86
250	0.46	0.70	0.70	0.66	0.69*
300	0.37	0.55	0.59	0.52	0.56*
350	0.33	0.45	--	0.44	0.48*
400	0.27	0.38	--	0.37	0.42*
450	0.23	0.32	--	0.32	0.34*
500	0.21	0.29	--	0.28*	0.30*
	Humble	Humble	AOR Co.	FRDC	FRDC

*Extrapolated Data

Notes: JP-4 and JP-5 Viscosity Data From "Data Book for Designers," Humble Oil & Refining Co., 1969.

JP-5 Data From "Supersonic Fuels and Lubricants," Ashland Oil & Refining Co., 1962.

JP-7 and JET A-1 Viscosity Data From Experimental Work at FRDC.

Table XXXVIII. Jet Engine Fuels Vapor Pressure-Temperature Relationship

Temperature, °F	Vapor Pressure, psia				
	JP-4	JP-5	JP-6	JP-7	JP-8 and JET A-1
50	1.05	--	--	0.008*	--
100	3.00	--	0.25	0.026	0.028
150	6.30	0.14	0.70	0.090	0.14
200	14.00	0.49	1.75	0.31	0.59
250	25.50	1.30	4.00	0.85	1.50
300	40.00	2.50	8.70	2.40	3.60
350	65.00	6.60	16.50	5.50	7.50
400	100.00	14.50	30.00	12.00	15.5*
450	--	25.00	50.00	23.00	32.00*
500	--	--	84.00	42.00	60.00*
	Humble	Humble	AOR Co.	FRDC PWA 535 5/9/67	FRDC

*Extrapolated Data

Notes: JP-4 and JP-5 Data From "Data Book for Designers," Humble Oil & Refining Co., 1969.

JP-6 Data From "Supersonic Fuels & Lubricants," Ashland Oil & Refining Co., 1962.

JP-7 and JET A-1 Data From Experimental Work at FRDC.

Table XXXIX. Jet Engine Fuels Enthalpy-Temperature Relationship

Temperature, °F	Enthalpy, Btu/lb					
	Liquid Phase			Vapor Phase		
	JP-4	JP-5	JP-6	JP-4	JP-5	JP-6
0	0	0	0	160	160	150
50	20	20	20	180	180	170
100	44	42	45	196	198	188
150	70	68	70	216	216	210
200	96	92	95	238	236	235
250	124	120	124	260	260	255
300	152	148	154	280	280	275
350	184	179	182	304	304	300
400	214*	208	213	328	328	325
450	246*	240	245	348	352	350
500	282*	272	280	368	380	380
550	320*	308	314	388	404	410
600	356*	344	350	406	436	440

*Extrapolated Data

Notes: JP-4 and JP-5 Enthalpy Data From "Data Book for Designers," Humble Oil & Refining Co., 1969.

JP-6 Enthalpy Data From "Supersonic Fuels & Lubricants," Ashland Oil & Refining Co., 1962.

Table XL. Jet Engine Fuels Specific Heat-Temperature Relationship

Temperature, °F	Specific Heat, Btu/lb/°F			
	JP-4	JP-5	JP-6	JP-8 and JET A-1
0	0.455	0.435	0.468	0.445
50	0.485	0.460	0.493	0.470
100	0.510	0.485	0.518	0.495
150	0.535	0.510	0.542	0.520
200	0.565	0.535	0.567	0.545
250	0.590	0.560	0.592	0.570
300	0.620	0.585	0.616	0.600
350	0.645	0.615	0.640	0.625
400	0.670	0.640	0.666	0.650
450	0.700	0.665	0.690	0.675
500	0.725	0.690	0.715	0.705

Notes: JP-4, JP-5, and JET A-1 Specific Heat Data From "Data Book for Designers," Humble Oil & Refining Co., 1969.

JP-6 Specific Heat Data From "Supersonic Fuels & Lubricants," Ashland Oil & Refining Co., 1962.

Table XLI. Jet Engine Fuels Average Thermal Conductivity Data

Temperature, °F	Thermal Conductivity, Btu/ft^2 (hr) (°F/°F)
0	0.0816
50	0.0802
100	0.0790
150	0.0776
200	0.0764
250	0.0750
300	0.0738
350	0.0725
400	0.0712
450	0.0699
500	0.0686

Notes: Thermal Conductivity Data From J. B. Maxwell, "Data Book on Hydrocarbons."

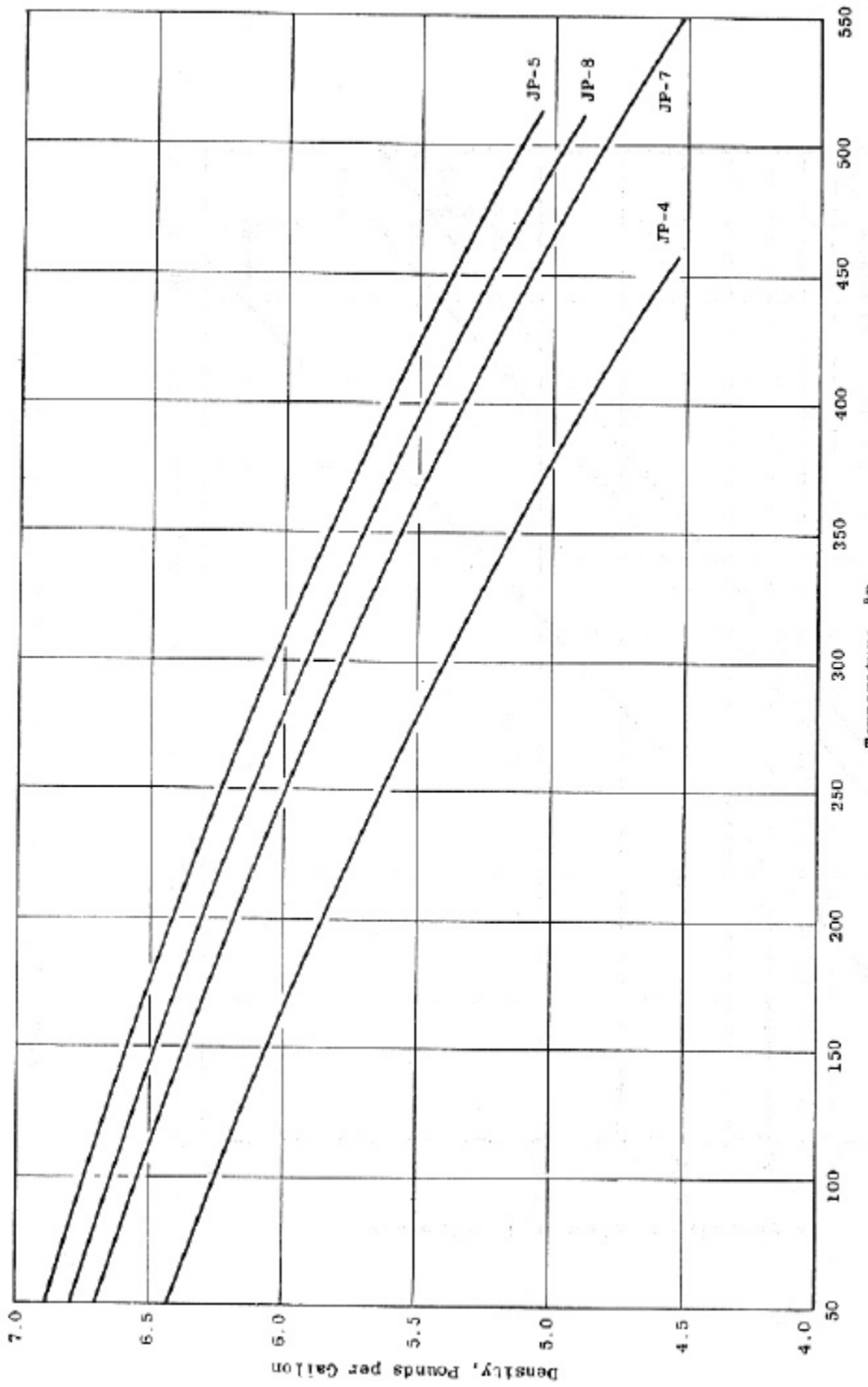

Figure 26. Densities of Fuels Used in FLITE Program.

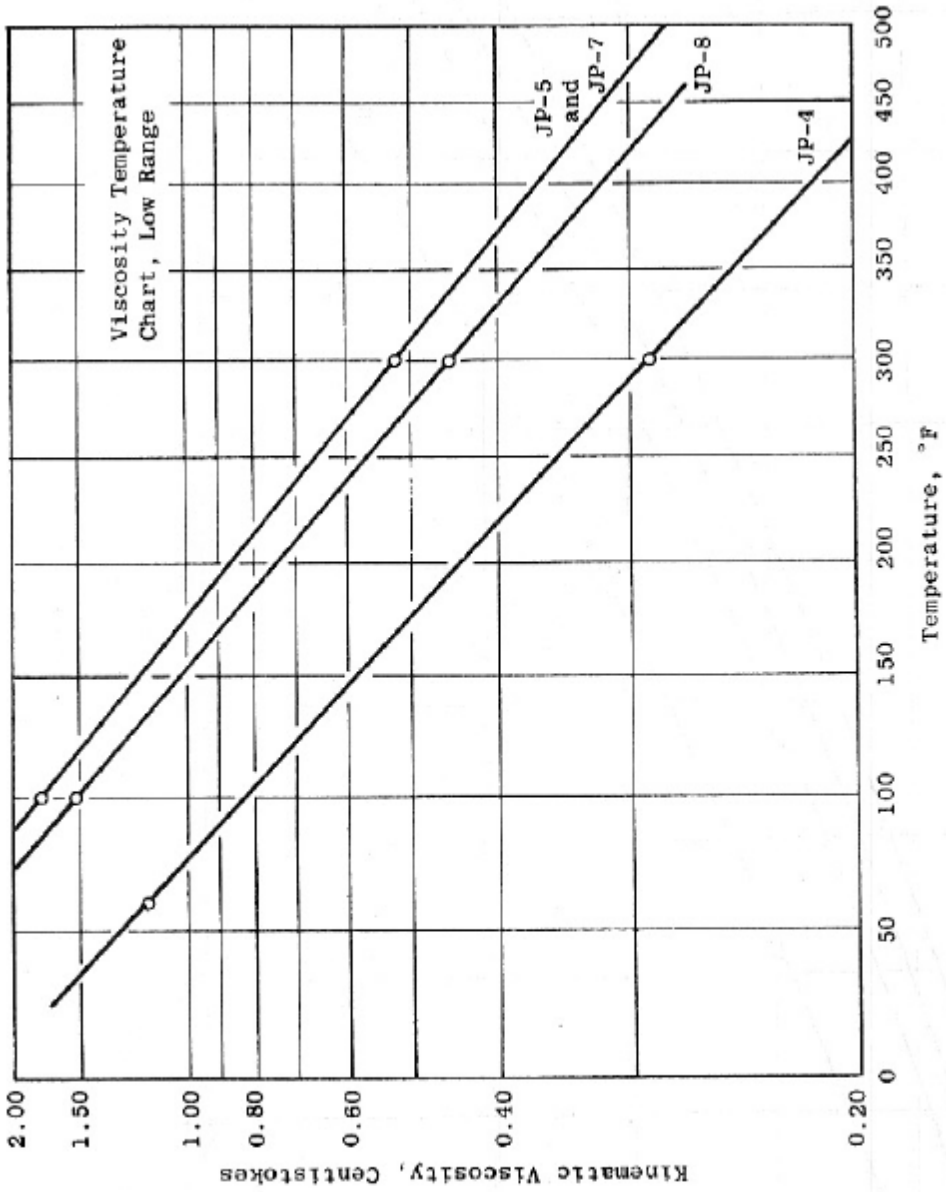

Figure 27. Viscosities of Fuels Used in FLITE Program.

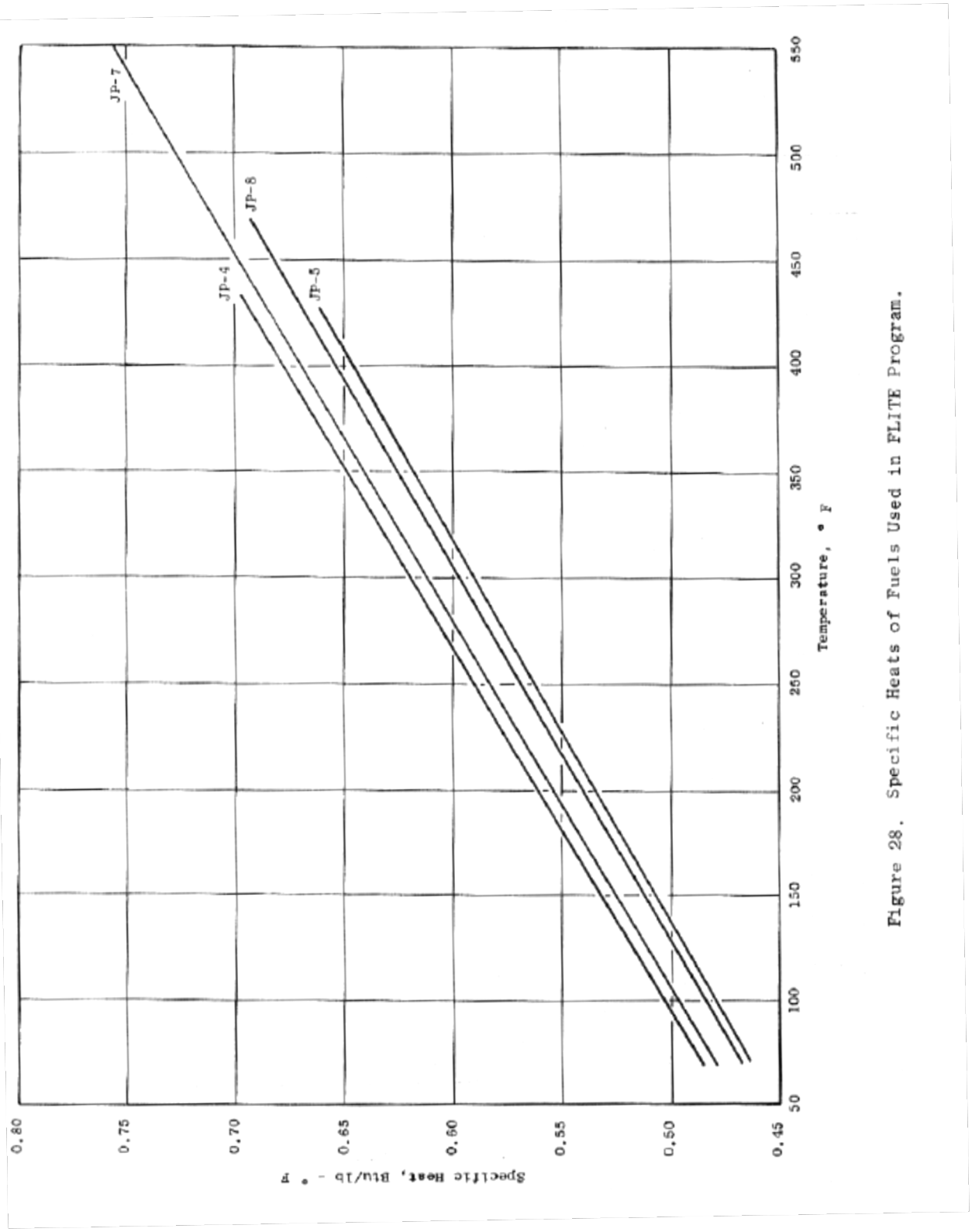

Figure 28. Specific Heats of Fuels Used in FLITE Program.

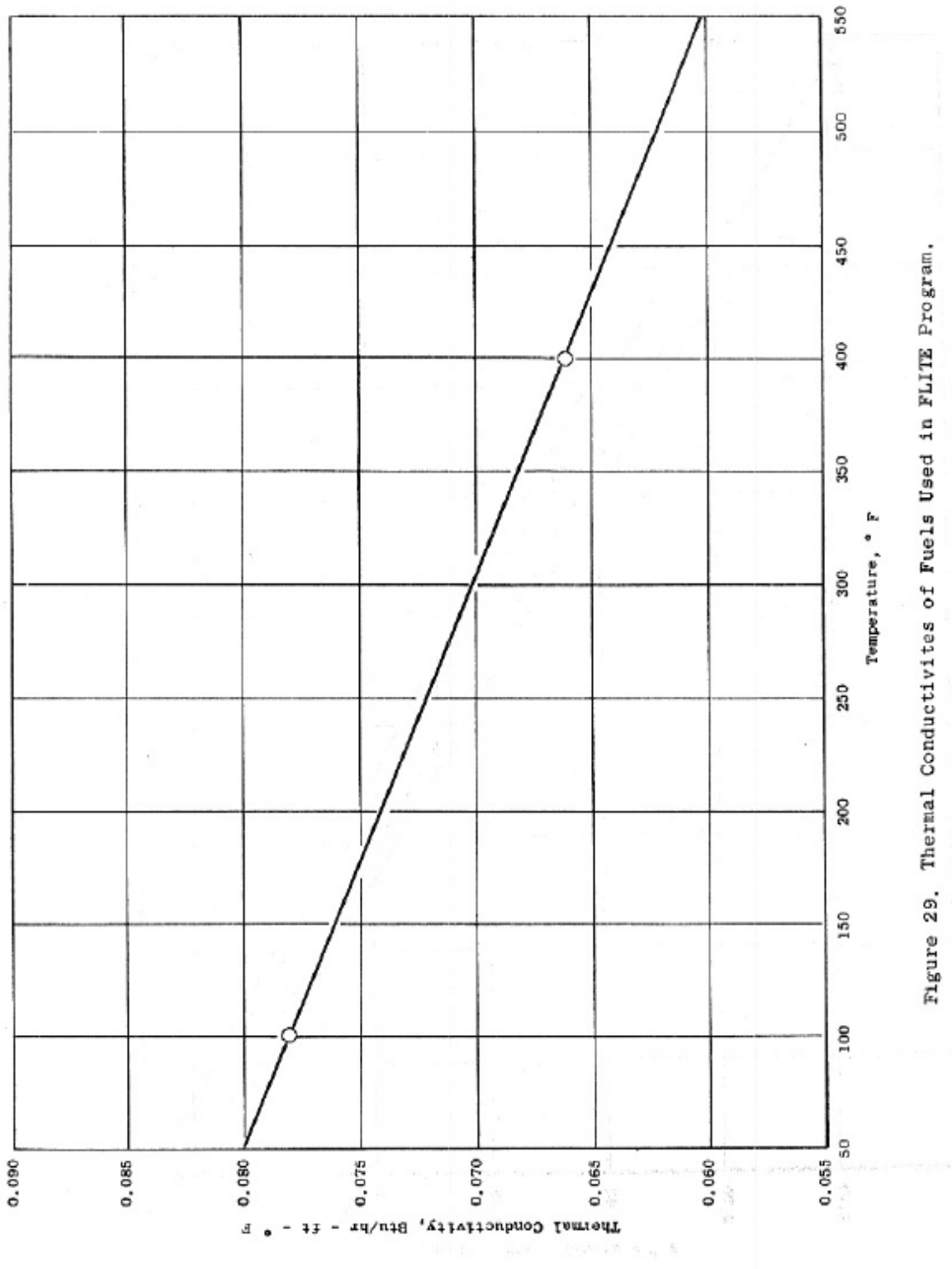

Figure 29. Thermal Conductivites of Fuels Used in FLITE Program.

Table XIX. GAS PROPERTIES OF JET A FUEL

Compressibility Factor

Temp., °F (°C)	Pressure, psia (MN/m²)		
	0 (0)	500 (3.45)	1000 (6.90)
750 (399)	1	0.305	0.470
800 (427)	1	0.357	0.494
850 (454)	1	0.436	0.524
900 (482)	1	0.528	0.559
950 (510)	1	0.615	0.601
1000 (538)	1	0.689	0.650

Density, lb/ft³ (kg/m³)

Temp., °F (°C)	Pressure, psia (MN/m²)		
	0 (0)	500 (3.45)	1000 (6.90)
750 (399)	0	21.5 (345)	27.9 (446)
800 (427)	0	17.6 (282)	25.5 (408)
850 (454)	0	13.88 (222)	23.1 (370)
900 (482)	0	11.04 (177)	20.9 (334)
950 (510)	0	9.14 (146)	18.7 (300)
1000 (538)	0	7.88 (126)	16.7 (268)

Enthalpy, Btu/lb (kJ/kg)

Temp., °F (°C)	Pressure, psia (MN/m²)		
	0 (0)	500 (3.45)	1000 (6.90)
750 (399)	565 (1313)	495 (1149)	489 (1136)
800 (427)	602 (1400)	542 (1260)	533 (1240)
850 (454)	640 (1488)	591 (1373)	578 (1344)
900 (482)	679 (1577)	639 (1485)	623 (1449)
950 (510)	718 (1669)	686 (1593)	669 (1554)
1000 (538)	758 (1763)	731 (1699)	714 (1659)

Specific Heat at Constant Pressure, Btu/lb-°F (kJ/kg-°C)

Temp., °F (°C)	Pressure, psia (MN/m²)		
	0 (0)	500 (3.45)	1000 (6.90)
750 (399)	0.730 (3.06)	0.945 (3.95)	0.894 (3.74)
800 (427)	0.748 (3.13)	0.965 (4.04)	0.866 (3.75)
850 (454)	0.765 (3.20)	0.973 (4.07)	0.899 (3.76)
900 (482)	0.781 (3.27)	0.948 (3.97)	0.902 (3.77)
950 (510)	0.797 (3.34)	0.917 (3.84)	0.905 (3.79)
1000 (538)	0.812 (3.40)	0.899 (3.76)	0.908 (3.80)

Viscosity, lb/ft-hr (μN·s/m²)

Temp., °F (°C)	Pressure, psia (MN/m²)		
	0 (0)	500 (3.45)	1000 (6.90)
750 (399)	0.0256 (10.6)	0.0836 (36.6)	0.1333 (55.1)
800 (427)	0.0266 (11.0)	0.0696 (28.8)	0.1148 (47.4)
850 (454)	0.0276 (11.4)	0.0559 (23.1)	0.1003 (41.5)
900 (482)	0.0285 (11.8)	0.0461 (19.9)	0.0879 (36.3)
950 (510)	0.0295 (12.2)	0.0442 (18.3)	0.0775 (32.0)
1000 (538)	0.0305 (12.6)	0.0423 (17.5)	0.0695 (28.7)

Thermal Conductivity, Btu/hr-ft-°F (mW/m·°C)

Temp., °F (°C)	Pressure, psia (MN/m²)		
	0 (0)	500 (3.45)	1000 (6.90)
750 (399)	0.0231 (39.9)	0.0344 (59.4)	0.0407 (70.3)
800 (427)	0.0246 (42.5)	0.0328 (56.7)	0.0395 (68.4)
850 (454)	0.0260 (45.0)	0.0318 (55.0)	0.0387 (67.0)
900 (482)	0.0275 (47.6)	0.0317 (54.8)	0.0383 (66.2)
950 (510)	0.0291 (50.3)	0.0322 (55.8)	0.0381 (65.9)
1000 (538)	0.0306 (52.9)	0.0332 (57.4)	0.0382 (66.0)

S-14115
67374

TABLE 7. THERMOPHYSICAL PROPERTIES OF JP-5

			Pressure, psia									
			330			430			530			
Temp. °F	Enthal. BTU/lb	Sp. Heat BTU/lb-°F	Density lbm/cft	Cond. BTU/ft-°F-hr	Visc. × 10^6 lb/ft-s	Density lbm/cft	Cond. BTU/ft-°F-hr	Visc. × 10^6 lb/ft-s	Density lbm/cft	Cond. BTU/ft-°F-hr	Visc. × 10^6 lb/ft-s
0	0.000	0.380	51.200	0.084	3300.000	51.200	0.084	3300.000	51.200	0.084	3300.000
50	20.667	0.402	49.950	0.081	2100.000	49.950	0.081	2100.000	49.950	0.081	2100.000
100	41.333	0.431	48.700	0.079	900.000	48.700	0.079	900.000	48.700	0.079	900.000
150	62.000	0.467	47.450	0.077	655.000	47.450	0.077	655.000	47.450	0.077	655.000
200	88.000	0.502	46.200	0.075	410.000	46.200	0.075	410.000	46.200	0.075	410.000
250	114.000	0.535	44.850	0.072	315.000	44.850	0.072	315.000	44.850	0.072	315.000
300	140.000	0.565	43.500	0.070	220.000	43.500	0.070	220.000	43.500	0.070	220.000
350	171.250	0.595	42.250	0.068	172.500	42.250	0.068	172.500	42.250	0.068	172.500
400	202.500	0.625	41.000	0.066	125.000	41.000	0.066	125.000	41.000	0.066	125.000
450	233.750	0.633	39.600	0.064	101.500	39.600	0.064	101.500	39.600	0.064	101.500
500	265.000	0.642	38.200	0.062	78.000	38.200	0.062	78.000	38.200	0.062	78.000
550	297.500	0.650	36.100	0.059	66.000	36.100	0.059	66.000	36.100	0.059	66.000
600	330.000	0.700	34.000	0.056	54.000	34.455	0.057	54.000	34.700	0.057	54.000
650	367.500	0.750	30.750	0.052	45.000	31.432	0.053	45.000	31.850	0.053	45.000
700	405.000	0.850	27.500	0.048	36.000	28.409	0.048	34.991	29.000	0.048	34.350
750	450.000	1.317	18.733	0.032	22.301	24.856	0.040	29.767	25.884	0.041	31.963
800	520.000	1.063	11.164	0.020	8.805	19.076	0.029	16.342	21.968	0.032	24.076
850	560.000	0.800	6.328	0.014	8.270	12.612	0.018	10.178	17.215	0.023	11.900
900	600.000	0.767	5.490	0.014	8.075	8.975	0.017	9.309	12.100	0.020	10.387
950	635.000	0.700	5.048	0.014	7.952	7.884	0.017	8.770	10.294	0.018	9.411
1000	670.000	0.725	4.607	0.015	7.914	6.792	0.017	8.620	8.487	0.018	9.065

TABLE 141 SHELL DEVELOPMENT COMPANY

CHARACTERISTIC PROPERTIES OF JP-5

MOLECULAR WEIGHT	169.0		169.0	
ACENTRIC FACTOR	.514		.514	
CRITICAL PRESSURE	22.8	ATM	330.0	PSIA
CRITICAL TEMPERATURE	411.8	C	773.0	F
CRITICAL COMPRESSIBILITY FACTOR	.250		.250	
CRITICAL DENSITY	.270	GM/CUCM	16.865	LB/CUFT
NORMAL BOILING POINT	199.1	C	390.3	F
NORMAL ENTHALPY OF VAPORIZATION	67.2	CAL/GM	120.9	BTU/LB

TABLE 142 SHELL DEVELOPMENT COMPANY

LIQUID PROPERTIES OF JP-5 AT SATURATION

TEMP, C	VAPOR PRESS, ATM	ENTHALPY OF VAP, CAL/GM	ENTHALPY, CAL/GM	ENTROPY, CAL/GM-K	SPEC HEAT AT CONST P, CAL/GM-K	DENSITY, GM/CUCM	VISCOSITY, CP	THERMAL COND, CAL/CM-SEC-K	PRANDTL NUMBER
-60	2.4462-07	9.0928+01	-2.2573+01	-1.8451-01	3.4016-01	8.7161-01	3.0333+01	3.4705-04	2.9731+02
-40	2.6783-06	8.9443+01	-1.5527+01	-1.1663-01	3.6437-01	8.5802-01	1.1723+01	3.3283-04	1.2835+02
-20	2.0091-05	8.7917+01	-8.0005+00	-5.5812-02	3.8825-01	8.4449-01	5.6135+00	3.1976-04	6.8158+01
0	1.1220-04	8.6346+01	0.0000	0.0000	4.1182-01	8.3100-01	3.1359+00	3.0766-04	4.1976+01
20	4.9548-04	8.4727+01	8.4672+00	5.1275-02	4.3510-01	8.1752-01	1.9630+00	2.9634-04	2.8821+01
40	1.8097-03	8.3056+01	1.7393+01	9.9004-02	4.5814-01	8.0404-01	1.3389+00	2.8570-04	2.1470+01
60	5.6554-03	8.1329+01	2.6767+01	1.4378-01	4.8102-01	7.9052-01	9.7544+01	2.7566-04	1.7021+01
80	1.5521-02	7.9539+01	3.6577+01	1.8606-01	5.0382-01	7.7695-01	7.4829+01	2.6616-04	1.4165+01
100	3.8168-02	7.7681+01	4.6804+01	2.2819-01	5.2670-01	7.6328-01	5.9797-01	2.5717-04	1.2247+01
120	8.5423-02	7.5747+01	5.7429+01	2.6945-01	5.4984-01	7.4947-01	4.9379-01	2.4868-04	1.0916+01
140	1.7610-01	7.3730+01	6.8427+01	3.0103-01	5.7347-01	7.3547-01	4.1879-01	2.4069-04	9.9781+00
160	3.3750-01	7.1618+01	7.9772+01	3.3612-01	5.9787-01	7.2123-01	3.6305-01	2.3319-04	9.3083+00
180	6.0568-01	6.9399+01	9.1442+01	3.6985-01	6.2334-01	7.0668-01	3.1944-01	2.2616-04	8.8044+00
200	1.0237+00	6.7058+01	1.0342+02	4.0243-01	6.5020-01	6.9172-01	2.8246-01	2.1956-04	8.3640+00
220	1.6379+00	6.4576+01	1.1571+02	4.3393-01	6.7878-01	6.7624-01	2.5061-01	2.1340-04	7.9714+00
240	2.4923+00	6.1927+01	1.2831+02	4.6451-01	7.0947-01	6.6010-01	2.2301-01	2.0758-04	7.6226+00
260	3.6238+00	5.9079+01	1.4124+02	4.9431-01	7.4279-01	6.4311-01	1.9893-01	2.0201-04	7.3145+00
280	5.0591+00	5.5988+01	1.5453+02	5.2343-01	7.7876-01	6.2501-01	1.7775-01	1.9680-04	7.0442+00
300	6.8136+00	5.2589+01	1.6817+02	5.5192-01	8.1841-01	6.0541-01	1.5894-01	1.9182-04	6.8098+00
320	8.8934+00	4.8789+01	1.8224+02	5.7997-01	8.6913-01	5.8379-01	1.4201-01	1.8672-04	6.6101+00
340	1.1297+01	4.4431+01	1.9682+02	6.0774-01	9.3436-01	5.5908-01	1.2646-01	1.8372-04	6.4453+00
360	1.4019+01	3.9234+01	2.1209+02	6.3550-01	1.0383+00	5.2967-01	1.1178-01	1.8357-04	6.3177+00
380	1.7049+01	3.2570+01	2.2842+02	6.6360-01	1.2356+00	4.9158-01	9.6740-02	1.9178-04	6.2353+00
400	2.0379+01	2.2273+01	2.4713+02	6.9456-01	1.9592+00	4.3073-01	7.8641-02	2.4738-04	6.2303+00

LIQUID PROPERTIES OF JP-5 AT SATURATION

TEMP, F	VAPOR PRESS, PSIA	ENTHALPY OF VAP, BTU/LB	ENTHALPY, BTU/LB	ENTROPY, BTU/LB-R	SPEC HEAT AT CONST P, BTU/LB-R	DENSITY, LB/CUFT	VISCOSITY, LB/FT-HR	THERMAL COND, BTU/FT-HR-R	PRANDTL NUMBER
-50	2.1119-05	1.6175+02	-1.8716+01	-8.5528-02	3.5768-01	5.3802+01	3.6028+01	8.1433-02	1.5825+02
0	3.6223-04	1.5794+02	0.0000	0.0000	3.9089-01	5.2628+01	1.2643+01	7.7014-02	6.4168+01
50	3.5572-03	1.5398+02	2.0359+01	7.5313-02	4.2349-01	5.1458+01	5.9287+00	7.3032-02	3.4379+01
100	2.3221-02	1.4984+02	4.2325+01	1.4304-01	4.5559-01	5.0290+01	3.3674+00	6.9395-02	2.2109+01
150	1.1135-01	1.4551+02	6.5851+01	2.0495-01	4.8735-01	4.9117+01	2.1819+00	6.6031-02	1.6104+01
200	4.2023-01	1.4095+02	9.0873+01	2.6223-01	5.1905-01	4.7937+01	1.5525+00	6.2921-02	1.2807+01
250	1.3096+00	1.3615+02	1.1730+02	3.1571-01	5.5113-01	4.6741+01	1.1628+00	6.0044-02	1.0857+01
300	3.4852+00	1.3103+02	1.4501+02	3.6599-01	5.8420-01	4.5523+01	9.4841-01	5.7402-02	9.6523+00
350	8.1093+00	1.2560+02	1.7390+02	4.1353-01	6.1901-01	4.4271+01	7.8901-01	5.4984-02	8.8827+00
400	1.6778+01	1.1974+02	2.0387+02	4.5871-01	6.5639-01	4.2972+01	6.6516-01	5.2776-02	8.2728+00
450	3.1287+01	1.1334+02	2.3491+02	5.0191-01	6.9723-01	4.1608+01	5.6431-01	5.0749-02	7.7932+00
500	5.3255+01	1.0634+02	2.6708+02	5.4350-01	7.4279-01	4.0130+01	4.8120-01	4.8867-02	7.3145+00
550	8.3810+01	9.8473+01	3.0048+02	5.8376+01	7.9216-01	3.8556+01	4.1167+01	4.6930-02	6.9489+00
600	1.2349+02	8.9414+01	3.3517+02	6.2296-01	8.5679-01	3.6758+01	3.5229+01	4.5079-02	6.6515+00
650	1.7237+02	7.8541+01	3.7181+02	6.6155-01	9.5015-01	3.4622+01	2.9987+01	4.4371-02	6.4213+00
700	2.3021+02	6.4409+01	4.1063+02	7.0028-01	1.1278+00	3.1841+01	2.5039+01	4.5065-02	6.2654+00
750	2.9665+02	4.1506+01	4.5556+02	7.4187-01	1.8663+00	2.7188+01	1.9325+01	5.7922-02	6.2266+00